IEEE Access
Multidisciplinary : Rapid Review : Open Access Journal

Received 22 August 2023, accepted 19 September 2023, date of publication 5 October 2023, date of current version 19 October 2023.

*Digital Object Identifier 10.1109/ACCESS.2023.3322278*

RESEARCH ARTICLE

# Modeling of Electric Vehicle Charging Demand and Coincidence of Large-Scale Charging Loads in Different Charging Locations

**ILKKA JOKINEN AND MATTI LEHTONEN**
Department of Electrical Engineering and Automation, Aalto University, 00076 Aalto, Finland
Corresponding author: Ilkka Jokinen (ilkka.a.jokinen@aalto.fi)

This work was supported by the Academy of Finland through the Profi5 Project. The work of Ilkka Jokinen was supported by the Walter Ahlström Foundation.

**ABSTRACT** Battery electric vehicles (BEVs) are becoming more widespread and consequently the charging load from vehicles is rapidly increasing. For energy system and grid planning, the magnitude and coincidence of these charging loads are crucial parameters. Furthermore, to determine the charging power demand in different charging locations, the coincidence of charging in them must be examined. Thus, in this study, the coincidence factors of charging loads in different charging locations were analyzed for a large-scale BEV fleet, considering available charging power and ambient temperature. In addition, the mean charging load, deviation of load, and flexibility potential within charging events, were examined based on the same parameters. The coincidence factors of charging increased with lower available charging power and lower ambient temperature. By location type, the highest factors were at work, at hotel, and at home, but overall, the coincidence of charging remained low for a large-scale BEV fleet. Moreover, the relative standard deviation of a composite load for a large number of BEVs was low, whereas the opposite was found for a small number of BEVs. The modeling of the charging loads in this study was based on activity-travel schedules from travel survey data, from which 12773 respondents with 40321 trips were included.

**INDEX TERMS** Charging load, coincidence factor, electric vehicle, load deviation.

## I. INTRODUCTION

The number of electric vehicles (EVs) is likely to grow significantly in the coming decades, due to technological advancements, cost decreases, and decarbonization targets. Globally, the International Energy Agency predicts, in their Stated Policies Scenario, that the number of passenger light duty electric vehicles will increase from 10 to 125 million by 2030 from 2020 [1]. This trend is evident in the European Union (EU), where the share of EVs from the newly registered vehicles has increased from a near 2% level (in 2015 – 2018) to 17.8% in 2021 [2]. Moreover, the EU plans to end the sale of new $CO_2$ emitting cars by 2035 [3]. Likewise in Finland, the share of battery electric vehicles (BEVs) and plug-in hybrid electric vehicles (PHEVs), from the new registrations in 2022, were 17.8% and 19.8% respectively [4]. As the number of EVs increase, consequently so does the energy and power demands of the transportation sector. For energy system operation and planning, it is crucial to estimate the characteristics of these charging loads, to maintain reliability and efficiency of the system.

The estimation of the EV charging loads can be based on data from travel surveys, vehicle trials, or EV charger trials [5]. Further, whichever the source of data, methods for estimating the demand are numerous. Travel surveys, often conducted on a national level, are a widely used source of data for this estimation. For example, in [6], [7], and [8] survey data was used to form charging profiles with the Monte Carlo method, whereas [9], [10], [11] used Direct use of observed activity-travel schedules (DUOATS), as classified in [12], for the formulation. Moreover, the Markov chain model was used in [13] to assess effects of EV charging to residential load,

The associate editor coordinating the review of this manuscript and approving it for publication was Emanuele Crisostomi.

while [14] used artificial neural networks to forecast travel behavior.

As the number of EVs on roads has increased, such have studies based on vehicle trials. For example, in [15] EV data of commercial and shared vehicles were used to forecast charging demand with the Monte Carlo method, while [16] developed a machine learning method, and compared it to several others, which utilized vehicle data to predict the demand. Moreover, vehicle measurement data was used in [17] to formulate usage patterns of vehicles, and in [18] to estimate power demand and the flexibility of charging.

Charging point data has been utilized e.g. in [19], where time series models, such as autoregressive integrated moving average, were used for forecasting aggregate charging load, or in [20] where time series models were compared to machine learning methods. Moreover, in [21] data mining methods for forecasting the charging load with case studies were utilized, while [22] used charging point data to estimate the future loading of commercial charging.

Even though there are several studies utilizing EV trials and charging point measurements, the data from these are scarce and often publicly not available [5]. Thus, in this study the data from the national household travel survey (NHTS) in Finland [23], was utilized to formulate charging profiles, by using the DUOATS [12] type modeling. In the survey, all respondents recorded all their trips on a given day, with detailed information on the departure and arrival times, locations, length, and mean of transport for the trips, which allowed the derivation of driving profiles. Shortcoming of using DUAOTS, based on survey data, is that it results in predetermined profiles where the driving patterns are fixed, and thus for example estimations of EV policy effects are not possible to be conducted [12]. However, in [9] Pareschi et al. compared the DUOATS type modeled charging load to electric vehicle trial data and concluded that travel surveys can be utilized for EV load modeling with reasonable accuracy.

For studies which utilize the characteristics of the charging profiles, case studies are required, for which the used source data almost always reflects a particular area, e.g., a country. In the case of Finland, large-scale EV charging has been estimated for BEVs in [11] and [24], and for PHEVs in [25].

The charging profiles can be utilized in a great number of analyses, including generation planning and scheduling, grid expansion and resiliency, and economics and environmental studies. Moreover, the effect of different parameters to the profiles can be considered in the analysis. The majority of studies consider the effect of available charging power on the estimated load. In addition, several studies consider the energy consumption of the vehicles based on ambient temperature [7], [8], [16], [24], or estimate different consumption scenarios [9], [25], and the vehicle's driving speed. However, while the ambient temperature is considered in several studies, a very low temperature is not. Thus, in this study, to fill this research gap, the charging load of a large-scale BEV fleet is examined with a very low ambient temperature of −20°C.

One key characteristic for generation and grid planning is the coincidence of EV charging load. This has been studied in small scale for example in [26], in the case of apartment buildings, analyzing the effects of available charging power, and in [27] by number of EVs considered. For a larger number of EVs, the coincidence factor has been studied in [28] with different available charging powers, while the effect of the number of EVs considered was studied in [29], [30], and [31]. In addition, in [32] the coincidence factor was analyzed based on charging power, battery size, and plug-in behavior. Moreover, [33] studied the coincidence of charging in terms of change in peak load by EV penetration level. However, there is a research gap on studying the variation of the coincidence of charging of large-scale EV fleets in different charging locations. Moreover, while ambient temperature was considered in studies [29], [30] on the coincidence factor, no analysis was conducted for a very low ambient temperature. This study examines these research gaps by analyzing the coincidence factor of charging in different charging locations, considering available charging power and ambient temperature, including a low temperature of −20°C. Moreover, as mentioned earlier, also the magnitude of the charging load is studied at very low ambient temperature, which lacks from the current literature. By analyzing the coincidence of charging in different charging locations, the location types where greater charging capacity is required, can be determined. This may be useful when planning charging point availability or dimensioning the distribution grid. By including the analysis of a very low temperature of −20°C, the magnitude, and the coincidence of the charging load, can be examined in a situation when the whole energy system is often under heavy loading. Thus, this knowledge can be useful when studying e.g., the reliability of the power system or generation planning.

In addition, in this study, the deviation of composite load, together with the flexibility potential of charging within charging events, which may lessen the burden of the charging load for the system, are examined based on the available charging power and ambient temperature.

The rest of the paper is formed as follows. Section II presents the materials and methods used to formulate the charging profiles, Section III presents the results, and Section IV concludes the study with discussion on the results.

## II. MATERIALS AND METHODS

### A. NATIONAL HOUSEHOLD TRAVEL SURVEY TO DRIVING PATTERNS

The driving patterns of BEVs were based on the driving patterns derived from the Finnish NHTS from 2016, conducted by the Finnish Transport and Communications Agency [23]. In the survey, the respondents recorded all their trips during one given day. For this study, the data used from the survey included the departure and arrival times, departure and arrival location types, trip distances, and mean of transport for the trips. From them, only the trips completed with passenger cars or vans with the respondent as a driver were included.

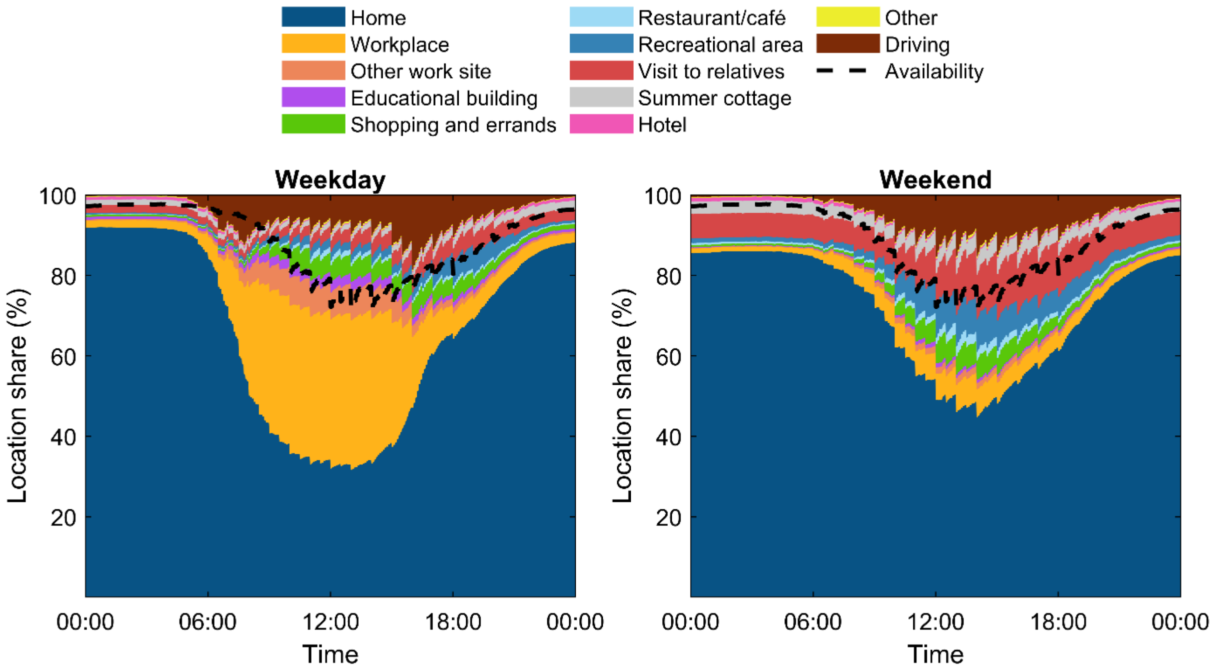


**FIGURE 1.** Share of vehicles in locations during week and weekend days, based on NHTS data [23]. Availability represents vehicles in locations with available charging power, in this study, as presented in Table 1.

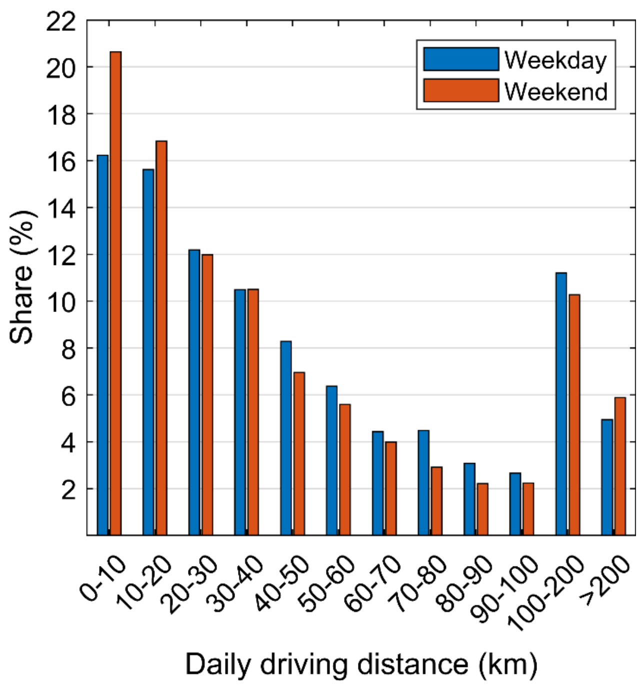


**FIGURE 2.** Daily driving distance distribution of vehicles during week and weekend days [23].

In addition, only continuous trips were included, where a later trip began from the same location as the earlier trip ended. Only exception was that the last trip of the day did not have to end at the same location as the first trip of the day began, to include long one-way trips. In addition, if the calculated mean velocity of the vehicle to complete a trip was greater than 130 km/h, or the departure time was later than the arrival time, the answers were eliminated. In total, the analysis included 13 323 responses with 43 348 trips, from which 12 733 and 40 321 were included after the elimination.

In the NHTS the respondents had 23 options to choose from as the location type of arrival and departure. Similar location types were here grouped together and treated as one, after verifying the continuity of trips. BEV driving profiles were formed such that one respondent was assumed to correspond to one BEV, regardless of the motive power of the respondent's vehicle in the survey. Further, it was assumed that the vehicle moved with a mean velocity during the trips

**TABLE 1.** Location types for vehicles based on the NHTS data [23], and the assumed available charging power (kW) in them, in this study, for three different charging power scenarios.

| Location type | Charging power in each scenario (kW) Low | Medium | High |
|---|---|---|---|
| Home | 3.68 | 7.36 | 11.0 |
| Workplace | 3.68 | 7.36 | 11.0 |
| Other work site | - | - | - |
| Educational building | - | - | - |
| Shopping and errands | 7.36 | 11.0 | 22.1 |
| Restaurant/café/pub | - | - | - |
| Sports or recreational area | - | - | - |
| Visit to relatives or friends | 3.68 | 7.36 | 11.0 |
| Summer cottage or vacation home | 3.68 | 7.36 | 11.0 |
| Hotel or motel | 7.36 | 11.0 | 22.1 |
| Other destination | - | - | - |
| Fast charging | 50 | 50 | 100 |

and was stationary between them. By so, a time series was formed for each vehicle, where its location for every time step, stationary or driving, was defined. In addition, while driving, the distance driven and driving speed, for each time step was defined from the survey data. The distance driven was multiplied by the energy consumption rate (ECR) of the vehicle, defined in Section II-C, which formed a consumption time series for each vehicle. Based on the location, charging power was either always or never available, and formed another time series for each vehicle. Moreover, three charging power scenarios (CPS) were analyzed (Low, Medium, and High power), which are presented in Table 1 for the different location groups. Charging was considered widely available in different location types, to represent a situation where the transportation sector is widely electrified, and thus the availability of charging points can be assumed high. All the 23 locations and their grouping are presented in Table 10 in Appendix A.

The responses were divided into weekday and weekend profiles. The share of active vehicles in each location, including driving, at every 1-minute time step are presented in Fig. 1 for week and weekend days. Notably, the share of vehicles at home were never below 31.7% and 44.8% during week and weekend days, respectively. The dashed line in the figure represents the share of vehicles with available charging. Moreover, in Fig. 2 the daily driving distance distribution of the formulated driving profiles is presented for week and weekend days, for which the average daily driving distances were 59.7 km and 60.9 km respectively.

To formulate driving profiles over one week, to have a continuous transfer from weekday to weekend, each of the weekday vehicle profiles was randomly coupled with a weekend profile. For this, conditions were that the weekday profile's last trip ended in the same location type as the weekend profile's first trip began, but if not possible, the profile was chosen such that the locations were similar in terms of available charging power. The total number of weekday profiles were 9744 and weekend profiles 2989.

Furthermore, it is important to note that the values in the tables and figures in this study refer to the active vehicles, i.e., the ones driven during the survey day. Thus, the resulting charging profiles from a number of active vehicles should be considered to occur for a larger BEV stock, which also includes the vehicles that are not driven on a given day [9]. The share of inactive vehicles can be derived as in (1) [9],

$$\text{Inactive share} = 1 - \frac{\left(\frac{d_{person} \cdot \#\text{Adults}_{\text{Finland}}}{\#\text{Cars}_{\text{Finland}}}\right)}{d_{active}} \approx 28.1\% \qquad (1)$$

where $d_{active}$ (60.0km) is the mean daily driving distance of active vehicles and $d_{person}$ (28.9km) is the daily driving distance per adult in the NHTS. Also included are the number of adults (4 429 921 [34]) in Finland and the number of vehicles in traffic (2 968 860 [35]) in Finland in 2016.

### B. ELECTRIC VEHICLE CHARGING PROFILES

Based on the driving profiles, minimum and maximum state of charge (SoC) levels of each individual BEV battery can be determined. Previously Zhang et al. [36] have studied aggregated charging profiles for BEVs with energy and power boundaries, to model charging and discharging of a large-scale BEV fleet. This study utilizes some of these same principles for calculating the minimum and maximum SoC levels for single BEV battery.

First the minimum ($e_i^{min}$) and maximum ($e_i^{max}$) representations of a BEV battery SoC through time were formulated, which were used for two purposes: to determine if the BEV was able to complete the trips assigned to it, and to formulate two charging profiles, one related to $e_i^{min}$ and one to $e_i^{max}$. These battery SoC levels should be thought as representations if the BEV would be either charged such that its battery level through time is as low as possible to complete the trips assigned to it ($e_i^{min}$), or such that the battery level is as high as possible ($e_i^{max}$). By so, the charging profile related to $e_i^{min}$ is one that delays the charging as late as possible, whereas the one related to $e_i^{max}$ charges immediately. Moreover, they are levels which can be sustained, and repeated, by the BEV if its trips over a time period, here a week, remain the same. Further, by calculating two charging profiles which either charged immediately or delayed the charging, allowed the flexibility potential, and thus demand response capacity, within charging events to be analyzed.

The process of calculating the $e_i^{min}$ and $e_i^{max}$, and the charging profiles is presented in Fig. 3. If the BEV was unable to complete its trips based on the NHTS, fast charging events were added to the profile. However, if the BEV was still unable to complete its trips, the profile was defined as non-electrifiable (6.1% of BEVs in the end). The calculations were performed over a three-week period with 1-minute resolution, from which the middle week was considered as an example week for further analysis. The three-week period was chosen to obtain a balance where during the middle week the BEV charged and consumed the same amount of energy. The process in Fig. 3 is explained in detail in the following subsections.

#### 1) MINIMUM BATTERY SOC LEVEL FOR A BEV TO COMPLETE ITS TRIPS

In blocks A.1, A.2, and A.3 in Fig. 3, the minimum battery SoC level of a BEV required to complete its trips was determined based on the consumption and location of the vehicle, and the available charging power. In block A.1 the location, and available charging power, of the vehicle were directly as the formulated vehicle profile from the NHTS, whereas in blocks A.2 and A.3 the location and available charging power were altered by the addition of stops for fast charging. However, in all the blocks A.1, A.2, and A.3 the calculations were completed in a similar manner based on the input information.

For each individual BEV (i) the required energy for its individual trip (j) was calculated as $e_{i,j}^{trip}$ in for each moment of departure $t_{i,j}^{d}$, i.e., the last moment the vehicle was stationary before a trip, as in (2). There, $t$ is time step, $d$ depict departure, $a$ depict arrival i.e., the first moment stationary after a trip, and $c_i(t)$ is the consumption of the vehicle. If a later trip had a large energy demand, or the charging power between the trips was limited, part, or all, of the energy demand of a later trip might have to be considered in the energy demand of the earlier trip. Thus, the total energy demand before each trip was represented as $e_{i,j}^{need}$ for each moment of departure $t_{i,j}^{d}$ as presented in (3-4) and visualized in Fig. 4.

$$e_{i,j}^{trip} = \sum\nolimits_{t=t_{i,j}^{d}+1}^{t_{i,j}^{a}-1} c_i(t), \quad \forall i, \ \forall j \tag{2}$$

$$e_{i,j}^{need} = e_{i,j}^{trip}, \quad j = J \tag{3}$$

$$e_{i,j}^{need} = e_{i,j}^{trip} + e_{i,j+1}^{min}\left(t_{i,j}^{d}\right), \quad j < J \tag{4}$$

Starting from the last trip, with $e_{i,j}^{need}$ and the available charging power for the vehicle $p_i^{available}(t)$, the minimum SoC level of the battery, $e_{i,j}^{min}(t)$, for each trip for the preceding timesteps, was determined such that the SoC of the battery reaches the $e_{i,j}^{need}$ at $t_{i,j}^{d}$, as in (5-6), which are a close resemblance to [36, eq. (6)], and where $\eta^{ch}$ is the charging efficiency. In addition, the minimum SoC of the battery during the trip was calculated based on the consumption of the vehicle during the trip as in (7).

$$e_{i,j}^{min}(t) = \max\left(e_{i,j}^{need} - \sum_{t=t+1}^{t_{i,j}^{d}} \eta^{ch} p_i^{available}(t), 0\right), \quad t < t_{i,j}^{d} \tag{5}$$

$$e_{i,j}^{min}(t) = e_{i,j}^{need}, \quad t = t_{i,j}^{d} \tag{6}$$

$$e_{i,j}^{min}(t) = \max\left(e_{i,j}^{min}(t-1) - c_i(t), 0\right), \quad t > t_{i,j}^{d} \tag{7}$$

From $e_{i,j}^{min}(t)$ for each single trip, the minimum SoC level of the BEV battery considering all its trips, $e_i^{min}(t)$, was determined as the maximum value for each time step of the individual trips $e_{i,j}^{min}(t)$ for the vehicle as in (8).

$$e_i^{min}(t) = \max(e_{i,j=1}^{min}(t), \ldots, e_{i,j=J}^{min}(t)), \quad \forall t, \ \forall j \tag{8}$$

In Fig. 4 an example vehicle profile with two trips is presented, seen as when $p_i^{available}(t)$ is zero. Both trips have the same energy demand when considered individually ($e_{i,j}^{trip}$), but the charging time between the trips is too short for charging the total energy demand of the later trip during the stop, and thus part of the demand must be considered in the energy demand of the earlier trip. Hence, the $e_{i,J-1}^{need}$, for the earlier trip, is greater than $e_{i,J-1}^{trip}$, by $e_{i,J}^{min}\left(t_{i,J-1}^{d}\right)$. For the later trip $e_{i,J}^{need} = e_{i,J}^{trip}$. The minimum SoC levels of each of the trips which reach their energy demands $e_{i,j}^{need}$ at $t_{i,j}^{d}$ are presented in green and yellow in the figure. In addition, it shows how the later trip's energy demand $e_{i,J}^{min}\left(t_{i,J-1}^{d}\right)$ is added to the previous trip's energy demand at $t_{i,J-1}^{d}$. The minimum level of the battery SoC of the BEV, which considers all the trips, is presented in blue and the maximum SoC in red, which is defined in Section II-B-III.

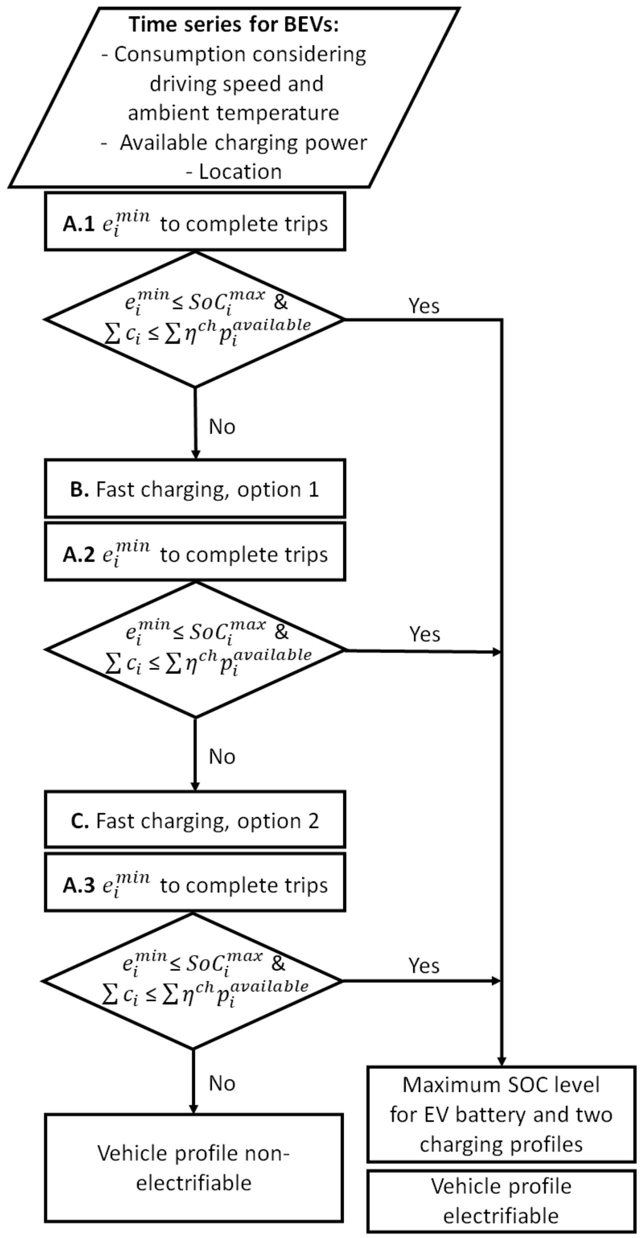


**FIGURE 3.** **The process of calculating the minimum, $e_i^{min}$, and maximum, $e_i^{max}$, levels of battery SoC to complete the trips by a vehicle profile, and the related two charging profiles. $SoC_i^{max}$ refers to the battery capacity, $\sum c_i$ to the daily energy consumption, $\sum \eta^{ch} p_i^{available}$ to the possible daily charged energy, and $\eta^{ch}$ is the charging efficiency. If the driving profile, formed from the survey data, was unable to be completed by the BEV, fast charging stops were added by two occasions, after which the profile was either defined as electrifiable or non-electrifiable.**

#### 2) CHARGING EVENTS FOR FAST CHARGING

If the minimum SOC level for the BEV, $e_i^{min}(t)$, to complete all its trips, as calculated in block A.1 in Fig. 3, was greater than the maximum available capacity of the BEV battery $SoC_i^{max}$, or the charging was not realizable, that is, the possible energy charged daily was less than the daily consumption, fast charging stops were added to the driving profiles. First, they were added to trips which consumption was greater than $SoC_i^{max}$, in block B in Fig 3. These stops were added by modifying the location data of the vehicle profiles such that the departure times of the trips in question were moved earlier, and the arrival times were not altered. The energy demand for fast charging was determined as the energy demand of the trip, reduced by the possible charge in the battery at the beginning of the trip, based on the past 24 hours. After the BEVs location profile was altered, the $e_i^{min}(t)$, was recalculated as in (2-8). If the $e_i^{min}(t)$ remained greater than the BEV's battery capacity, or there were no single trips with greater energy consumption than it, fast charging stops were added considering the too high energy demand due to multiple consecutive trips, in block C in Fig. 3. Now the energy demand for fast charging was determined as the lack of possible charging during days where the BEV consumed more than it charged. For these days, fast charging stops were added to the trip with the highest consumption, and the $e_i^{min}(t)$ recalculated with the altered vehicle location profile. In addition, conditions for adding the fast charging stops were that the duration that the BEV was stationary before the trip where fast charging was added must be longer than the duration for fast charging, and the last fast charging event must end 15 minutes before the trip's arrival time.

#### 3) CHARGING PROFILES FOR ELECTRIC VEHICLES

For the vehicles which driving profiles were electrifiable, the maximum level of the BEV battery SoC $e_i^{max}(t)$ was determined as in (9-10), which are a close resemblance of [36, eq. (5)]. The $e_i^{max}(t)$ was assumed to begin from the maximum battery capacity at the beginning of the three-week period and then represent a level of a battery which is charged immediately at every opportunity.

$$e_i^{max}(t) = \min(e_i^{max}(t-1) + \eta^{ch} p_i^{available}(t) - c_{i,j}(t), \mathrm{SoC}_i^{max}), t > 1 \quad (9)$$

$$e_i^{max}(t) = \mathrm{SoC}_i^{max}, \quad t = 1 \quad (10)$$

Moreover, two charging scenarios were determined which followed either $e_i^{min}(t)$ or $e_i^{max}(t)$. As described in Section II-B, $e_i^{min}(t)$ reached the required charge at the moment of departure for a trip. Thus, a charging profile related to $e_i^{min}(t)$ resulted in one which delayed the charging as late as possible, formally $p_i^{delayed}(t)$, as presented in (11). Likewise, $e_i^{max}(t)$ resulted in a situation where the BEV was charged immediately after a trip. Thus, the charging profile related to $e_i^{max}(t)$, $p_i^{immediate}(t)$, was defined as in (12). Importantly, both charging profiles $p_i^{delayed}(t)$ and $p_i^{immediate}(t)$ charged the same amount as the BEV consumed over the example week, i.e., the middle week of the three-week period. The difference in charged amounts of energy was then during single stops, but as the trips occurred in repetitive manner, in total the profiles charged the same amount. Thus, it can be considered that these profiles change the time of charging but not the amount, when considering the example week.

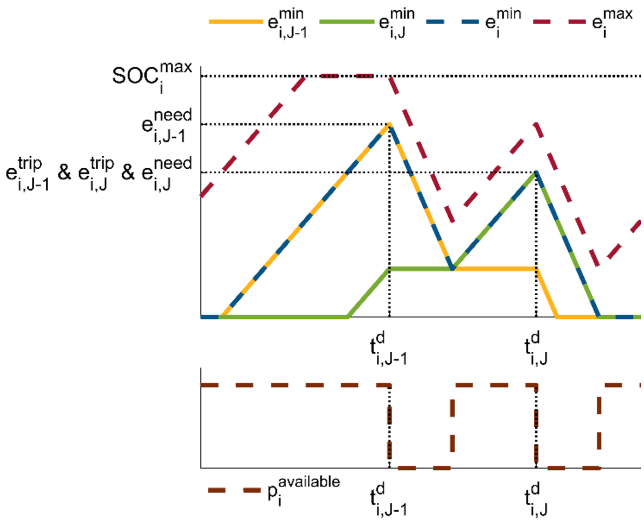


**FIGURE 4.** **The formulation of the minimum and maximum battery SoC levels for a single BEV (i) with two trips (j) with limited charging time between them.**

The two charging profiles were formed as described in (11) and (12) for the example week. As the calculations were conducted with a 1-minute interval, time steps between 10081 and 20160 were considered, i.e., from Monday to Sunday of the middle week of the three-week period. The consumption was added since during trips both the $e_i^{min}(t)$ and $e_i^{max}(t)$ decreased and thus the charging profiles would have been otherwise negative for these moments, whereas now they are zero.

$$p_i^{delayed}(t) = e_i^{min}(t) - e_i^{min}(t-1) + c_{i,j}(t), \quad 10081 \le t \le 20160 \quad (11)$$

$$p_i^{immediate}(t) = e_i^{max}(t) - e_i^{max}(t-1) + c_{i,j}(t), \quad 10081 \le t \le 20160 \quad (12)$$

### C. OTHER PARAMETERS CONSIDERED FOR CHARGING PROFILES

Electric vehicles' energy consumption rate, ECR, depends on several parameters, of which two major ones were considered in this study. These were the vehicle driving speed and the ambient temperature ($T^{amb}$), as their effect on the ECR is well studied in the existing literature. The effect of the driving speed was based on the studies presented in Table 2, from which a mean consumption rate, kWh/km, was determined from 10 km/h to 120 km/h.

The effect of the ambient temperature on the ECR was based on the studies presented in Table 3. The lowest consumption was in general determined to occur when the

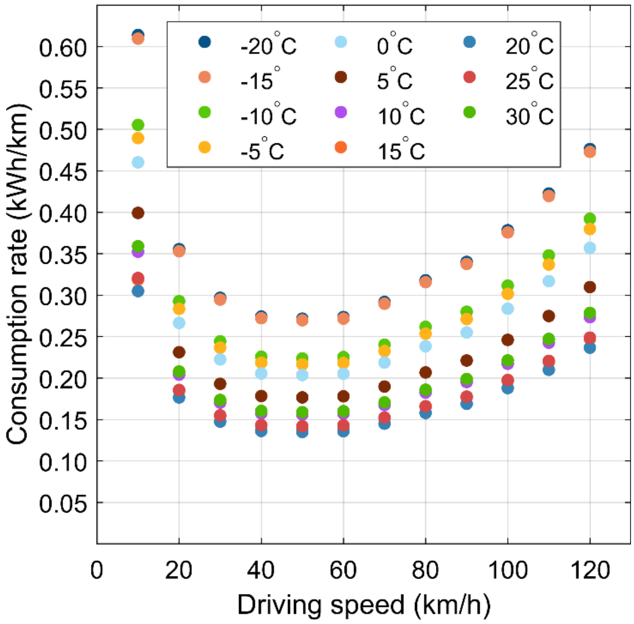


**FIGURE 5.** Electric vehicle energy consumption rate in terms of vehicle driving speed and ambient temperature, based on the mean values presented in Table 2 and Table 3 [13], [24], [37], [38], [39], [40], [44], [45], [46], [47].

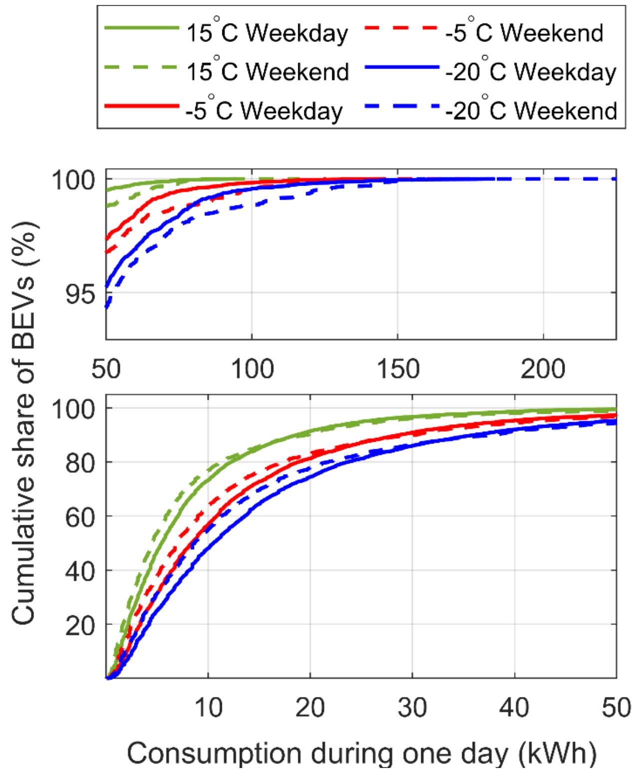


**FIGURE 6.** Cumulative share of electric vehicle's tank-to-wheel energy consumption during a week and weekend day.

ambient temperature was approximately 20°C, and thus it was chosen as the base value for which the other temperatures were compared to. This is also visible in Table 3, except for [37] where the consumption was lowest for 25°C. For the values in Table 3, which required conversion from the original studies, the original values are presented in Table 11 in Appendix A. Moreover, as presented in Table 3, the ECR increases when the temperature decreases, and may double at temperatures of −15°C and −20°C. This is due to increased cabin and battery heating [13], [37], [38], [39], [40], output energy losses [40], efficiency of regenerative braking [38], and increased air density [40]. Similarly with higher than 20°C temperatures, the ECR increases due to cabin and battery cooling needs [13], [39].

The BEV energy consumption rate for each of its trips was calculated such that the consumption rate based on the BEV's driving speed during the trip, from Table 2, was multiplied by the relative energy consumption rate based on the ambient temperature, from Table 3. For both, the mean values presented in Tables 2 and 3 were used, which were considered to represent well the generic ECR of a large-scale BEV fleet. Moreover, these energy consumption rates, considering both the vehicle driving speed and ambient temperature are presented in Fig. 5.

The consumption was examined with a typical summer (15°C) and winter (−5°C) temperatures in Finland, based on the monthly mean temperatures from 1991-2020, in the four climate zones in Finland [41], [42], which were weighted by the number of registered vehicles [43] in 2020, with minor effect, for each climate zone and rounded to the closest 5 degree Celsius. These are presented in Table 4. Moreover, a −20°C scenario was added to examine the charging profiles with very low temperature, as then the whole energy system is often under heavy loading. Between 2010-2020 there were on, vehicle weighted by the climate zones, average 118 hours annually, when the temperature in Finland was −20°C or lower [48].

Vehicle battery capacities chosen for this study are presented in Table 5. Of the battery capacity 80% was assumed to be possible to be operated in the analysis in Section II-B similar to [9]. In addition, three different capacities for the vehicle batteries were assumed, depending on the daily distance driven, thus assuming that a driver travelling longer distances would prefer a vehicle with higher battery capacity. Moreover, the charging was assumed linear, with an efficiency of 90%, as in [24] and [49].

## III. RESULTS

In the following subsections the results for the charging profiles are presented for the three different temperatures (15°C, −5°C, and −20°C) and for the three different charging power scenarios (Low, Medium, and High). The results are presented for active vehicles which were electrifiable in every scenario. The share of electrifiable vehicles was 88.6% without fast charging, and 93.9% with fast charging. Moreover,

**TABLE 2.** Electric vehicle energy consumption rate (kWh/km) in terms of vehicle driving speed (km/h).

| Driving speed (km/h) | | | | | | | | | | | | | | |
|---|---|---|---|---|---|---|---|---|---|---|---|---|---|---|
| 10 | 20 | 30 | 40 | 50 | 60 | 70 | 80 | 90 | 100 | 110 | 120 | $T^{amb}$ (°C) | S/M [a] | Source (year) |
| - | - | 0.11 | 0.10 | 0.10 | 0.11 | 0.11 | 0.13 | 0.14 | 0.16 | - | - | 15-25 | M | [38] (2022) |
| 0.35 | 0.23 | 0.19 | 0.17 | 0.17 | 0.17 | 0.18 | 0.18 | 0.19 | 0.21 | 0.22 | 0.24 | - | S | [45] (2021) |
| 0.26 | 0.22 | 0.20 | 0.18 | 0.17 | 0.17 | 0.18 | 0.19 | 0.20 | 0.22 | - | - | - | M | [44] (2017) |
| - | 0.08 | 0.09 | - | 0.10 | 0.12 | - | 0.15 | - | 0.18 | 0.21 | 0.25 | 22 | M | [47] [b] (2017) |
| - | - | - | - | - | 0.11 | 0.12 | 0.14 | 0.15 | 0.17 | 0.20 | 0.22 | - | M | [46] (2016) |
| 0.31 | 0.18 | 0.15 | 0.15 | 0.14 | 0.14 | 0.15 | 0.16 | 0.17 | 0.19 | 0.21 | 0.24 | | | Mean |

[a] Whether the values were based on simulations (S) or measurements (M).
[b] Original publication was in miles per hour, which was here converted to km/h.

**TABLE 3.** Electric vehicle relative energy consumption rate, compared to 20°C, in terms of ambient temperature.

| Ambient temperature (°C) | | | | | | | | | | | | |
|---|---|---|---|---|---|---|---|---|---|---|---|---|
| -20 | -15 | -10 | -5 | 0 | 5 | 10 | 15 | 20 | 25 | 30 | S/M [c] | Source (year) |
| - | - | - | - | 2.00 | 1.57 | 1.21 | 1.00 | 1.00 | 1.07 | 1.21 | M | [38] [d] (2022) |
| 1.32 | 1.27 | 1.22 | 1.17 | 1.12 | 1.07 | 1.02 | 1.00 | 1.00 | 1.13 | 1.23 | S | [13] (2019) |
| - | - | - | 1.92 | 1.69 | 1.31 | 1.15 | 1.08 | 1.00 | 1.08 | 1.23 | M | [40] [d] (2018) |
| 1.79 | - | 1.57 | - | 1.36 | - | 1.21 | - | 1.00 | - | 1.07 | S | [39] [d] (2018) |
| 2.94 | 2.94 | 2.24 | 1.87 | 1.55 | 1.37 | 1.19 | 1.08 | 1.00 | 0.91 | - | M | [37] [e] (2016) |
| 2.00 | 1.78 | 1.60 | 1.46 | 1.33 | 1.23 | 1.14 | 1.07 | 1.00 | 1.07 | 1.14 | Mix | [24] (2016) |
| 2.01 | 2.00 | 1.66 | 1.60 | 1.51 | 1.31 | 1.16 | 1.04 | 1.00 | 1.05 | 1.18 | | Mean |

[c] Whether the values were based on simulations (S) or measurements (M).
[d] Original publication presented consumption as kWh/km, which was here converted to relative values. Original values in Table 11 in Appendix A.
[e] Original publication studied maximum range with different temperatures. This was here converted to relative consumption values. Original values in Table 11 in Appendix A.

**TABLE 4.** Mean monthly temperature from 1991-2020 [42] for each climate zone in Finland [41] and their weighted mean by the number of registered light vehicles in each climate zone in 2020 [43].

| Climate zone (Weather station) | Month 1 | 2 | 3 | 4 | 5 | 6 | 7 | 8 | 9 | 10 | 11 | 12 |
|---|---|---|---|---|---|---|---|---|---|---|---|---|
| I (Vantaa) | -4.3 | -4.9 | -1.4 | 4.5 | 10.9 | 15.3 | 18.3 | 16.6 | 11.6 | 5.8 | 1.4 | -1.9 |
| II (Jokioinen) | -4.8 | -5.4 | -1.9 | 3.9 | 10.0 | 14.3 | 17.0 | 15.5 | 10.6 | 4.9 | 0.7 | -2.6 |
| III (Jyväskylä) | -7.3 | -7.6 | -3.5 | 2.5 | 9.1 | 14.0 | 16.7 | 14.6 | 9.4 | 3.6 | -0.9 | -4.5 |
| IV (Sodankylä) | -12.5 | -12.1 | -7.1 | -0.8 | 5.6 | 11.9 | 15.0 | 12.4 | 7.0 | 0.0 | -5.8 | -9.6 |
| Mean | -7.2 | -7.5 | -3.5 | 2.5 | 8.9 | 13.9 | 16.8 | 14.8 | 9.7 | 3.6 | -1.2 | -4.7 |
| Weighted mean | -5.8 | -6.3 | -2.5 | 3.4 | 9.7 | 14.3 | 17.1 | 15.3 | 10.3 | 4.4 | 0.0 | -3.4 |
| Rounded weighted mean | -5 | -5 | -5 | 5 | 10 | 15 | 15 | 15 | 10 | 5 | 0 | -5 |

**TABLE 5.** Electric vehicle battery capacity based on the daily driving distance.

| Daily driving distance (D) | Battery capacity Total (kWh) | Battery capacity Usable (kWh) |
|---|---|---|
| D < 100 km | 40 | 32 |
| 100 km ≤ D < 200 km | 70 | 56 |
| D ≥ 200 km | 100 | 80 |

the mean and standard deviation of the weekly time series for the charging load profiles, considering all the scenarios, are presented Appendix C in Table 12 and Table 13.

## A. CHARGING PROFILES

The daily tank-to-wheel energy consumption of the BEVs by different temperatures are presented in Fig. 6 for week and weekend days. Notably, even with ambient temperature of −20°C, nearly half of the BEVs consumed 10 kWh or less, and close to 80% 20 kWh or less, daily. To be precise, the mean daily energy consumptions during a weekday (and weekend) were 8.2 (7.9), 12.7 (12.2), and 15.9 (15.3) kWh with 15°C, −5°C, and −20°C respectively. Moreover, the mean distance driven by BEVs were 51.2 km during weekdays and 49.1 km on weekends. Thus, the mean ECR of the vehicles during a weekday (and weekend) were 16.1 (16.1), 24.8 (24.8), and 31.1 (31.2) kWh per 100 km,

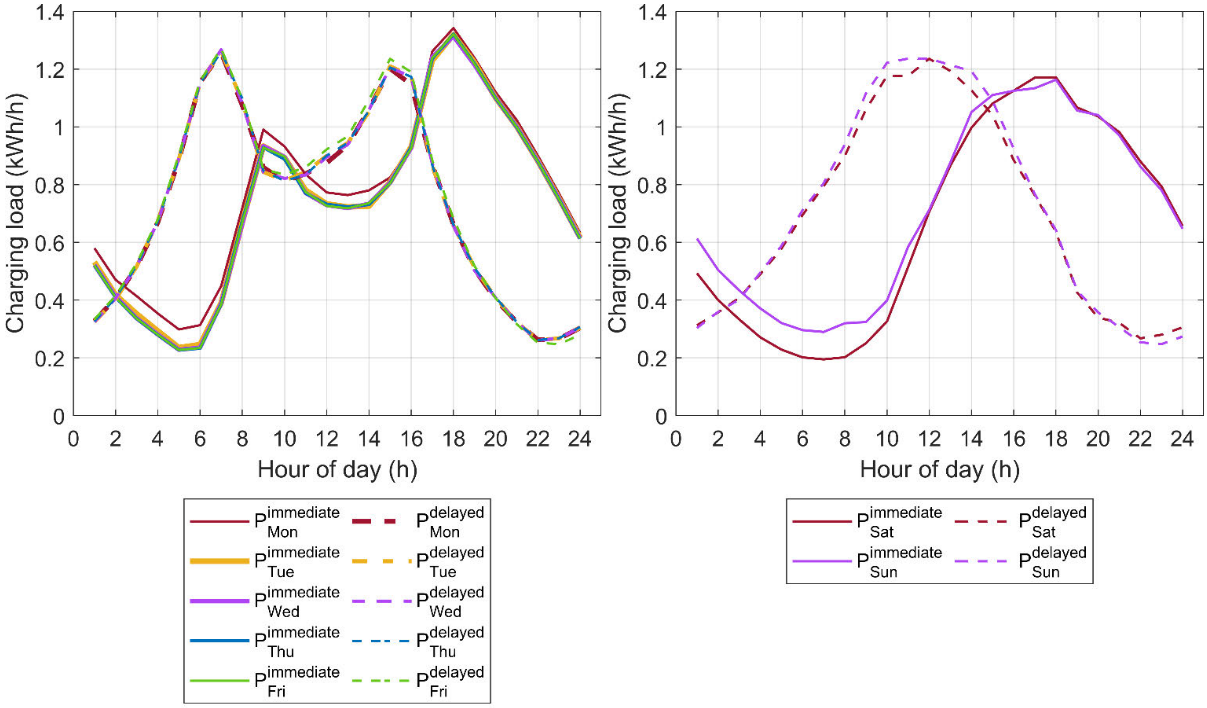


**FIGURE 7.** The hourly mean charging load for the $p^{immediate}$ and $p^{delayed}$ charging profiles for each week and weekend day with ambient temperature of −20°C and charging power scenario Low. Note that some of the lines have a slightly wider linewidth for better visibility. Moreover, all except Monday for $p^{immediate}$ are approximately on top each other, and likewise for all except Friday for $p^{delayed}$.

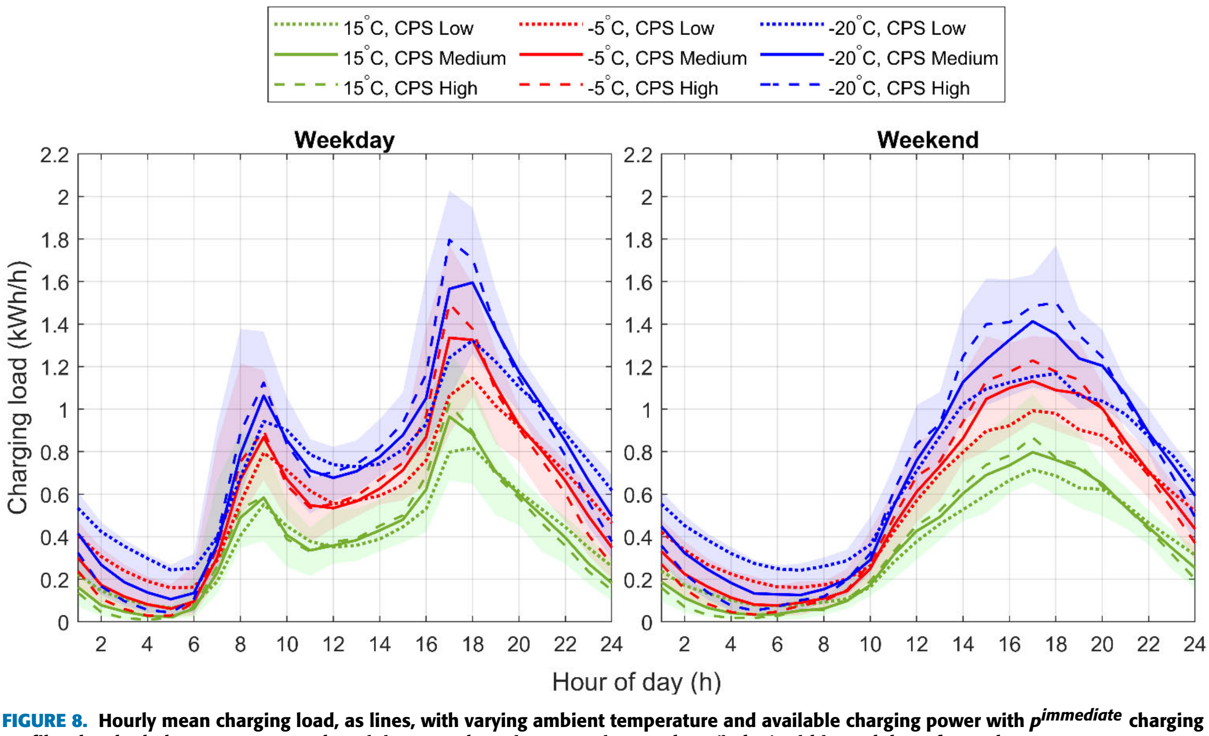


**FIGURE 8.** Hourly mean charging load, as lines, with varying ambient temperature and available charging power with $p^{immediate}$ charging profile. The shaded areas represent the minimum and maximum 1-minute values (in kW) within each hour for each temperature considering all the CPSs.

for 15°C, −5°C, and −20°C respectively. As presented in Section II-B-III, two charging profiles were formed for the BEVs: $p^{immediate}$ and $p^{delayed}$.

The hourly mean charging for both profiles are presented for each weekday and for Saturday and Sunday in Fig. 7. Although all weekdays used the same vehicle location

**TABLE 6.** Hourly mean peak charging load (kWh/h), the 1-minute mean peak load (kW), and the share of BEVs (%) charging simultaneously during the peak hour by ambient temperature and CPS.

| | Ambient temperature | | | | | | | | |
|---|---|---|---|---|---|---|---|---|---|
| | 15°C | | | -5°C | | | -20°C | | |
| | Charging power scenario | | | Charging power scenario | | | Charging power scenario | | |
| | Low | Medium | High | Low | Medium | High | Low | Medium | High |
| Peak hour, mean (kWh/h) | 0.81 | 0.97 | 1.03 | 1.14 | 1.34 | 1.50 | 1.32 | 1.60 | 1.80 |
| Peak hour, 1-min mean peak (kW) | 0.90 | 1.14 | 1.27 | 1.22 | 1.50 | 1.77 | 1.37 | 1.74 | 2.03 |
| Charging simultaneously (%) | 22.7 | 15.0 | 10.8 | 30.5 | 19.6 | 15.1 | 34.5 | 22.7 | 17.2 |

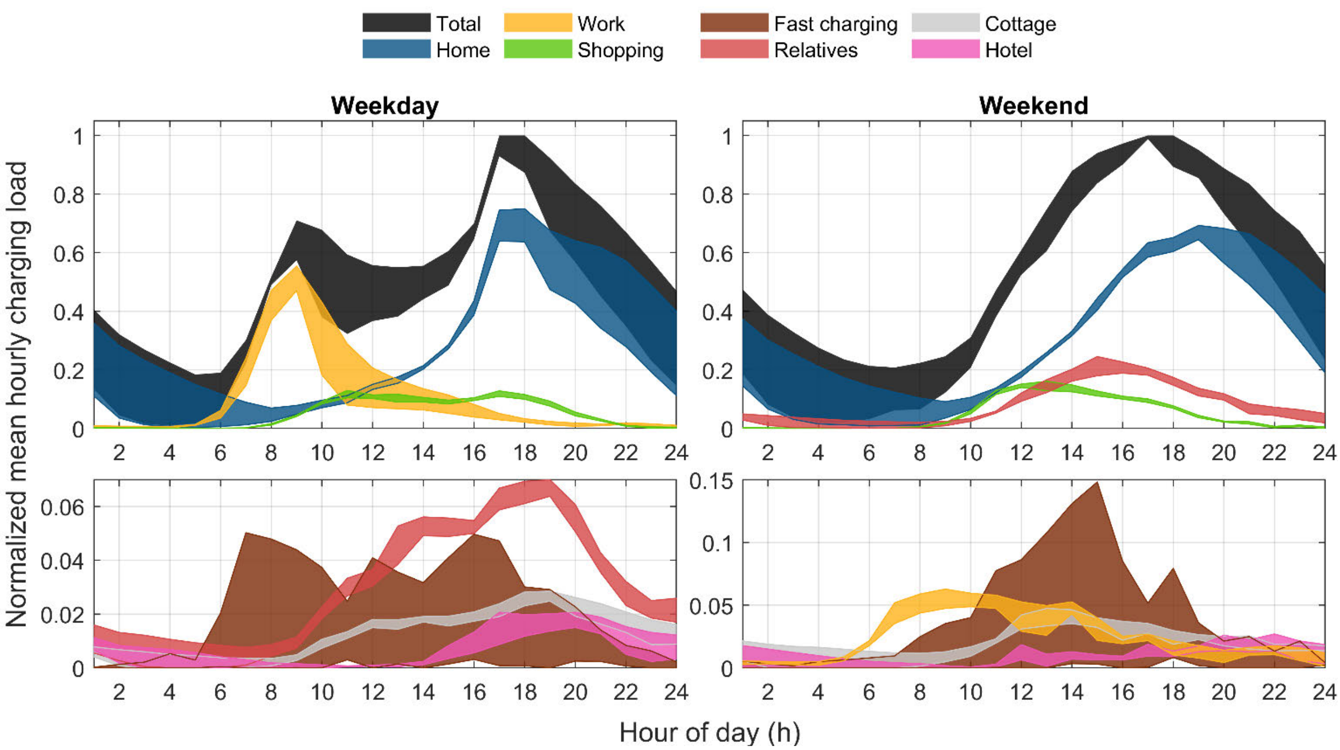


**FIGURE 9.** Normalized hourly mean charging in different locations during a mean week and weekend day. For each location, the shaded areas delimit the area in between which all the normalized values considering all the scenarios (temperature and CPS) fit into. Note, that both week and weekend days were normalized separately.

**TABLE 7.** Highest share of BEVs, from total, simultaneously charging at a location (CH) as %, and the summed 1-minute peak powers ($P_{peak}$) in kW for $p^{immediate}$ in the locations, divided by the total number of BEVs.

| | Ambient temperature | | | | | | | | | | | | | | | | | |
|---|---|---|---|---|---|---|---|---|---|---|---|---|---|---|---|---|---|---|
| | 15°C | | | | | | -5°C | | | | | | -20°C | | | | | |
| | Charging power scenario | | | | | | Charging power scenario | | | | | | Charging power scenario | | | | | |
| | Low | | Medium | | High | | Low | | Medium | | High | | Low | | Medium | | High | |
| Location | $P_{peak}$ | CH | $P_{peak}$ | CH | $P_{peak}$ | CH | $P_{peak}$ | CH | $P_{peak}$ | CH | $P_{peak}$ | CH | $P_{peak}$ | CH | $P_{peak}$ | CH | $P_{peak}$ | CH |
| Home | 0.68 | 18.5 | 0.87 | 12.0 | 0.94 | 8.70 | 0.89 | 24.2 | 1.14 | 15.7 | 1.32 | 12.2 | 1.01 | 27.5 | 1.34 | 18.3 | 1.50 | 13.8 |
| Work | 0.53 | 14.4 | 0.69 | 9.53 | 0.78 | 7.25 | 0.67 | 18.2 | 0.90 | 12.4 | 1.05 | 9.70 | 0.75 | 20.4 | 1.02 | 14.0 | 1.20 | 11.0 |
| Shopping & errands | 0.17 | 2.35 | 0.19 | 1.79 | 0.31 | 1.43 | 0.24 | 3.38 | 0.26 | 2.55 | 0.35 | 1.67 | 0.27 | 3.66 | 0.31 | 2.91 | 0.38 | 1.76 |
| Relatives & friends | 0.17 | 4.65 | 0.22 | 3.01 | 0.25 | 2.30 | 0.21 | 5.72 | 0.29 | 4.00 | 0.33 | 3.01 | 0.23 | 6.33 | 0.33 | 4.53 | 0.38 | 3.51 |
| Cottage | 0.04 | 1.13 | 0.04 | 0.58 | 0.06 | 0.50 | 0.05 | 1.38 | 0.07 | 1.02 | 0.07 | 0.66 | 0.06 | 1.68 | 0.08 | 1.12 | 0.09 | 0.82 |
| Hotel | 0.02 | 0.27 | 0.02 | 0.21 | 0.03 | 0.11 | 0.03 | 0.38 | 0.03 | 0.26 | 0.04 | 0.16 | 0.03 | 0.37 | 0.03 | 0.28 | 0.04 | 0.17 |
| Fast charging | 0.06 | 0.12 | 0.02 | 0.04 | 0.04 | 0.04 | 0.15 | 0.31 | 0.12 | 0.24 | 0.16 | 0.16 | 0.24 | 0.47 | 0.16 | 0.32 | 0.27 | 0.27 |

profiles, there were minor differences between Monday and the rest of the weekdays for $p^{immediate}$ due to the proximity of the weekend. Similarly for Saturday and Sunday. The profiles in Fig. 7 are presented for −20°C and CPS Low, as for it the summed absolute difference over a day between Monday and the rest of the weekdays, and between Saturday

**TABLE 8. Highest share of BEVs from total BEVs simultaneously at a location (%) and the share of BEVs visiting a location during a day (%).**

| | | Home | Work | Shopping & errands | Relatives & friends | Cottage | Hotel | FC [f] |
|---|---|---|---|---|---|---|---|---|
| Weekday | Simultaneously at | 92.73 | 38.72 | 5.18 | 4.54 | 2.07 | 0.57 | 0.22 |
| | Visiting a day | 97.62 | 46.57 | 42.49 | 13.83 | 3.76 | 0.83 | 2.80 |
| Weekend | Simultaneously at | 87.07 | 7.59 | 6.57 | 12.92 | 3.98 | 0.71 | 0.49 |
| | Visiting a day | 96.22 | 11.52 | 39.08 | 30.72 | 6.76 | 1.13 | 2.74 |

[f] Fast charging (FC) values for scenario -20°C and CPS Low as for it the values were the highest.

**TABLE 9. Coincidence factors per location by ambient temperature and charging power scenario.**

| | Ambient temperature | | | | | | | | |
|---|---|---|---|---|---|---|---|---|---|
| | 15°C | | | -5°C | | | -20°C | | |
| | Charging power scenario | | | Charging power scenario | | | Charging power scenario | | |
| Location | Low | Medium | High | Low | Medium | High | Low | Medium | High |
| Home | 0.188 | 0.121 | 0.088 | 0.247 | 0.158 | 0.123 | 0.281 | 0.186 | 0.140 |
| Work | 0.307 | 0.202 | 0.152 | 0.389 | 0.262 | 0.206 | 0.438 | 0.298 | 0.235 |
| Shopping & errands | 0.053 | 0.041 | 0.033 | 0.076 | 0.056 | 0.037 | 0.085 | 0.066 | 0.040 |
| Relatives & friends | 0.151 | 0.097 | 0.074 | 0.185 | 0.129 | 0.098 | 0.205 | 0.147 | 0.113 |
| Cottage | 0.165 | 0.086 | 0.074 | 0.203 | 0.147 | 0.090 | 0.249 | 0.165 | 0.117 |
| Hotel | 0.233 | 0.184 | 0.107 | 0.330 | 0.233 | 0.146 | 0.330 | 0.252 | 0.155 |
| Fast charging | 0.043 | 0.016 | 0.016 | 0.109 | 0.086 | 0.059 | 0.168 | 0.113 | 0.098 |

Shading: 0 ≤ white ≤ 0.10; 0.10 < light grey ≤ 0.20; 0.20 < dark grey

and Sunday, was the largest. From the figure the difference of the two profiles is clearly visible; the $p^{immediate}$ charges immediately after arrival, seen e.g. during weekdays as a peak after arriving to home from work in the afternoon, whereas the $p^{delayed}$ delays the charging as late as possible, seen e.g., as a peak before the departure from home to work during weekday mornings. Moreover, the charging profiles in Fig. 7, and all the consequent figures and tables, present the results from the grid's point of view, i.e., considering the charging efficiency of 90%.

In Fig. 8 the hourly mean charging load for $p^{immediate}$ is presented for the different ambient temperatures and charging power scenarios. The immediate charging profile was considered as the one, from the two, which the majority of BEV users would follow, since it assumed that the BEVs were charged when plugged in, whereas the delayed charging profile would require the drivers to time the charging exactly such that the vehicles would be charged as late as possible. This was considered unlikely, especially for charging which does not occur at home. That is, the $p^{immediate}$ charging profile corresponds to an uncontrolled charging profile. Nevertheless, the corresponding figure for $p^{delayed}$ is presented in Fig. 14 in Appendix B.

In addition to the hourly mean charging loads, presented as lines in Fig. 8, the maximum and minimum 1-minute power values within each hour are presented as the shaded areas in Fig. 8. These 1-minute values consider all the CPSs for each temperature. Moreover, in Table 6 the hourly mean peak charging load (kWh/h), for each scenario, is presented together with the mean peak 1-minute load (kW) within that peak hour. Overall, the mean charging load remained low compared to the available charging power, since the majority of BEVs did not charge simultaneously. This is highlighted in Table 6, where the shares of BEVs charging simultaneously

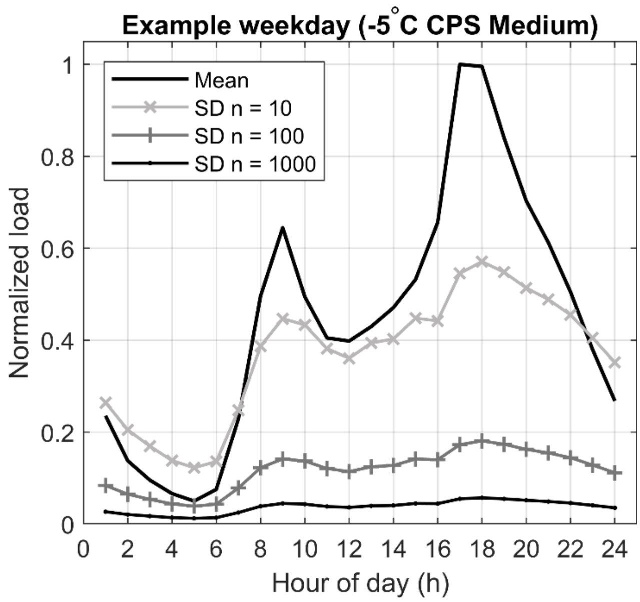


**FIGURE 10.** Normalized mean and standard deviation (SD) of a composite charging load by the number of groups (n) , representing electric vehicles with charging distributions, considered. Mean weekday with −5°C and CPS medium.

during the peak hours are presented. Furthermore, in Fig. 8, with lower available charging power the charging profiles were more even, whereas with higher available charging power there were larger differences between the peaks and valleys of charging.

In Fig. 9 the hourly normalized mean charging in different charging locations, for the $p^{immediate}$ charging profile, are presented for a mean week and weekend day. The shaded areas in the figure, per location, delimit the area in between

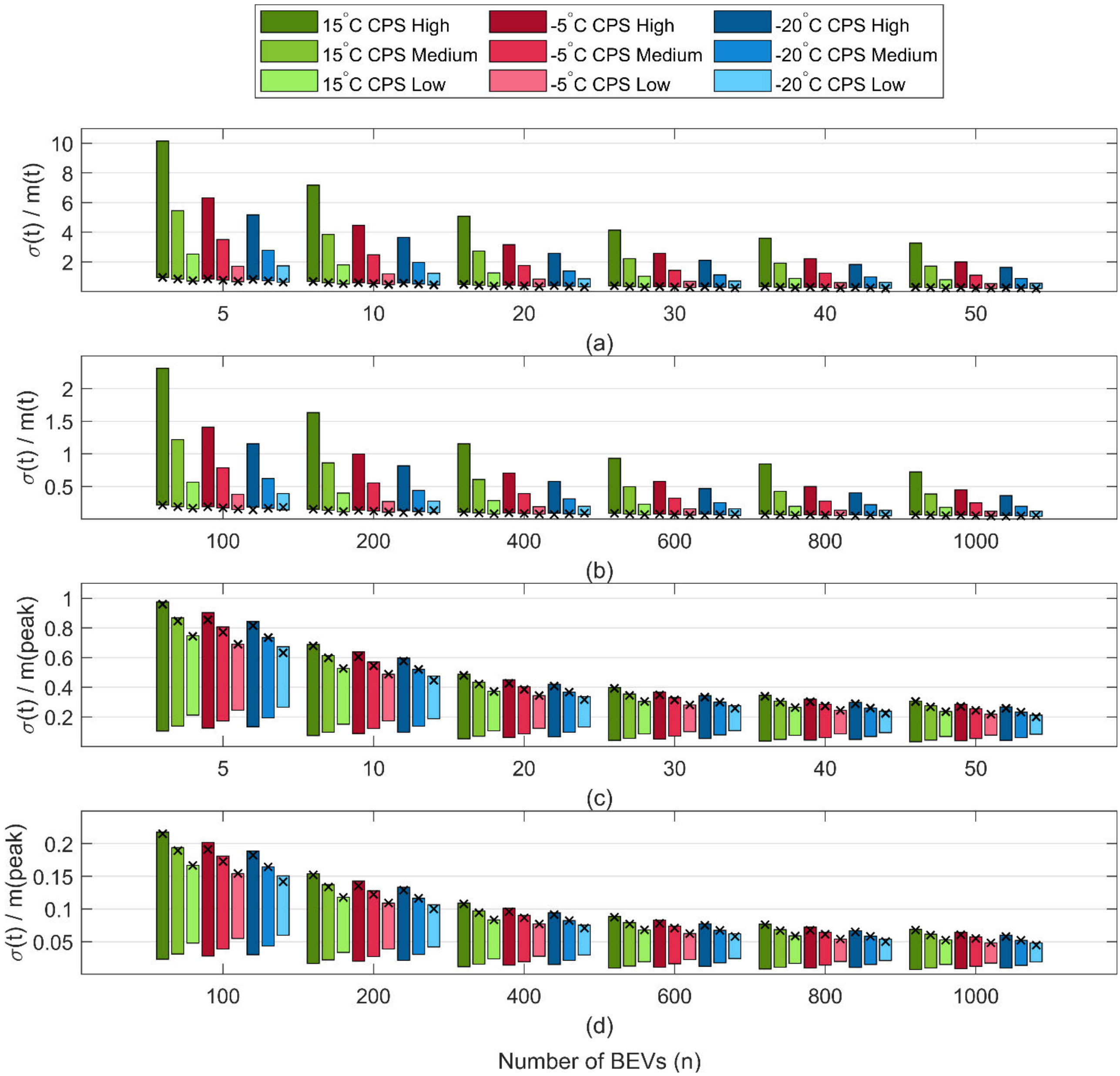


**FIGURE 11.** The share of standard deviation of a composite load ($\sigma$) compared to mean of a composite load ($m$) of the same hour by number of BEVs considered in a) and b). In c) and d) the share of composite SD to the composite mean of the peak hour during the day, by number of BEVs considered. Crosses represent the shares during peak hours. The shares are presented with bars in which all the hourly shares of the scenario fit into.

which all the normalized values, considering all the scenarios (temperatures and CPSs) fit into. During weekdays the peak in the morning is almost fully due to charging at work, and the peak in the afternoon largely due to charging at home. In the rest of the locations the charging load was significantly lower, and from them shopping and errands presented the highest charging load. Moreover, for fast charging the difference between the scenarios was considerable, seen as high vertical difference of the corresponding shaded area, as the number of BEVs required to utilize fast charging varied by temperature and CPS. During weekends, home charging dominated, and charging at relatives & friends and shopping & errands were the second and third most charged locations. Furthermore, also fast charging was notable with high variation.

### B. COINCIDENCE OF CHARGING IN CHARGING LOCATIONS

For energy system operation and planning, and especially for grid planning, the simultaneity of charging is highly important. By knowing the share of vehicles which charge simultaneously and the peak charging power, the requirement

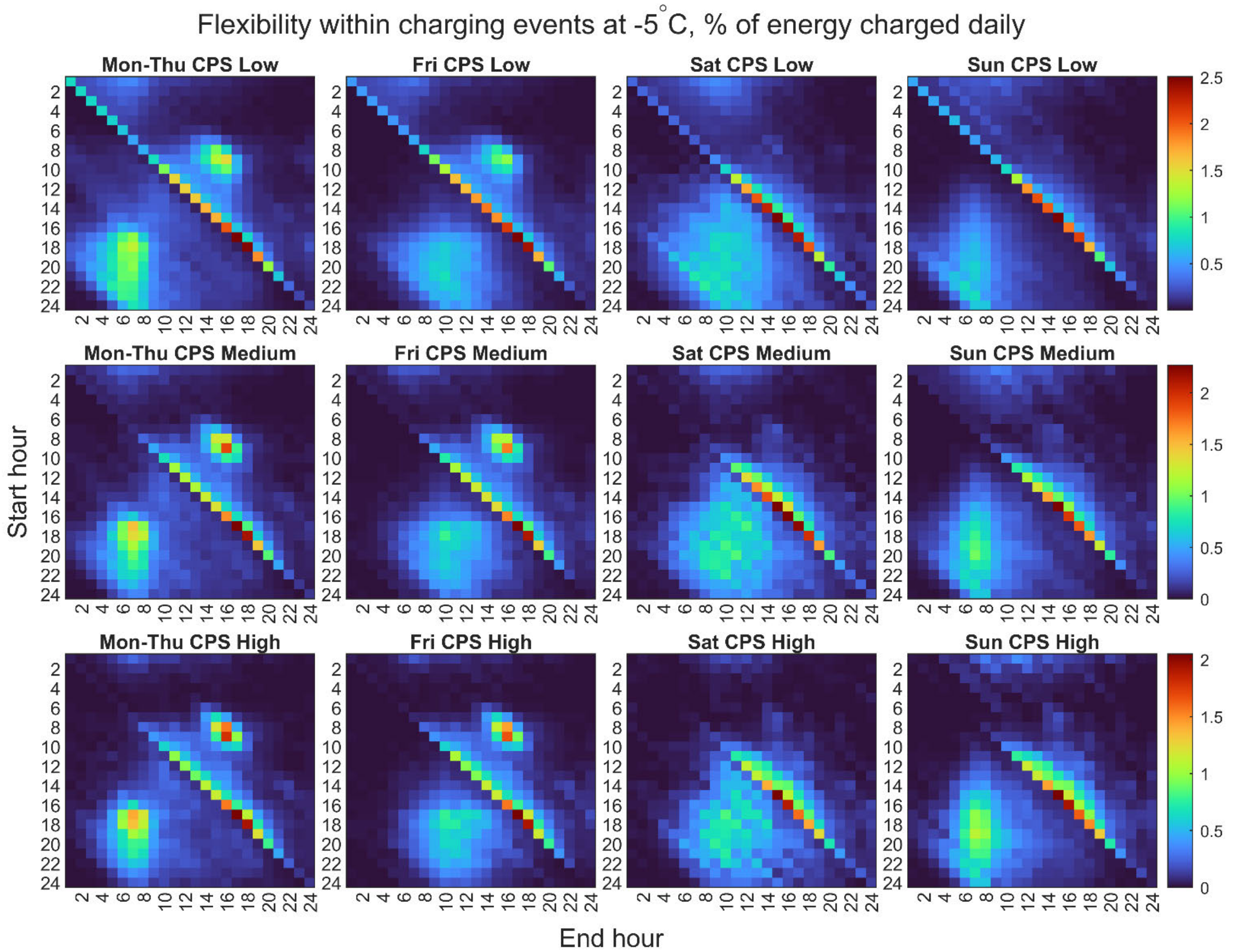


**FIGURE 12.** Flexibility within charging events represented as charging which can at most be shifted from start hour to end hour, as percentage of energy charged during a day with ambient temperature of −5°C. Monday to Thursday presented as a mean value of the respective days as they were nearly identical.

for the supply of charging power can be determined such that the charging demand can be fulfilled. In Table 7 the mean 1-minute peak powers, in kW, in the different charging locations are presented by ambient temperature and available charging power in the location. The mean peak powers were derived such that the summed peak powers for all the BEVs by location were divided by the total number of BEVs. Thus, the values in Table 7 are small for locations where the number of vehicles which charged in the location was low. Moreover, in Table 7 the maximum share of vehicles, from all BEVs, which charged simultaneously at each location is presented. These shares remained on a low level, and the highest share of BEVs charging in a particular location, 27.5%, was at home with −20°C and CPS Low.

The highest share of BEVs, which were simultaneously at a location, and the share of which visited a location during a week and weekend day, are presented in Table 8. From the values in Tables 7 and 8, the coincidence factors of the charging load per location type can be determined by temperature and CPS. In general, the coincidence factor is determined such that the peak power of a sum of loads is divided by the sum of individual peak loads. Here the summed peak load was as presented in Table 7, and the summed individual peak load was determined as share of BEVs visiting a location during a day times the available charging power in that location. The coincidence factors for each location are presented in Table 9. The available charging power affected the coincidence factors the most, as with a lower CPS they were the highest. Moreover, for lower ambient temperature, i.e., higher consumption, the coincidence factors increased. Furthermore, the factors were the highest for charging at work, at hotel, and at home.

### C. DEVIATION OF CHARGING

As presented previously, the coincidence of charging remained rather low, and such did the mean charging loads

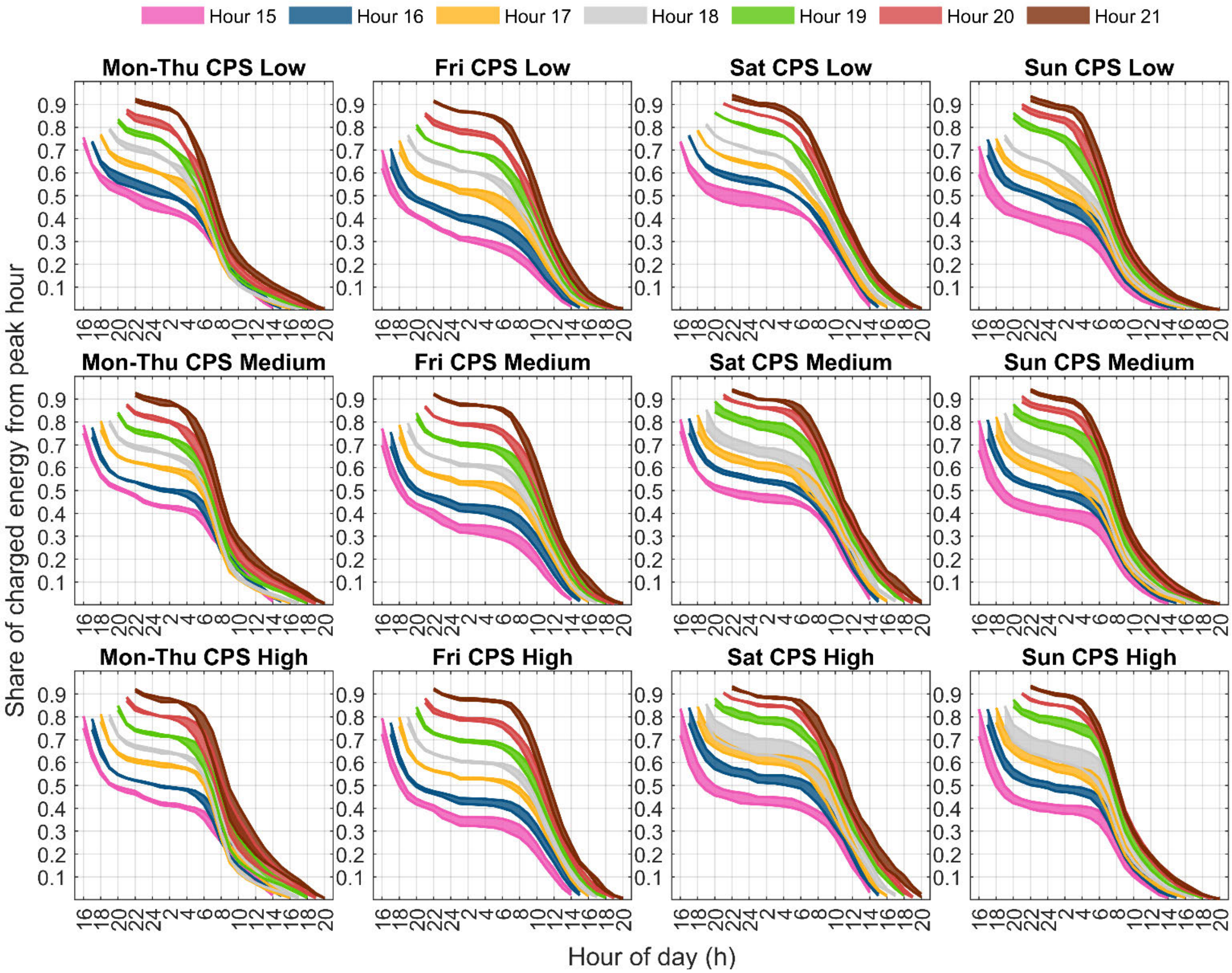


**FIGURE 13.** Share of charged energy, in the $p^{immediate}$ charging profile, during hours 15 to 21 which could be shifted at most to the following hours within charging events, presented for each evening hour. The shaded areas delimit the area in between which all the scenarios considering the ambient temperatures of 15°C, −5°C, and −20°C for each CPS fit into. Mon-Thu presents the mean values from Mondays to Thursdays. Note that hours from 1 to 20 refer to the next day from the header. For example, hour 2 on the Fri CPS Low graph refers to hour 2 on Saturday morning.

compared to the available charging power. Thus, the deviation of individual charging loads from the mean load was high. To analyze the standard deviation (SD) of a composite load of different number of BEVs, the BEVs were divided into groups which represented an electric vehicle as a variable with a distribution of charging for each hour. In other words, the total BEVs N were divided into n groups, with N/n BEVs in each group, and the BEVs in a group formed the distribution of charging for the group, which represented an electric vehicle. For these groups, the composite load mean ($m$) and standard deviation ($\sigma$) were calculated as in (13) and (14) [50], where $m_k$ and $\sigma_k$ are the mean and SD of a single group of BEVs and $\rho_{k,l}$ the correlation between two groups. In them, k and l represent the groups of vehicles. In Fig. 10, an example is given where the normalized composite mean and standard deviations are presented for different number of vehicles considered (n), represented by the aforementioned groups. There the absolute SD is the highest during the peak hour, but compared to the mean, the lowest. Moreover, in Fig. 10, the normalized mean was the same for all n, whereas the non-normalized mean, for example, for n = 100 was tenfold compared to n = 10.

$$m = \sum_{k=1}^{n} m_k \tag{13}$$

$$\sigma^2 = \sum_{k=1}^{n} \sum_{l=1}^{n} \sigma_k \sigma_l \rho_{k,l} \tag{14}$$

The mean and SD for a composite load were calculated for each scenario and the results presented in Fig. 11. In Fig. 11 a) and b) the share of composite SD to the composite mean of the same hour, by the number of vehicles, n, considered is displayed. In addition, as this share varied for every hour, as in Fig. 10, for each scenario the share is presented with a bar in which all the hourly shares fit into. Furthermore, the shares during peak hours are presented

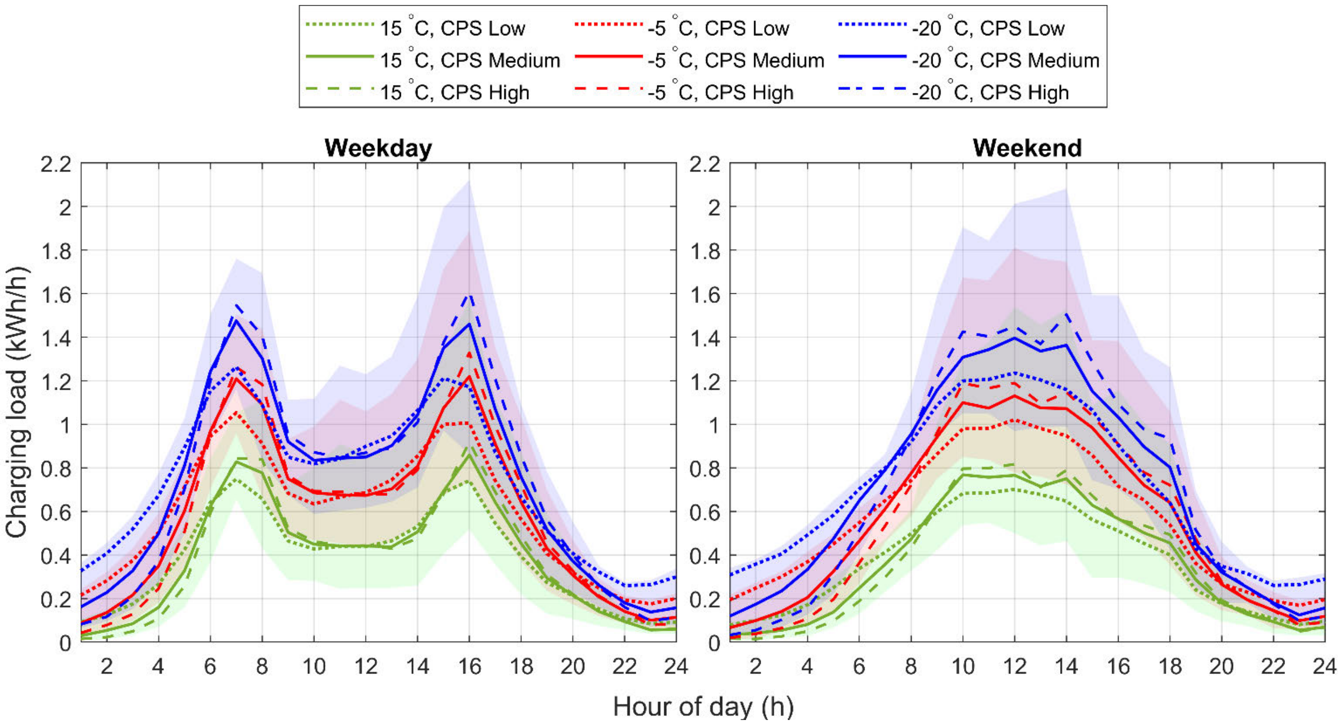


**FIGURE 14.** Hourly mean charging load, as lines, with varying ambient temperature and available charging power with $p^{delayed}$ charging profile. The shaded areas represent the minimum and maximum 1-minute values within each hour for each temperature considering all the CPSs.

**TABLE 10.** The grouping of all possible type locations as in the national household travel survey into groups of locations used in this study.

| Location type | Location number | Location group |
|---|---|---|
| Home | 1 | 1 |
| Other permanent residence | 2 | 1 |
| Workplace (primary) | 3 | 3 |
| Workplace (secondary) | 4 | 3 |
| Other work site | 5 | 5 |
| Educational building | 6 | 6 |
| Day care center | 7 | 6 |
| Stop for pick up or drop off | 8 | 6 |
| Grocery store | 9 | 9 |
| Bank/medical care/postal service, hairdresser etc. | 10 | 9 |
| Shopping center | 11 | 9 |
| Other place of purchase | 12 | 12 |
| Restaurant/café etc. | 13 | 12 |
| Pub/bar/night club | 14 | 12 |
| Sports or recreational area | 15 | 15 |
| Unbuilt nature area | 16 | 15 |
| Visit to relatives or friends | 18 | 18 |
| Cultural center | 19 | 15 |
| Summer cottage or vacation home | 20 | 20 |
| Other leisure time destination | 21 | 15 |
| Hotel or motel | 22 | 22 |
| Other destination | 23 | 23 |

with crosses, and they represent the lowest values for each scenario. In Fig. 11 c) and d) the share of composite SD to the composite mean of the peak hour during the day is presented, by number of vehicles considered. Again, for each scenario, the share is presented with a bar in which all the hourly shares fit into, and crosses represent the values during the peak hours. The peak hour values were in c) and d) almost always the highest values presented by the bars, but if not, nearly the highest. This means that during some hour (often +1h or −1h to the peak hour) the absolute SD was greater than during the peak hour. Moreover, the shares in c) and d) were significantly lower, compared to the ones in a) and b), highlighting that the composite SD at every hour was low compared to the composite mean of the peak hour. For both comparisons the shares decreased significantly as the number of vehicles increased, and for 1000 BEVs, when comparing to the peak hours in c) and d), the highest shares for CPS High were 0.069, 0.064, and 0.060 for 15°C, −5°C, and −20°C, respectively. The values in Fig. 11 considered a mean weekday as then the peak power was the greatest. For attaining the SD of a composite load, the correlations between groups of BEVs were determined, which were greater for groups with small amounts of BEVs, but always lower than 0.021 and greater than −0.019.

### D. FLEXIBILITY OF CHARGING WITHIN CHARGING EVENTS

As the $p^{immediate}$ charging profile charged immediately after arrival, it was possible to determine the charging which could be shifted within each charging event. This is visualized by matrixes in Fig. 12, where the mean amount of charging that could be shifted from 'Start hour' i.e., from hour where the charging would occur in $p^{immediate}$, to 'End hour', which represents the last hour where the charging could be shifted.

**TABLE 11.** Electric vehicle energy consumption rate (ECR) in terms of ambient temperature. Original values and the conversion to relative values, which are presented in Table 3 in Section II-C.

Values as in the original studies

| | | Ambient temperature T in °C | | | | | | | | | | | |
|---|---|---|---|---|---|---|---|---|---|---|---|---|---|
| Value | Unit | -20 | -15 | -10 | -5 | 0 | 5 | 10 | 15 | 20 | 25 | 30 | Source |
| ECR | kWh/km | - | - | - | - | 0.28 | 0.22 | 0.17 | 0.14 | 0.14 | 0.15 | 0.17 | [38] |
| ECR | kWh/km | - | - | - | 0.25 | 0.22 | 0.17 | 0.15 | 0.14 | 0.13 | 0.14 | 0.16 | [40] |
| ECR | kWh/km | 0.25 | - | 0.22 | - | 0.19 | - | 0.17 | - | 0.14 | - | 0.15 | [39] |
| Range, EV1 | km | 50 | 50 | 65 | 80 | 95 | 110 | 125 | 140 | 150 | 165 | - | [37] |
| Range, EV2 | km | 45 | 45 | 60 | 70 | 85 | 95 | 110 | 120 | 130 | - | - | [37] |

Relative consumption rate compared to 20°C

| | | Ambient temperature T in °C | | | | | | | | | | | |
|---|---|---|---|---|---|---|---|---|---|---|---|---|---|
| Value | Calculated as | -20 | -15 | -10 | -5 | 0 | 5 | 10 | 15 | 20 | 25 | 30 | Source |
| Relative ECR | ECR(T)/ECR(20°C) | - | - | - | - | 2.00 | 1.57 | 1.21 | 1.00 | 1.00 | 1.07 | 1.21 | [38] |
| Relative ECR | ECR(T)/ECR(20°C) | - | - | - | 1.92 | 1.69 | 1.31 | 1.15 | 1.08 | 1.00 | 1.08 | 1.23 | [40] |
| Relative ECR | ECR(T)/ECR(20°C) | 1.79 | - | 1.57 | - | 1.36 | - | 1.21 | - | 1.00 | - | 1.07 | [39] |
| Relative ECR, EV1 | Range(T)/Range(20°C) | 3.00 | 3.00 | 2.31 | 1.88 | 1.58 | 1.36 | 1.20 | 1.07 | 1.00 | 0.91 | - | [37] |
| Relative ECR, EV2 | Range(T)/Range(20°C) | 2.89 | 2.89 | 2.17 | 1.86 | 1.53 | 1.37 | 1.18 | 1.08 | 1.00 | - | - | [37] |
| Relative ECR, Mean | (EV1 + EV2)/2 | 2.94 | 2.94 | 2.24 | 1.87 | 1.55 | 1.37 | 1.19 | 1.08 | 1.00 | 0.91 | - | [37] |

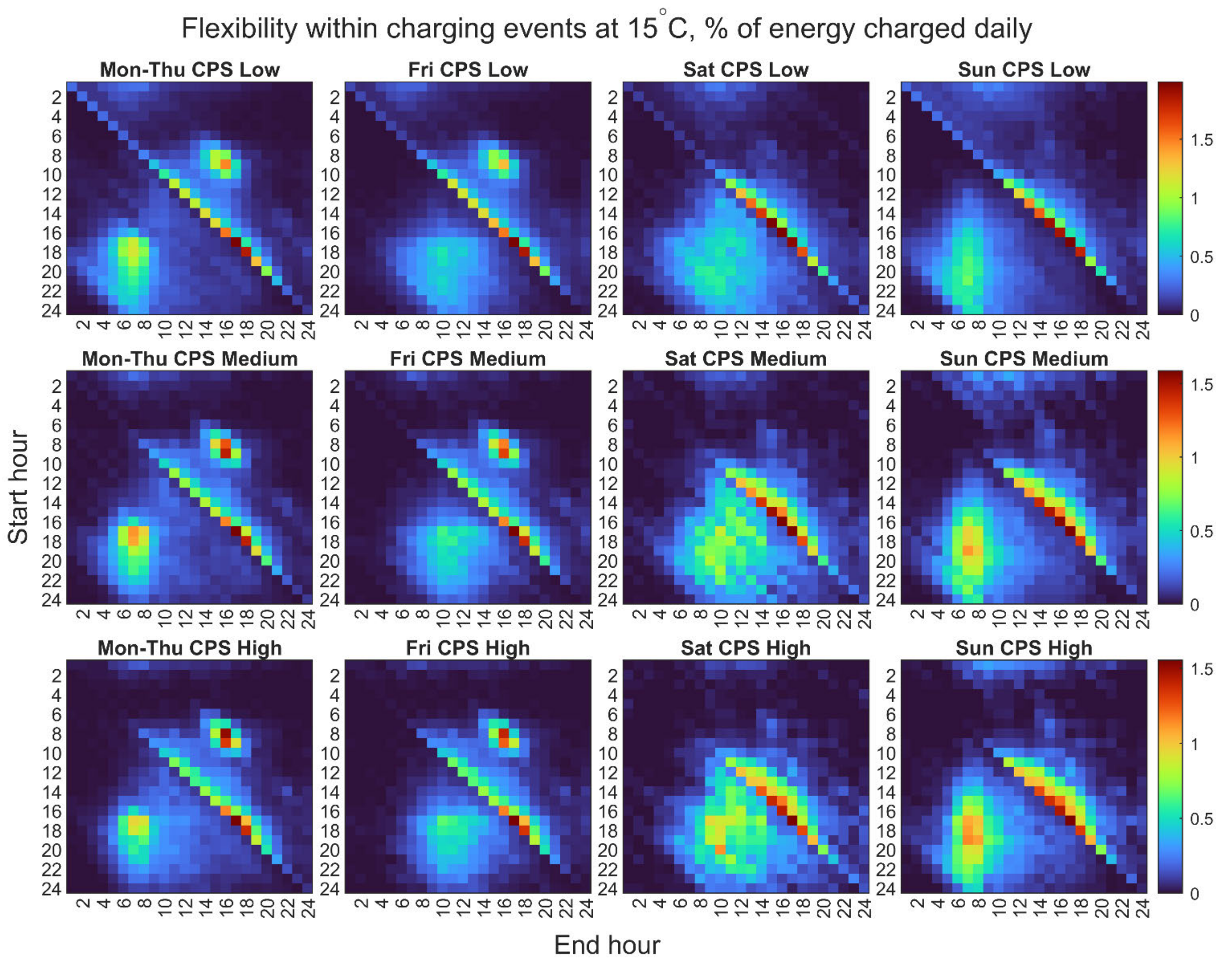


**FIGURE 15.** Flexibility within charging events represented as charging which can at most be shifted from start hour to end hour, as percentage of energy charged during a day with ambient temperature of 15°C. Monday to Thursday presented as a mean value of the respective days as they were nearly identical.

Thus, these amounts represent the flexibility of charging within charging events. In other words, they must be charged between the 'Start' and 'End' hours. The values in the matrixes in Fig. 12 represent the share of the daily charged energy during Monday to Thursday (mean), Friday, Saturday, and Sunday, with ambient temperature of −5°C for each CPS.

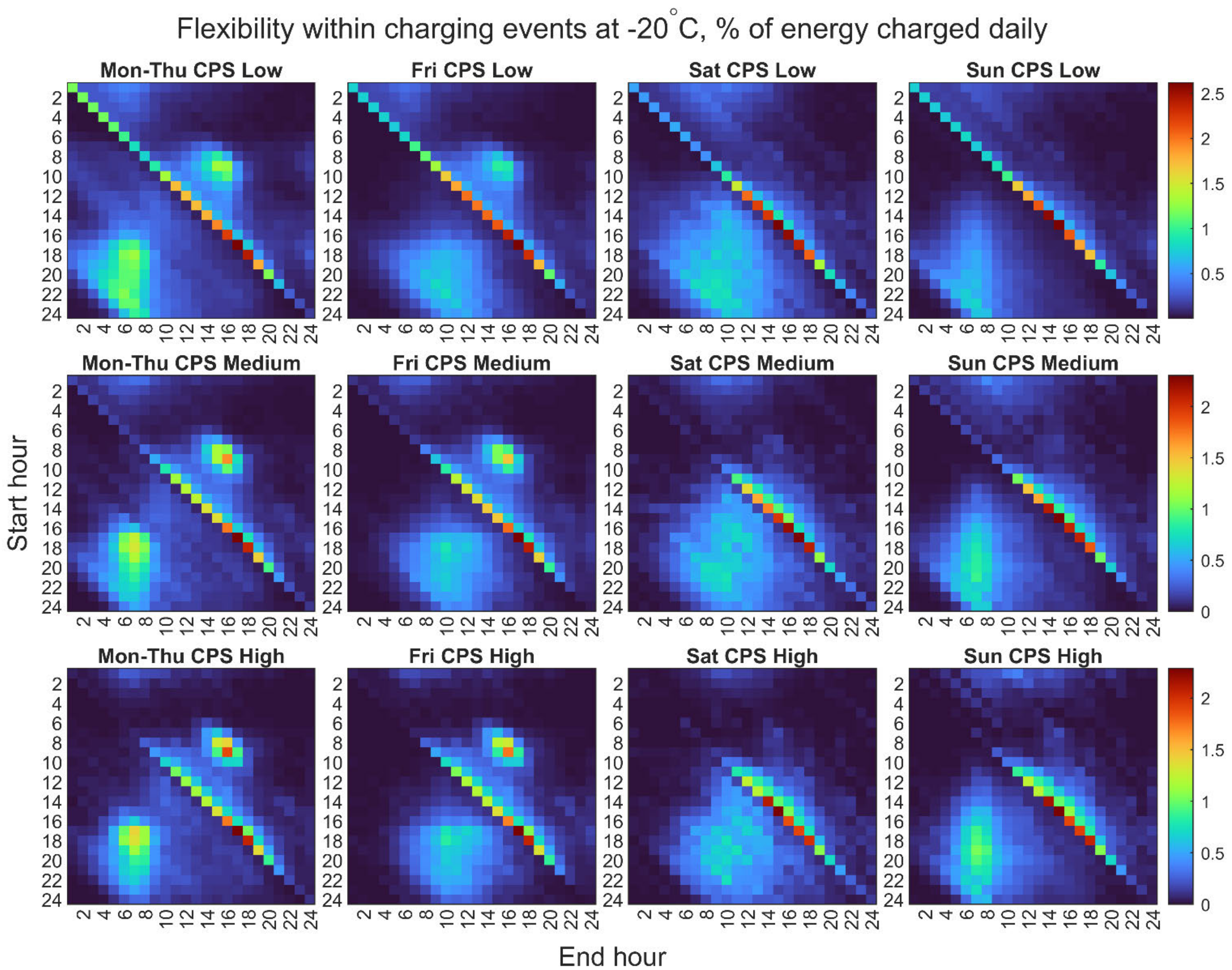


**FIGURE 16.** Flexibility within charging events represented as charging which can at most be shifted from start hour to end hour, as percentage of energy charged during a day with ambient temperature of −20°C. Monday to Thursday presented as a mean value of the respective days as they were nearly identical.

Corresponding figures for 15°C and −20°C are presented in Appendix [DCLseclabel9]B in Fig. 15 and 16. In Fig. 12 several clusters can be identified:

- Non-shiftable charging on the diagonal
- Charging which could be shifted a few hours forward as data points just above the diagonal
- Shiftable charging during common office hours from morning to afternoon on Monday to Friday
- Shiftable charging during night, i.e., from afternoon and evening to morning on all days

Moreover, and unsurprisingly, when the following day is a weekday, e.g. on Sunday, the shiftable charging overnight must be charged earlier compared to when the following day is a weekend day. In addition, with higher available charging power the clusters identified were slightly more concentrated and the non-shiftable charging during the night decreased.

The peak BEV charging load, with the $p^{immediate}$ charging profile, occurred during the evening hours, which is when there usually is higher power demand in the rest of the energy system too. Thus, from Fig. 12 the share of charging during peak hours which could be shifted forward can be further examined. In Fig. 13, the share of charged energy during the evening peak hours, from 15 to 21, which could be shifted at most to the following hours, is presented for each of the evening hours. The shaded areas delimit the area in between which all the scenarios considering the ambient temperatures for each CPS fit into. Thus, it includes data presented for 15°C in Fig. 15 and −20°C in Fig. 16 in Appendix B. For example, from Fig. 13 it can be determined that during Mondays to Thursdays, from hour 16 with CPS medium, approximately 75% of the charged energy can be shifted to hour 17, 50% to hour 2 the next day, and 30% to hour 7 the next day. Moreover, in Fig. 13. it is further visible that when the following day

**TABLE 12.** Mean and standard deviation (SD) of $p^{immediate}$ charging profile over the example week with 1-hour resolution by ambient temperature and charging power scenario Low (L), Medium (M), and High (H).

| | Ambient temperature | | | | | | | | | | | | | | | | | |
|---|---|---|---|---|---|---|---|---|---|---|---|---|---|---|---|---|---|---|
| | 15°C | | | | | | -5°C | | | | | | -20°C | | | | | |
| | Charging power scenario | | | | | | Charging power scenario | | | | | | Charging power scenario | | | | | |
| | L | L | M | M | H | H | L | L | M | M | H | H | L | L | M | M | H | H |
| h | Mean | SD | Mean | SD | Mean | SD | Mean | SD | Mean | SD | Mean | SD | Mean | SD | Mean | SD | Mean | SD |
| 1 | 0.275 | 0.950 | 0.238 | 1.230 | 0.208 | 1.365 | 0.463 | 1.216 | 0.392 | 1.584 | 0.333 | 1.771 | 0.580 | 1.335 | 0.516 | 1.827 | 0.434 | 2.045 |
| 2 | 0.199 | 0.829 | 0.138 | 0.956 | 0.072 | 0.796 | 0.358 | 1.086 | 0.262 | 1.342 | 0.176 | 1.305 | 0.470 | 1.231 | 0.367 | 1.569 | 0.259 | 1.603 |
| 3 | 0.160 | 0.748 | 0.081 | 0.726 | 0.026 | 0.447 | 0.289 | 0.982 | 0.197 | 1.155 | 0.091 | 0.915 | 0.414 | 1.176 | 0.281 | 1.379 | 0.154 | 1.219 |
| 4 | 0.126 | 0.665 | 0.053 | 0.588 | 0.013 | 0.325 | 0.243 | 0.913 | 0.142 | 0.975 | 0.047 | 0.625 | 0.354 | 1.106 | 0.214 | 1.202 | 0.079 | 0.847 |
| 5 | 0.106 | 0.593 | 0.043 | 0.508 | 0.018 | 0.332 | 0.216 | 0.860 | 0.098 | 0.780 | 0.033 | 0.497 | 0.298 | 1.003 | 0.157 | 1.000 | 0.055 | 0.678 |
| 6 | 0.113 | 0.571 | 0.071 | 0.494 | 0.069 | 0.491 | 0.214 | 0.837 | 0.116 | 0.727 | 0.094 | 0.666 | 0.313 | 1.266 | 0.173 | 0.960 | 0.112 | 0.771 |
| 7 | 0.218 | 0.706 | 0.233 | 0.860 | 0.262 | 0.982 | 0.331 | 1.065 | 0.315 | 1.108 | 0.351 | 1.294 | 0.447 | 1.557 | 0.385 | 1.341 | 0.398 | 1.440 |
| 8 | 0.426 | 0.954 | 0.492 | 1.298 | 0.532 | 1.506 | 0.594 | 1.434 | 0.677 | 1.660 | 0.755 | 1.997 | 0.719 | 1.682 | 0.795 | 1.860 | 0.893 | 2.325 |
| 9 | 0.567 | 1.113 | 0.586 | 1.454 | 0.592 | 1.645 | 0.815 | 1.595 | 0.866 | 1.874 | 0.902 | 2.223 | 0.990 | 2.049 | 1.069 | 2.215 | 1.125 | 2.630 |
| 10 | 0.468 | 1.096 | 0.413 | 1.272 | 0.395 | 1.394 | 0.747 | 1.516 | 0.673 | 1.820 | 0.649 | 2.000 | 0.933 | 1.830 | 0.862 | 2.062 | 0.843 | 2.434 |
| 11 | 0.395 | 1.107 | 0.341 | 1.156 | 0.334 | 1.279 | 0.649 | 1.531 | 0.558 | 1.675 | 0.544 | 2.006 | 0.837 | 1.778 | 0.726 | 2.042 | 0.693 | 2.214 |
| 12 | 0.370 | 0.994 | 0.360 | 1.152 | 0.378 | 1.353 | 0.595 | 1.540 | 0.540 | 1.531 | 0.558 | 1.807 | 0.773 | 1.656 | 0.690 | 1.919 | 0.712 | 2.339 |
| 13 | 0.369 | 0.943 | 0.387 | 1.228 | 0.395 | 1.399 | 0.589 | 1.334 | 0.574 | 1.665 | 0.596 | 1.944 | 0.765 | 1.775 | 0.713 | 1.876 | 0.746 | 2.402 |
| 14 | 0.398 | 0.976 | 0.434 | 1.287 | 0.454 | 1.489 | 0.598 | 1.305 | 0.633 | 1.718 | 0.675 | 2.048 | 0.781 | 1.854 | 0.782 | 2.078 | 0.825 | 2.329 |
| 15 | 0.452 | 1.093 | 0.483 | 1.388 | 0.503 | 1.639 | 0.667 | 1.517 | 0.715 | 1.880 | 0.751 | 2.179 | 0.826 | 1.834 | 0.879 | 2.179 | 0.941 | 2.716 |
| 16 | 0.539 | 1.106 | 0.625 | 1.480 | 0.690 | 1.819 | 0.768 | 1.458 | 0.871 | 1.841 | 0.974 | 2.372 | 0.935 | 1.827 | 1.049 | 2.192 | 1.168 | 2.694 |
| 17 | 0.803 | 1.294 | 0.967 | 1.824 | 1.027 | 2.197 | 1.078 | 1.646 | 1.333 | 2.257 | 1.499 | 2.867 | 1.261 | 2.001 | 1.565 | 2.578 | 1.792 | 3.266 |
| 18 | 0.823 | 1.367 | 0.884 | 1.871 | 0.896 | 2.224 | 1.156 | 1.796 | 1.332 | 2.459 | 1.375 | 2.968 | 1.341 | 1.900 | 1.601 | 2.695 | 1.716 | 3.443 |
| 19 | 0.711 | 1.347 | 0.707 | 1.746 | 0.691 | 2.050 | 1.027 | 1.700 | 1.114 | 2.341 | 1.093 | 2.773 | 1.239 | 1.988 | 1.381 | 2.674 | 1.380 | 3.222 |
| 20 | 0.616 | 1.366 | 0.602 | 1.699 | 0.586 | 1.917 | 0.934 | 1.676 | 0.928 | 2.157 | 0.911 | 2.543 | 1.120 | 1.801 | 1.182 | 2.467 | 1.151 | 2.973 |
| 21 | 0.532 | 1.294 | 0.503 | 1.611 | 0.466 | 1.769 | 0.824 | 1.513 | 0.807 | 2.085 | 0.763 | 2.413 | 1.023 | 1.698 | 1.016 | 2.282 | 0.968 | 2.712 |
| 22 | 0.449 | 1.179 | 0.398 | 1.444 | 0.360 | 1.552 | 0.715 | 1.443 | 0.665 | 1.910 | 0.607 | 2.199 | 0.900 | 1.530 | 0.850 | 2.138 | 0.786 | 2.488 |
| 23 | 0.351 | 1.071 | 0.276 | 1.235 | 0.238 | 1.328 | 0.599 | 1.325 | 0.500 | 1.706 | 0.410 | 1.828 | 0.770 | 1.526 | 0.668 | 1.986 | 0.568 | 2.195 |
| 24 | 0.263 | 0.922 | 0.183 | 1.049 | 0.149 | 1.081 | 0.474 | 1.215 | 0.352 | 1.481 | 0.270 | 1.550 | 0.634 | 1.377 | 0.503 | 1.776 | 0.380 | 1.857 |
| 25 | 0.210 | 0.830 | 0.144 | 0.929 | 0.120 | 0.997 | 0.398 | 1.128 | 0.278 | 1.319 | 0.215 | 1.408 | 0.533 | 1.279 | 0.391 | 1.574 | 0.297 | 1.675 |
| 26 | 0.132 | 0.681 | 0.063 | 0.645 | 0.039 | 0.623 | 0.300 | 1.002 | 0.151 | 1.008 | 0.091 | 0.967 | 0.419 | 1.165 | 0.244 | 1.286 | 0.144 | 1.205 |
| 27 | 0.093 | 0.575 | 0.040 | 0.524 | 0.014 | 0.324 | 0.233 | 0.893 | 0.099 | 0.825 | 0.052 | 0.713 | 0.354 | 1.152 | 0.163 | 1.053 | 0.083 | 0.901 |
| 28 | 0.070 | 0.505 | 0.021 | 0.356 | 0.010 | 0.266 | 0.182 | 0.796 | 0.067 | 0.670 | 0.024 | 0.442 | 0.295 | 1.059 | 0.119 | 0.901 | 0.050 | 0.679 |
| 29 | 0.057 | 0.452 | 0.019 | 0.314 | 0.017 | 0.332 | 0.147 | 0.721 | 0.053 | 0.583 | 0.027 | 0.448 | 0.237 | 0.921 | 0.094 | 0.794 | 0.040 | 0.570 |
| 30 | 0.073 | 0.442 | 0.059 | 0.420 | 0.070 | 0.512 | 0.156 | 0.817 | 0.091 | 0.609 | 0.090 | 0.628 | 0.246 | 1.168 | 0.127 | 0.804 | 0.107 | 0.736 |
| 31 | 0.183 | 0.624 | 0.230 | 0.851 | 0.263 | 0.984 | 0.284 | 1.124 | 0.299 | 1.062 | 0.349 | 1.286 | 0.389 | 1.621 | 0.359 | 1.377 | 0.398 | 1.435 |
| 32 | 0.401 | 0.920 | 0.489 | 1.291 | 0.530 | 1.500 | 0.551 | 1.383 | 0.668 | 1.648 | 0.752 | 1.990 | 0.669 | 1.813 | 0.785 | 1.890 | 0.889 | 2.316 |
| 33 | 0.548 | 1.092 | 0.583 | 1.448 | 0.587 | 1.629 | 0.789 | 1.633 | 0.871 | 1.954 | 0.898 | 2.212 | 0.933 | 1.896 | 1.059 | 2.170 | 1.128 | 2.701 |
| 34 | 0.447 | 1.072 | 0.407 | 1.257 | 0.387 | 1.368 | 0.707 | 1.504 | 0.669 | 1.848 | 0.639 | 1.976 | 0.894 | 1.927 | 0.855 | 2.089 | 0.831 | 2.407 |
| 35 | 0.372 | 1.076 | 0.335 | 1.141 | 0.330 | 1.265 | 0.606 | 1.503 | 0.545 | 1.619 | 0.534 | 1.995 | 0.781 | 1.790 | 0.711 | 2.023 | 0.677 | 2.169 |
| 36 | 0.347 | 0.921 | 0.358 | 1.147 | 0.375 | 1.345 | 0.548 | 1.308 | 0.532 | 1.520 | 0.553 | 1.789 | 0.733 | 1.871 | 0.675 | 1.861 | 0.701 | 2.316 |
| 37 | 0.357 | 0.932 | 0.383 | 1.218 | 0.391 | 1.389 | 0.565 | 1.411 | 0.565 | 1.637 | 0.591 | 1.930 | 0.723 | 1.835 | 0.706 | 1.907 | 0.740 | 2.384 |
| 38 | 0.388 | 0.964 | 0.429 | 1.280 | 0.451 | 1.482 | 0.592 | 1.644 | 0.624 | 1.693 | 0.668 | 2.038 | 0.726 | 1.672 | 0.776 | 2.121 | 0.815 | 2.312 |
| 39 | 0.444 | 1.103 | 0.480 | 1.383 | 0.500 | 1.631 | 0.640 | 1.503 | 0.714 | 1.920 | 0.746 | 2.171 | 0.809 | 2.089 | 0.877 | 2.184 | 0.934 | 2.692 |
| 40 | 0.529 | 1.081 | 0.621 | 1.473 | 0.686 | 1.810 | 0.755 | 1.578 | 0.871 | 1.856 | 0.966 | 2.347 | 0.931 | 2.089 | 1.056 | 2.299 | 1.167 | 2.721 |
| 41 | 0.796 | 1.277 | 0.964 | 1.821 | 1.025 | 2.195 | 1.059 | 1.649 | 1.333 | 2.296 | 1.497 | 2.873 | 1.229 | 1.879 | 1.563 | 2.610 | 1.796 | 3.288 |
| 42 | 0.817 | 1.364 | 0.882 | 1.870 | 0.894 | 2.221 | 1.144 | 1.824 | 1.322 | 2.407 | 1.373 | 2.970 | 1.318 | 1.870 | 1.590 | 2.634 | 1.704 | 3.377 |
| 43 | 0.706 | 1.343 | 0.705 | 1.742 | 0.688 | 2.043 | 1.009 | 1.663 | 1.110 | 2.327 | 1.081 | 2.697 | 1.222 | 1.931 | 1.369 | 2.607 | 1.376 | 3.209 |
| 44 | 0.611 | 1.359 | 0.598 | 1.692 | 0.580 | 1.904 | 0.914 | 1.605 | 0.923 | 2.150 | 0.907 | 2.545 | 1.100 | 1.825 | 1.170 | 2.392 | 1.144 | 2.961 |
| 45 | 0.527 | 1.290 | 0.497 | 1.601 | 0.461 | 1.758 | 0.809 | 1.509 | 0.798 | 2.031 | 0.756 | 2.400 | 1.000 | 1.671 | 1.015 | 2.323 | 0.962 | 2.702 |
| 46 | 0.445 | 1.179 | 0.395 | 1.439 | 0.357 | 1.548 | 0.701 | 1.434 | 0.662 | 1.908 | 0.602 | 2.192 | 0.881 | 1.517 | 0.849 | 2.139 | 0.778 | 2.477 |
| 47 | 0.348 | 1.069 | 0.273 | 1.228 | 0.236 | 1.323 | 0.587 | 1.316 | 0.495 | 1.698 | 0.406 | 1.818 | 0.752 | 1.515 | 0.664 | 1.980 | 0.561 | 2.182 |
| 48 | 0.260 | 0.919 | 0.182 | 1.046 | 0.149 | 1.079 | 0.463 | 1.206 | 0.348 | 1.476 | 0.271 | 1.553 | 0.617 | 1.363 | 0.495 | 1.762 | 0.377 | 1.851 |
| 49 | 0.210 | 0.829 | 0.144 | 0.929 | 0.120 | 0.997 | 0.390 | 1.119 | 0.278 | 1.318 | 0.215 | 1.408 | 0.521 | 1.268 | 0.389 | 1.569 | 0.297 | 1.675 |
| 50 | 0.132 | 0.679 | 0.062 | 0.640 | 0.039 | 0.623 | 0.292 | 0.989 | 0.150 | 1.003 | 0.091 | 0.967 | 0.412 | 1.190 | 0.243 | 1.284 | 0.144 | 1.205 |
| 51 | 0.092 | 0.572 | 0.040 | 0.523 | 0.014 | 0.324 | 0.225 | 0.879 | 0.099 | 0.823 | 0.052 | 0.713 | 0.337 | 1.070 | 0.162 | 1.049 | 0.083 | 0.901 |
| 52 | 0.068 | 0.495 | 0.021 | 0.356 | 0.010 | 0.266 | 0.177 | 0.786 | 0.067 | 0.670 | 0.024 | 0.442 | 0.281 | 1.030 | 0.119 | 0.899 | 0.050 | 0.679 |
| 53 | 0.056 | 0.446 | 0.019 | 0.314 | 0.017 | 0.332 | 0.145 | 0.746 | 0.052 | 0.575 | 0.027 | 0.448 | 0.228 | 0.937 | 0.094 | 0.790 | 0.040 | 0.570 |
| 54 | 0.073 | 0.442 | 0.059 | 0.420 | 0.070 | 0.512 | 0.147 | 0.698 | 0.090 | 0.599 | 0.089 | 0.627 | 0.236 | 1.095 | 0.124 | 0.762 | 0.106 | 0.735 |
| 55 | 0.183 | 0.623 | 0.230 | 0.851 | 0.263 | 0.984 | 0.279 | 1.095 | 0.299 | 1.060 | 0.349 | 1.286 | 0.387 | 1.670 | 0.356 | 1.347 | 0.399 | 1.436 |
| 56 | 0.401 | 0.920 | 0.489 | 1.291 | 0.530 | 1.500 | 0.553 | 1.417 | 0.667 | 1.648 | 0.751 | 1.990 | 0.664 | 1.806 | 0.786 | 1.947 | 0.889 | 2.316 |
| 57 | 0.548 | 1.093 | 0.583 | 1.448 | 0.587 | 1.629 | 0.787 | 1.606 | 0.867 | 1.901 | 0.898 | 2.212 | 0.932 | 1.918 | 1.059 | 2.170 | 1.122 | 2.624 |
| 58 | 0.445 | 1.035 | 0.407 | 1.257 | 0.387 | 1.368 | 0.704 | 1.444 | 0.670 | 1.858 | 0.639 | 1.975 | 0.896 | 1.926 | 0.853 | 2.068 | 0.837 | 2.473 |
| 59 | 0.375 | 1.138 | 0.335 | 1.141 | 0.330 | 1.265 | 0.608 | 1.475 | 0.546 | 1.626 | 0.534 | 1.992 | 0.771 | 1.650 | 0.706 | 1.994 | 0.677 | 2.169 |
| 60 | 0.347 | 0.921 | 0.358 | 1.147 | 0.375 | 1.345 | 0.546 | 1.267 | 0.533 | 1.541 | 0.553 | 1.789 | 0.728 | 1.856 | 0.674 | 1.834 | 0.701 | 2.316 |
| 61 | 0.357 | 0.932 | 0.383 | 1.218 | 0.391 | 1.389 | 0.564 | 1.431 | 0.565 | 1.637 | 0.591 | 1.930 | 0.719 | 1.813 | 0.706 | 1.903 | 0.740 | 2.384 |
| 62 | 0.387 | 0.960 | 0.429 | 1.280 | 0.451 | 1.482 | 0.591 | 1.668 | 0.624 | 1.693 | 0.668 | 2.038 | 0.734 | 1.808 | 0.773 | 2.078 | 0.815 | 2.312 |
| 63 | 0.445 | 1.112 | 0.480 | 1.383 | 0.500 | 1.631 | 0.639 | 1.472 | 0.711 | 1.898 | 0.746 | 2.171 | 0.807 | 2.088 | 0.878 | 2.211 | 0.935 | 2.698 |
| 64 | 0.529 | 1.081 | 0.621 | 1.473 | 0.686 | 1.810 | 0.760 | 1.658 | 0.869 | 1.850 | 0.966 | 2.349 | 0.927 | 2.059 | 1.050 | 2.251 | 1.164 | 2.705 |

**TABLE 12.** *(Continued.)* **Mean and standard deviation (SD) of $p^{immediate}$ charging profile over the example week with 1-hour resolution by ambient temperature and charging power scenario Low (L), Medium (M), and High (H).**

| | | | | | | | | | | | | | | | | | | |
|---|---|---|---|---|---|---|---|---|---|---|---|---|---|---|---|---|---|---|
| 65 | 0.796 | 1.277 | 0.964 | 1.821 | 1.025 | 2.195 | 1.059 | 1.617 | 1.337 | 2.359 | 1.495 | 2.863 | 1.241 | 1.970 | 1.566 | 2.651 | 1.797 | 3.294 |
| 66 | 0.817 | 1.364 | 0.881 | 1.869 | 0.894 | 2.221 | 1.142 | 1.790 | 1.323 | 2.408 | 1.379 | 3.079 | 1.312 | 1.833 | 1.595 | 2.653 | 1.706 | 3.397 |
| 67 | 0.706 | 1.343 | 0.705 | 1.742 | 0.688 | 2.043 | 1.013 | 1.713 | 1.110 | 2.332 | 1.081 | 2.697 | 1.215 | 1.889 | 1.375 | 2.645 | 1.375 | 3.210 |
| 68 | 0.610 | 1.359 | 0.598 | 1.692 | 0.580 | 1.904 | 0.913 | 1.604 | 0.923 | 2.149 | 0.907 | 2.545 | 1.100 | 1.839 | 1.174 | 2.446 | 1.143 | 2.961 |
| 69 | 0.527 | 1.290 | 0.497 | 1.601 | 0.461 | 1.758 | 0.809 | 1.508 | 0.802 | 2.079 | 0.756 | 2.400 | 1.000 | 1.662 | 1.010 | 2.276 | 0.962 | 2.702 |
| 70 | 0.444 | 1.178 | 0.395 | 1.439 | 0.357 | 1.548 | 0.700 | 1.433 | 0.661 | 1.906 | 0.602 | 2.192 | 0.881 | 1.517 | 0.847 | 2.136 | 0.778 | 2.477 |
| 71 | 0.347 | 1.067 | 0.273 | 1.228 | 0.236 | 1.323 | 0.585 | 1.313 | 0.495 | 1.698 | 0.406 | 1.818 | 0.751 | 1.513 | 0.662 | 1.975 | 0.561 | 2.182 |
| 72 | 0.259 | 0.917 | 0.182 | 1.046 | 0.148 | 1.076 | 0.461 | 1.202 | 0.348 | 1.476 | 0.270 | 1.552 | 0.614 | 1.361 | 0.496 | 1.766 | 0.377 | 1.851 |
| 73 | 0.210 | 0.828 | 0.144 | 0.929 | 0.120 | 0.997 | 0.390 | 1.118 | 0.278 | 1.318 | 0.215 | 1.408 | 0.520 | 1.266 | 0.390 | 1.571 | 0.297 | 1.675 |
| 74 | 0.131 | 0.678 | 0.062 | 0.640 | 0.039 | 0.623 | 0.291 | 0.989 | 0.150 | 1.004 | 0.091 | 0.967 | 0.409 | 1.175 | 0.243 | 1.284 | 0.144 | 1.205 |
| 75 | 0.092 | 0.572 | 0.040 | 0.523 | 0.014 | 0.324 | 0.225 | 0.878 | 0.098 | 0.816 | 0.052 | 0.713 | 0.336 | 1.072 | 0.162 | 1.050 | 0.083 | 0.901 |
| 76 | 0.068 | 0.495 | 0.021 | 0.356 | 0.010 | 0.266 | 0.176 | 0.784 | 0.066 | 0.660 | 0.024 | 0.442 | 0.280 | 1.033 | 0.117 | 0.892 | 0.050 | 0.679 |
| 77 | 0.056 | 0.446 | 0.019 | 0.314 | 0.017 | 0.332 | 0.144 | 0.727 | 0.052 | 0.572 | 0.027 | 0.448 | 0.227 | 0.929 | 0.093 | 0.784 | 0.040 | 0.570 |
| 78 | 0.073 | 0.442 | 0.059 | 0.420 | 0.070 | 0.512 | 0.150 | 0.733 | 0.091 | 0.604 | 0.089 | 0.627 | 0.233 | 1.081 | 0.126 | 0.804 | 0.106 | 0.734 |
| 79 | 0.183 | 0.623 | 0.230 | 0.851 | 0.263 | 0.984 | 0.279 | 1.108 | 0.299 | 1.062 | 0.349 | 1.286 | 0.385 | 1.628 | 0.355 | 1.309 | 0.397 | 1.432 |
| 80 | 0.401 | 0.920 | 0.489 | 1.291 | 0.530 | 1.500 | 0.550 | 1.376 | 0.668 | 1.648 | 0.751 | 1.990 | 0.675 | 1.897 | 0.788 | 1.934 | 0.889 | 2.316 |
| 81 | 0.548 | 1.093 | 0.583 | 1.448 | 0.587 | 1.629 | 0.793 | 1.718 | 0.868 | 1.905 | 0.898 | 2.212 | 0.928 | 1.861 | 1.062 | 2.186 | 1.125 | 2.644 |
| 82 | 0.445 | 1.036 | 0.407 | 1.257 | 0.387 | 1.368 | 0.702 | 1.414 | 0.670 | 1.858 | 0.639 | 1.975 | 0.888 | 1.846 | 0.851 | 2.034 | 0.834 | 2.421 |
| 83 | 0.374 | 1.128 | 0.335 | 1.141 | 0.330 | 1.265 | 0.607 | 1.494 | 0.545 | 1.617 | 0.534 | 1.997 | 0.770 | 1.639 | 0.707 | 1.995 | 0.677 | 2.169 |
| 84 | 0.347 | 0.921 | 0.358 | 1.147 | 0.375 | 1.345 | 0.543 | 1.237 | 0.534 | 1.544 | 0.553 | 1.789 | 0.732 | 1.868 | 0.673 | 1.834 | 0.701 | 2.316 |
| 85 | 0.357 | 0.932 | 0.383 | 1.218 | 0.391 | 1.389 | 0.566 | 1.458 | 0.565 | 1.637 | 0.591 | 1.930 | 0.723 | 1.897 | 0.707 | 1.910 | 0.740 | 2.384 |
| 86 | 0.387 | 0.960 | 0.429 | 1.280 | 0.451 | 1.482 | 0.594 | 1.677 | 0.624 | 1.693 | 0.668 | 2.038 | 0.731 | 1.755 | 0.775 | 2.095 | 0.815 | 2.312 |
| 87 | 0.445 | 1.117 | 0.480 | 1.383 | 0.500 | 1.631 | 0.637 | 1.437 | 0.714 | 1.920 | 0.746 | 2.171 | 0.805 | 2.063 | 0.880 | 2.216 | 0.935 | 2.698 |
| 88 | 0.529 | 1.081 | 0.621 | 1.473 | 0.686 | 1.810 | 0.758 | 1.628 | 0.869 | 1.850 | 0.966 | 2.349 | 0.930 | 2.098 | 1.052 | 2.260 | 1.163 | 2.704 |
| 89 | 0.796 | 1.277 | 0.964 | 1.821 | 1.025 | 2.195 | 1.057 | 1.617 | 1.337 | 2.359 | 1.495 | 2.863 | 1.235 | 1.921 | 1.566 | 2.651 | 1.798 | 3.308 |
| 90 | 0.817 | 1.364 | 0.881 | 1.869 | 0.894 | 2.221 | 1.141 | 1.793 | 1.324 | 2.412 | 1.379 | 3.078 | 1.320 | 1.914 | 1.592 | 2.644 | 1.705 | 3.397 |
| 91 | 0.705 | 1.343 | 0.705 | 1.742 | 0.688 | 2.043 | 1.014 | 1.710 | 1.110 | 2.333 | 1.081 | 2.697 | 1.219 | 1.913 | 1.374 | 2.652 | 1.376 | 3.219 |
| 92 | 0.610 | 1.359 | 0.598 | 1.692 | 0.580 | 1.904 | 0.912 | 1.604 | 0.924 | 2.157 | 0.907 | 2.545 | 1.100 | 1.838 | 1.168 | 2.391 | 1.143 | 2.961 |
| 93 | 0.527 | 1.289 | 0.497 | 1.601 | 0.461 | 1.758 | 0.809 | 1.508 | 0.797 | 2.029 | 0.756 | 2.400 | 0.999 | 1.660 | 1.014 | 2.321 | 0.962 | 2.702 |
| 94 | 0.444 | 1.178 | 0.395 | 1.439 | 0.357 | 1.548 | 0.700 | 1.433 | 0.661 | 1.906 | 0.602 | 2.192 | 0.880 | 1.516 | 0.847 | 2.137 | 0.778 | 2.477 |
| 95 | 0.347 | 1.067 | 0.273 | 1.228 | 0.236 | 1.323 | 0.585 | 1.315 | 0.495 | 1.698 | 0.406 | 1.818 | 0.749 | 1.511 | 0.662 | 1.975 | 0.561 | 2.182 |
| 96 | 0.259 | 0.917 | 0.182 | 1.046 | 0.148 | 1.076 | 0.462 | 1.204 | 0.348 | 1.476 | 0.270 | 1.551 | 0.613 | 1.358 | 0.495 | 1.764 | 0.377 | 1.851 |
| 97 | 0.210 | 0.828 | 0.144 | 0.929 | 0.120 | 0.997 | 0.390 | 1.119 | 0.278 | 1.317 | 0.215 | 1.408 | 0.520 | 1.266 | 0.390 | 1.571 | 0.297 | 1.675 |
| 98 | 0.131 | 0.678 | 0.062 | 0.640 | 0.039 | 0.623 | 0.292 | 0.990 | 0.150 | 1.004 | 0.091 | 0.967 | 0.410 | 1.178 | 0.243 | 1.285 | 0.144 | 1.205 |
| 99 | 0.092 | 0.572 | 0.040 | 0.523 | 0.014 | 0.324 | 0.225 | 0.878 | 0.099 | 0.823 | 0.052 | 0.713 | 0.336 | 1.071 | 0.162 | 1.050 | 0.083 | 0.901 |
| 100 | 0.068 | 0.495 | 0.021 | 0.356 | 0.010 | 0.266 | 0.176 | 0.785 | 0.067 | 0.666 | 0.024 | 0.442 | 0.280 | 1.032 | 0.119 | 0.899 | 0.050 | 0.679 |
| 101 | 0.056 | 0.446 | 0.019 | 0.314 | 0.017 | 0.332 | 0.144 | 0.728 | 0.052 | 0.571 | 0.027 | 0.448 | 0.227 | 0.930 | 0.093 | 0.785 | 0.040 | 0.570 |
| 102 | 0.073 | 0.442 | 0.059 | 0.420 | 0.070 | 0.512 | 0.148 | 0.718 | 0.090 | 0.599 | 0.089 | 0.627 | 0.235 | 1.097 | 0.127 | 0.865 | 0.106 | 0.735 |
| 103 | 0.183 | 0.623 | 0.230 | 0.851 | 0.263 | 0.984 | 0.278 | 1.105 | 0.299 | 1.060 | 0.348 | 1.283 | 0.385 | 1.638 | 0.352 | 1.282 | 0.398 | 1.433 |
| 104 | 0.401 | 0.920 | 0.489 | 1.291 | 0.530 | 1.500 | 0.551 | 1.390 | 0.667 | 1.648 | 0.751 | 1.990 | 0.669 | 1.848 | 0.784 | 1.905 | 0.889 | 2.316 |
| 105 | 0.548 | 1.093 | 0.583 | 1.448 | 0.587 | 1.629 | 0.789 | 1.641 | 0.867 | 1.902 | 0.898 | 2.212 | 0.927 | 1.845 | 1.065 | 2.220 | 1.124 | 2.631 |
| 106 | 0.445 | 1.035 | 0.407 | 1.257 | 0.387 | 1.368 | 0.702 | 1.415 | 0.670 | 1.858 | 0.639 | 1.975 | 0.897 | 1.942 | 0.851 | 2.044 | 0.835 | 2.442 |
| 107 | 0.375 | 1.132 | 0.335 | 1.141 | 0.330 | 1.265 | 0.609 | 1.496 | 0.545 | 1.621 | 0.534 | 1.995 | 0.774 | 1.673 | 0.706 | 1.991 | 0.677 | 2.169 |
| 108 | 0.347 | 0.921 | 0.358 | 1.147 | 0.375 | 1.345 | 0.545 | 1.263 | 0.533 | 1.541 | 0.553 | 1.789 | 0.726 | 1.811 | 0.672 | 1.831 | 0.701 | 2.316 |
| 109 | 0.357 | 0.932 | 0.383 | 1.218 | 0.391 | 1.389 | 0.566 | 1.472 | 0.565 | 1.637 | 0.591 | 1.930 | 0.718 | 1.838 | 0.706 | 1.908 | 0.740 | 2.384 |
| 110 | 0.387 | 0.960 | 0.429 | 1.280 | 0.451 | 1.482 | 0.589 | 1.606 | 0.624 | 1.693 | 0.668 | 2.038 | 0.736 | 1.833 | 0.774 | 2.087 | 0.815 | 2.312 |
| 111 | 0.445 | 1.114 | 0.480 | 1.383 | 0.500 | 1.631 | 0.638 | 1.467 | 0.711 | 1.898 | 0.746 | 2.171 | 0.805 | 2.070 | 0.877 | 2.196 | 0.935 | 2.698 |
| 112 | 0.529 | 1.081 | 0.621 | 1.473 | 0.686 | 1.810 | 0.758 | 1.633 | 0.869 | 1.850 | 0.966 | 2.349 | 0.926 | 2.053 | 1.050 | 2.249 | 1.163 | 2.704 |
| 113 | 0.796 | 1.277 | 0.964 | 1.821 | 1.025 | 2.195 | 1.061 | 1.631 | 1.337 | 2.359 | 1.495 | 2.863 | 1.238 | 1.938 | 1.566 | 2.651 | 1.798 | 3.308 |
| 114 | 0.817 | 1.364 | 0.881 | 1.869 | 0.894 | 2.221 | 1.141 | 1.776 | 1.325 | 2.421 | 1.379 | 3.078 | 1.320 | 1.913 | 1.597 | 2.682 | 1.705 | 3.397 |
| 115 | 0.705 | 1.343 | 0.705 | 1.742 | 0.688 | 2.043 | 1.012 | 1.691 | 1.109 | 2.310 | 1.081 | 2.697 | 1.217 | 1.897 | 1.373 | 2.634 | 1.376 | 3.217 |
| 116 | 0.611 | 1.378 | 0.598 | 1.692 | 0.580 | 1.904 | 0.914 | 1.637 | 0.925 | 2.191 | 0.911 | 2.570 | 1.100 | 1.848 | 1.176 | 2.473 | 1.148 | 3.003 |
| 117 | 0.526 | 1.287 | 0.497 | 1.601 | 0.461 | 1.758 | 0.808 | 1.507 | 0.802 | 2.079 | 0.755 | 2.396 | 0.999 | 1.661 | 1.010 | 2.275 | 0.962 | 2.701 |
| 118 | 0.444 | 1.177 | 0.395 | 1.439 | 0.357 | 1.548 | 0.700 | 1.433 | 0.661 | 1.905 | 0.600 | 2.189 | 0.880 | 1.516 | 0.846 | 2.135 | 0.777 | 2.475 |
| 119 | 0.346 | 1.066 | 0.273 | 1.228 | 0.236 | 1.323 | 0.584 | 1.312 | 0.494 | 1.697 | 0.405 | 1.815 | 0.749 | 1.513 | 0.661 | 1.974 | 0.560 | 2.179 |
| 120 | 0.259 | 0.916 | 0.181 | 1.045 | 0.148 | 1.076 | 0.460 | 1.200 | 0.347 | 1.473 | 0.269 | 1.547 | 0.614 | 1.360 | 0.495 | 1.765 | 0.376 | 1.847 |
| 121 | 0.185 | 0.779 | 0.112 | 0.831 | 0.079 | 0.793 | 0.359 | 1.079 | 0.236 | 1.225 | 0.163 | 1.219 | 0.493 | 1.272 | 0.345 | 1.493 | 0.234 | 1.477 |
| 122 | 0.130 | 0.672 | 0.065 | 0.637 | 0.041 | 0.570 | 0.290 | 1.058 | 0.150 | 0.995 | 0.093 | 0.925 | 0.401 | 1.148 | 0.242 | 1.282 | 0.145 | 1.171 |
| 123 | 0.095 | 0.573 | 0.038 | 0.483 | 0.020 | 0.379 | 0.223 | 0.868 | 0.102 | 0.816 | 0.053 | 0.680 | 0.334 | 1.099 | 0.171 | 1.084 | 0.091 | 0.911 |
| 124 | 0.070 | 0.489 | 0.024 | 0.371 | 0.014 | 0.331 | 0.182 | 0.905 | 0.068 | 0.656 | 0.029 | 0.497 | 0.271 | 0.949 | 0.125 | 0.960 | 0.050 | 0.652 |
| 125 | 0.053 | 0.428 | 0.020 | 0.321 | 0.018 | 0.351 | 0.140 | 0.683 | 0.053 | 0.724 | 0.027 | 0.455 | 0.229 | 0.952 | 0.092 | 0.877 | 0.040 | 0.598 |
| 126 | 0.054 | 0.405 | 0.031 | 0.368 | 0.028 | 0.355 | 0.124 | 0.635 | 0.058 | 0.551 | 0.044 | 0.523 | 0.202 | 0.887 | 0.091 | 0.851 | 0.068 | 0.922 |
| 127 | 0.059 | 0.384 | 0.052 | 0.408 | 0.056 | 0.471 | 0.124 | 0.604 | 0.081 | 0.593 | 0.075 | 0.583 | 0.196 | 1.021 | 0.101 | 0.692 | 0.096 | 0.787 |
| 128 | 0.076 | 0.456 | 0.062 | 0.472 | 0.056 | 0.483 | 0.141 | 0.760 | 0.102 | 0.711 | 0.097 | 0.770 | 0.202 | 0.958 | 0.137 | 0.850 | 0.116 | 0.833 |
| 129 | 0.097 | 0.483 | 0.099 | 0.579 | 0.106 | 0.687 | 0.176 | 0.891 | 0.141 | 0.766 | 0.150 | 0.865 | 0.247 | 1.223 | 0.195 | 1.335 | 0.197 | 1.407 |
| 130 | 0.156 | 0.607 | 0.174 | 0.802 | 0.191 | 0.968 | 0.237 | 0.795 | 0.247 | 1.089 | 0.277 | 1.326 | 0.325 | 1.290 | 0.293 | 1.243 | 0.322 | 1.465 |
| 131 | 0.273 | 0.811 | 0.315 | 1.038 | 0.329 | 1.197 | 0.400 | 1.308 | 0.450 | 1.450 | 0.488 | 1.622 | 0.516 | 2.004 | 0.529 | 1.733 | 0.613 | 2.083 |
| 132 | 0.373 | 0.942 | 0.428 | 1.259 | 0.455 | 1.449 | 0.540 | 1.482 | 0.614 | 1.803 | 0.687 | 2.200 | 0.706 | 2.231 | 0.743 | 2.038 | 0.838 | 2.606 |

**TABLE 12.** *(Continued.)* Mean and standard deviation (SD) of $p^{immediate}$ charging profile over the example week with 1-hour resolution by ambient temperature and charging power scenario Low (L), Medium (M), and High (H).

| | | | | | | | | | | | | | | | | | | |
|---|---|---|---|---|---|---|---|---|---|---|---|---|---|---|---|---|---|---|
| 133 | 0.455 | 1.004 | 0.496 | 1.305 | 0.526 | 1.541 | 0.671 | 1.610 | 0.734 | 1.704 | 0.759 | 2.006 | 0.865 | 2.401 | 0.926 | 2.244 | 0.935 | 2.312 |
| 134 | 0.531 | 1.154 | 0.607 | 1.546 | 0.644 | 1.820 | 0.816 | 2.118 | 0.860 | 1.926 | 0.945 | 2.398 | 0.997 | 2.423 | 1.149 | 3.102 | 1.254 | 3.877 |
| 135 | 0.594 | 1.147 | 0.694 | 1.625 | 0.742 | 1.950 | 0.889 | 2.034 | 1.046 | 2.537 | 1.139 | 3.046 | 1.081 | 2.633 | 1.224 | 2.643 | 1.406 | 3.750 |
| 136 | 0.670 | 1.266 | 0.738 | 1.673 | 0.784 | 2.073 | 0.933 | 1.717 | 1.109 | 2.334 | 1.179 | 2.870 | 1.126 | 2.186 | 1.328 | 2.582 | 1.414 | 3.058 |
| 137 | 0.720 | 1.403 | 0.800 | 1.845 | 0.869 | 2.279 | 0.982 | 1.800 | 1.136 | 2.260 | 1.232 | 2.846 | 1.171 | 2.181 | 1.413 | 2.783 | 1.490 | 3.384 |
| 138 | 0.690 | 1.608 | 0.765 | 1.890 | 0.775 | 2.215 | 0.975 | 1.844 | 1.092 | 2.364 | 1.181 | 2.931 | 1.172 | 2.118 | 1.359 | 2.988 | 1.504 | 3.827 |
| 139 | 0.633 | 1.243 | 0.723 | 1.813 | 0.741 | 2.166 | 0.911 | 1.643 | 1.080 | 2.375 | 1.142 | 2.919 | 1.069 | 1.732 | 1.238 | 2.439 | 1.355 | 3.111 |
| 140 | 0.627 | 1.360 | 0.652 | 1.760 | 0.640 | 2.086 | 0.878 | 1.605 | 0.999 | 2.290 | 1.003 | 2.732 | 1.037 | 1.658 | 1.206 | 2.459 | 1.250 | 3.075 |
| 141 | 0.557 | 1.267 | 0.543 | 1.671 | 0.543 | 2.054 | 0.801 | 1.525 | 0.848 | 2.129 | 0.822 | 2.542 | 0.983 | 1.732 | 1.074 | 2.429 | 1.049 | 2.913 |
| 142 | 0.467 | 1.158 | 0.446 | 1.558 | 0.436 | 1.888 | 0.713 | 1.470 | 0.709 | 2.015 | 0.689 | 2.445 | 0.881 | 1.695 | 0.896 | 2.248 | 0.874 | 2.745 |
| 143 | 0.391 | 1.095 | 0.347 | 1.439 | 0.319 | 1.618 | 0.615 | 1.346 | 0.580 | 1.851 | 0.533 | 2.202 | 0.794 | 1.706 | 0.746 | 2.109 | 0.693 | 2.490 |
| 144 | 0.315 | 1.025 | 0.254 | 1.261 | 0.202 | 1.322 | 0.521 | 1.304 | 0.439 | 1.681 | 0.371 | 1.831 | 0.656 | 1.436 | 0.595 | 1.961 | 0.494 | 2.146 |
| 145 | 0.292 | 0.981 | 0.262 | 1.268 | 0.242 | 1.429 | 0.485 | 1.252 | 0.428 | 1.645 | 0.379 | 1.871 | 0.613 | 1.438 | 0.551 | 1.877 | 0.483 | 2.132 |
| 146 | 0.212 | 0.854 | 0.160 | 1.017 | 0.100 | 0.930 | 0.383 | 1.133 | 0.299 | 1.427 | 0.215 | 1.415 | 0.505 | 1.324 | 0.404 | 1.648 | 0.307 | 1.722 |
| 147 | 0.172 | 0.775 | 0.092 | 0.775 | 0.043 | 0.593 | 0.313 | 1.030 | 0.227 | 1.232 | 0.114 | 1.034 | 0.434 | 1.203 | 0.321 | 1.472 | 0.186 | 1.329 |
| 148 | 0.135 | 0.681 | 0.059 | 0.608 | 0.021 | 0.399 | 0.269 | 0.999 | 0.159 | 1.035 | 0.063 | 0.729 | 0.371 | 1.126 | 0.241 | 1.266 | 0.102 | 0.969 |
| 149 | 0.106 | 0.607 | 0.047 | 0.542 | 0.019 | 0.361 | 0.238 | 1.095 | 0.110 | 0.835 | 0.042 | 0.592 | 0.321 | 1.083 | 0.174 | 1.103 | 0.064 | 0.766 |
| 150 | 0.097 | 0.560 | 0.042 | 0.441 | 0.027 | 0.328 | 0.204 | 0.858 | 0.095 | 0.746 | 0.051 | 0.582 | 0.296 | 1.161 | 0.167 | 1.151 | 0.073 | 0.731 |
| 151 | 0.096 | 0.519 | 0.053 | 0.415 | 0.054 | 0.446 | 0.199 | 0.909 | 0.099 | 0.684 | 0.077 | 0.604 | 0.290 | 1.111 | 0.151 | 0.927 | 0.107 | 0.979 |
| 152 | 0.106 | 0.557 | 0.062 | 0.476 | 0.056 | 0.482 | 0.206 | 0.835 | 0.117 | 0.777 | 0.099 | 0.768 | 0.319 | 1.509 | 0.169 | 1.012 | 0.120 | 0.855 |
| 153 | 0.121 | 0.558 | 0.097 | 0.563 | 0.105 | 0.683 | 0.228 | 1.031 | 0.148 | 0.795 | 0.149 | 0.858 | 0.320 | 1.373 | 0.205 | 1.278 | 0.197 | 1.406 |
| 154 | 0.169 | 0.639 | 0.171 | 0.788 | 0.189 | 0.957 | 0.289 | 1.116 | 0.252 | 1.215 | 0.273 | 1.314 | 0.397 | 1.617 | 0.290 | 1.159 | 0.319 | 1.455 |
| 155 | 0.286 | 0.903 | 0.312 | 1.028 | 0.328 | 1.185 | 0.443 | 1.415 | 0.449 | 1.400 | 0.485 | 1.604 | 0.585 | 2.317 | 0.555 | 1.945 | 0.609 | 2.068 |
| 156 | 0.382 | 0.987 | 0.425 | 1.255 | 0.451 | 1.444 | 0.599 | 1.943 | 0.608 | 1.729 | 0.682 | 2.193 | 0.711 | 2.074 | 0.774 | 2.241 | 0.833 | 2.600 |
| 157 | 0.464 | 1.134 | 0.490 | 1.292 | 0.519 | 1.523 | 0.723 | 2.083 | 0.729 | 1.705 | 0.751 | 1.991 | 0.875 | 2.327 | 0.914 | 2.173 | 0.925 | 2.294 |
| 158 | 0.524 | 1.085 | 0.600 | 1.534 | 0.636 | 1.801 | 0.778 | 1.672 | 0.864 | 2.070 | 0.935 | 2.378 | 1.050 | 2.846 | 1.106 | 2.873 | 1.241 | 3.865 |
| 159 | 0.599 | 1.277 | 0.687 | 1.610 | 0.735 | 1.925 | 0.905 | 2.339 | 1.049 | 2.589 | 1.127 | 3.025 | 1.109 | 2.792 | 1.242 | 2.861 | 1.392 | 3.729 |
| 160 | 0.661 | 1.223 | 0.733 | 1.664 | 0.779 | 2.066 | 0.912 | 1.548 | 1.090 | 2.245 | 1.171 | 2.855 | 1.125 | 2.331 | 1.322 | 2.563 | 1.404 | 3.055 |
| 161 | 0.710 | 1.391 | 0.795 | 1.837 | 0.865 | 2.270 | 1.003 | 2.015 | 1.128 | 2.250 | 1.225 | 2.838 | 1.134 | 1.847 | 1.412 | 2.867 | 1.478 | 3.367 |
| 162 | 0.683 | 1.600 | 0.758 | 1.880 | 0.768 | 2.201 | 0.986 | 1.924 | 1.087 | 2.362 | 1.171 | 2.916 | 1.163 | 2.185 | 1.347 | 2.943 | 1.499 | 3.851 |
| 163 | 0.626 | 1.233 | 0.718 | 1.806 | 0.737 | 2.158 | 0.896 | 1.606 | 1.068 | 2.355 | 1.134 | 2.910 | 1.056 | 1.702 | 1.240 | 2.541 | 1.341 | 3.079 |
| 164 | 0.618 | 1.351 | 0.647 | 1.753 | 0.634 | 2.073 | 0.873 | 1.617 | 1.008 | 2.417 | 0.997 | 2.724 | 1.041 | 1.804 | 1.202 | 2.479 | 1.242 | 3.066 |
| 165 | 0.550 | 1.258 | 0.537 | 1.662 | 0.539 | 2.049 | 0.791 | 1.513 | 0.850 | 2.200 | 0.813 | 2.529 | 0.971 | 1.709 | 1.065 | 2.463 | 1.042 | 2.918 |
| 166 | 0.462 | 1.154 | 0.443 | 1.553 | 0.434 | 1.885 | 0.700 | 1.445 | 0.705 | 2.009 | 0.685 | 2.437 | 0.862 | 1.643 | 0.882 | 2.217 | 0.870 | 2.740 |
| 167 | 0.389 | 1.092 | 0.346 | 1.437 | 0.318 | 1.612 | 0.607 | 1.333 | 0.576 | 1.845 | 0.530 | 2.197 | 0.781 | 1.698 | 0.742 | 2.104 | 0.689 | 2.483 |
| 168 | 0.313 | 1.021 | 0.253 | 1.257 | 0.200 | 1.316 | 0.519 | 1.301 | 0.433 | 1.668 | 0.369 | 1.825 | 0.647 | 1.427 | 0.590 | 1.950 | 0.489 | 2.135 |

is a weekend day the charging can be shifted to a later hour overnight. In addition, with higher available charging power a slightly larger part of the charging could be shifted closer to the 'End' hour.

## IV. DISCUSSION AND CONCLUSION

In this study, the charging of a large-scale BEV fleet was analyzed in terms of ambient temperature and available charging power. Moreover, the coincidence of charging was examined, with the coincidence factor, in different charging locations, together with the possible flexibility of charging within charging events, and the deviation of the charging load. The examination included a very low ambient temperature of −20°C, to provide knowledge of conditions when the energy system is often as a whole under heavy loading. The results show that with higher available charging power the peaks of charging increased, and the valleys became deeper. Whereas with lower charging power the charging demand was more even. With higher ambient temperature the BEVs consumed, and consequently charged, less, compared to low ambient temperature, including during the peak hours. Moreover, the maximum hourly mean charging load increased to 1.80 kWh/h, with −20°C and CPS High, whereas the peak 1-minute load within that hour, and same scenario, reached 2.03 kW. Furthermore, compared to previous studies, the charging profiles presented in this study were in the same order of magnitude as in studies [11] and [24].

The coincidence of charging increased with lower available charging power and lower ambient temperature. By location type, the highest coincidence factors were at workplace, at hotel, and at home. However, the factors were never above 0.438 (workplace), which reflects that in a large-scale BEV fleet the simultaneity of charging is rather low, even with ambient temperature of −20°C. However, as presented in Fig. 10 and Fig. 11 the standard deviation of charging was considerable for a small number of BEVs. Thus, when considering e.g., a single location with a small number of BEVs, the deviation of charging would be high, and such the coincidence of charging could be too. Compared to previous studies, which included a large number of EVs [28], [32] similar effects were observed for a change in the available charging power; the coincidence factor decreased with higher available charging power. Moreover, the magnitude of the coincidence factors, for large number of EVs were in the range of 0.07 – 0.45 in studies [28], [29], [30], [31] which are comparable to the coincidence factors presented this study.

**TABLE 13.** Mean and standard deviation (SD) of $p^{delayed}$ charging profile over the example week with 1-hour resolution by ambient temperature and charging power scenario Low (L), Medium (M), and High (H).

| | Ambient temperature | | | | | | | | | | | | | | | | | |
|---|---|---|---|---|---|---|---|---|---|---|---|---|---|---|---|---|---|---|
| | 15°C | | | | | | -5°C | | | | | | -20°C | | | | | |
| | Charging power scenario | | | | | | Charging power scenario | | | | | | Charging power scenario | | | | | |
| | L | L | M | M | H | H | L | L | M | M | H | H | L | L | M | M | H | H |
| h | Mean | SD | Mean | SD | Mean | SD | Mean | SD | Mean | SD | Mean | SD | Mean | SD | Mean | SD | Mean | SD |
| 1 | 0.090 | 0.551 | 0.029 | 0.422 | 0.015 | 0.345 | 0.215 | 0.848 | 0.088 | 0.775 | 0.042 | 0.616 | 0.328 | 1.035 | 0.162 | 1.040 | 0.082 | 0.894 |
| 2 | 0.123 | 0.646 | 0.053 | 0.583 | 0.023 | 0.434 | 0.281 | 0.958 | 0.136 | 0.942 | 0.078 | 0.860 | 0.407 | 1.139 | 0.228 | 1.234 | 0.117 | 1.071 |
| 3 | 0.173 | 0.756 | 0.084 | 0.737 | 0.049 | 0.656 | 0.374 | 1.088 | 0.215 | 1.185 | 0.127 | 1.093 | 0.515 | 1.261 | 0.328 | 1.463 | 0.210 | 1.416 |
| 4 | 0.264 | 0.913 | 0.158 | 0.996 | 0.108 | 0.963 | 0.502 | 1.229 | 0.349 | 1.485 | 0.245 | 1.514 | 0.669 | 1.404 | 0.498 | 1.762 | 0.370 | 1.861 |
| 5 | 0.422 | 1.110 | 0.326 | 1.363 | 0.256 | 1.446 | 0.709 | 1.396 | 0.602 | 1.877 | 0.504 | 2.083 | 0.886 | 1.532 | 0.809 | 2.164 | 0.702 | 2.470 |
| 6 | 0.639 | 1.271 | 0.623 | 1.755 | 0.592 | 2.005 | 0.939 | 1.515 | 0.968 | 2.208 | 0.948 | 2.650 | 1.153 | 1.836 | 1.238 | 2.492 | 1.198 | 3.004 |
| 7 | 0.747 | 1.270 | 0.827 | 1.813 | 0.843 | 2.127 | 1.046 | 1.575 | 1.208 | 2.266 | 1.260 | 2.750 | 1.257 | 2.028 | 1.467 | 2.533 | 1.544 | 3.107 |
| 8 | 0.656 | 1.153 | 0.775 | 1.667 | 0.837 | 1.998 | 0.910 | 1.621 | 1.089 | 2.082 | 1.180 | 2.538 | 1.074 | 1.839 | 1.293 | 2.309 | 1.404 | 2.880 |
| 9 | 0.462 | 1.055 | 0.502 | 1.431 | 0.521 | 1.662 | 0.675 | 1.539 | 0.744 | 1.835 | 0.762 | 2.173 | 0.859 | 2.144 | 0.918 | 2.156 | 0.947 | 2.549 |
| 10 | 0.427 | 1.080 | 0.448 | 1.390 | 0.462 | 1.643 | 0.637 | 1.496 | 0.681 | 1.882 | 0.691 | 2.150 | 0.811 | 1.845 | 0.833 | 2.078 | 0.868 | 2.563 |
| 11 | 0.436 | 1.156 | 0.441 | 1.386 | 0.442 | 1.580 | 0.664 | 1.525 | 0.677 | 1.869 | 0.689 | 2.304 | 0.838 | 1.831 | 0.850 | 2.208 | 0.849 | 2.508 |
| 12 | 0.438 | 1.079 | 0.440 | 1.340 | 0.442 | 1.568 | 0.691 | 1.607 | 0.670 | 1.752 | 0.677 | 2.081 | 0.875 | 1.707 | 0.851 | 2.127 | 0.868 | 2.609 |
| 13 | 0.461 | 1.068 | 0.436 | 1.337 | 0.429 | 1.511 | 0.733 | 1.482 | 0.704 | 1.867 | 0.676 | 2.120 | 0.937 | 1.876 | 0.900 | 2.137 | 0.890 | 2.644 |
| 14 | 0.528 | 1.130 | 0.505 | 1.453 | 0.475 | 1.610 | 0.830 | 1.519 | 0.807 | 1.957 | 0.790 | 2.312 | 1.061 | 2.000 | 1.045 | 2.426 | 1.009 | 2.662 |
| 15 | 0.681 | 1.294 | 0.691 | 1.685 | 0.677 | 1.932 | 1.001 | 1.795 | 1.076 | 2.339 | 1.072 | 2.618 | 1.202 | 2.171 | 1.356 | 2.722 | 1.380 | 3.272 |
| 16 | 0.741 | 1.251 | 0.858 | 1.706 | 0.917 | 2.047 | 0.993 | 1.574 | 1.215 | 2.150 | 1.337 | 2.759 | 1.147 | 1.963 | 1.449 | 2.487 | 1.620 | 3.206 |
| 17 | 0.545 | 1.113 | 0.642 | 1.469 | 0.688 | 1.730 | 0.736 | 1.479 | 0.901 | 1.902 | 0.990 | 2.295 | 0.868 | 1.876 | 1.065 | 2.270 | 1.198 | 2.668 |
| 18 | 0.391 | 0.961 | 0.451 | 1.236 | 0.486 | 1.441 | 0.561 | 1.473 | 0.645 | 1.735 | 0.716 | 2.072 | 0.661 | 1.590 | 0.758 | 1.925 | 0.859 | 2.443 |
| 19 | 0.272 | 0.874 | 0.293 | 1.016 | 0.308 | 1.171 | 0.401 | 1.257 | 0.430 | 1.485 | 0.462 | 1.709 | 0.506 | 1.623 | 0.516 | 1.772 | 0.559 | 2.062 |
| 20 | 0.213 | 0.941 | 0.216 | 0.996 | 0.219 | 1.038 | 0.320 | 1.211 | 0.307 | 1.261 | 0.325 | 1.430 | 0.402 | 1.349 | 0.377 | 1.483 | 0.401 | 1.782 |
| 21 | 0.152 | 0.835 | 0.143 | 0.871 | 0.144 | 0.881 | 0.246 | 0.959 | 0.213 | 1.113 | 0.215 | 1.242 | 0.324 | 1.176 | 0.263 | 1.168 | 0.256 | 1.314 |
| 22 | 0.109 | 0.712 | 0.097 | 0.746 | 0.099 | 0.806 | 0.195 | 0.903 | 0.144 | 0.942 | 0.144 | 1.130 | 0.262 | 0.959 | 0.185 | 1.036 | 0.163 | 1.107 |
| 23 | 0.086 | 0.631 | 0.057 | 0.567 | 0.059 | 0.669 | 0.178 | 0.807 | 0.103 | 0.807 | 0.081 | 0.815 | 0.266 | 1.045 | 0.145 | 0.979 | 0.101 | 0.923 |
| 24 | 0.095 | 0.586 | 0.060 | 0.603 | 0.066 | 0.765 | 0.206 | 0.864 | 0.121 | 0.895 | 0.091 | 0.933 | 0.304 | 1.031 | 0.167 | 1.057 | 0.124 | 1.096 |
| 25 | 0.090 | 0.551 | 0.029 | 0.422 | 0.015 | 0.345 | 0.212 | 0.839 | 0.086 | 0.759 | 0.041 | 0.605 | 0.324 | 1.027 | 0.160 | 1.030 | 0.081 | 0.889 |
| 26 | 0.124 | 0.647 | 0.053 | 0.583 | 0.023 | 0.434 | 0.278 | 0.948 | 0.134 | 0.932 | 0.078 | 0.860 | 0.402 | 1.131 | 0.225 | 1.224 | 0.116 | 1.065 |
| 27 | 0.174 | 0.757 | 0.084 | 0.737 | 0.049 | 0.656 | 0.371 | 1.083 | 0.213 | 1.176 | 0.127 | 1.093 | 0.516 | 1.311 | 0.324 | 1.454 | 0.210 | 1.414 |
| 28 | 0.264 | 0.913 | 0.158 | 0.996 | 0.108 | 0.963 | 0.500 | 1.224 | 0.346 | 1.478 | 0.245 | 1.514 | 0.675 | 1.511 | 0.495 | 1.756 | 0.370 | 1.861 |
| 29 | 0.422 | 1.111 | 0.326 | 1.363 | 0.256 | 1.446 | 0.708 | 1.393 | 0.599 | 1.871 | 0.504 | 2.083 | 0.890 | 1.617 | 0.807 | 2.162 | 0.702 | 2.470 |
| 30 | 0.639 | 1.271 | 0.623 | 1.755 | 0.592 | 2.005 | 0.943 | 1.563 | 0.966 | 2.204 | 0.948 | 2.650 | 1.153 | 1.811 | 1.240 | 2.503 | 1.198 | 3.004 |
| 31 | 0.747 | 1.270 | 0.827 | 1.813 | 0.843 | 2.127 | 1.054 | 1.677 | 1.206 | 2.264 | 1.260 | 2.750 | 1.260 | 2.045 | 1.475 | 2.588 | 1.544 | 3.107 |
| 32 | 0.656 | 1.153 | 0.775 | 1.667 | 0.837 | 1.998 | 0.909 | 1.588 | 1.089 | 2.082 | 1.180 | 2.537 | 1.088 | 2.014 | 1.300 | 2.355 | 1.403 | 2.880 |
| 33 | 0.462 | 1.055 | 0.502 | 1.431 | 0.521 | 1.662 | 0.683 | 1.610 | 0.752 | 1.920 | 0.762 | 2.173 | 0.843 | 1.914 | 0.915 | 2.117 | 0.954 | 2.639 |
| 34 | 0.427 | 1.086 | 0.448 | 1.390 | 0.462 | 1.643 | 0.633 | 1.496 | 0.684 | 1.922 | 0.691 | 2.151 | 0.814 | 1.902 | 0.836 | 2.118 | 0.868 | 2.560 |
| 35 | 0.436 | 1.159 | 0.441 | 1.386 | 0.442 | 1.580 | 0.662 | 1.527 | 0.675 | 1.838 | 0.690 | 2.316 | 0.844 | 1.870 | 0.844 | 2.202 | 0.846 | 2.497 |
| 36 | 0.435 | 1.045 | 0.440 | 1.340 | 0.442 | 1.568 | 0.682 | 1.431 | 0.670 | 1.758 | 0.677 | 2.081 | 0.899 | 1.955 | 0.847 | 2.090 | 0.868 | 2.609 |
| 37 | 0.462 | 1.076 | 0.436 | 1.337 | 0.429 | 1.511 | 0.744 | 1.580 | 0.700 | 1.850 | 0.676 | 2.120 | 0.945 | 1.958 | 0.900 | 2.153 | 0.889 | 2.636 |
| 38 | 0.529 | 1.132 | 0.505 | 1.453 | 0.475 | 1.610 | 0.856 | 1.833 | 0.803 | 1.944 | 0.790 | 2.312 | 1.052 | 1.864 | 1.041 | 2.405 | 1.006 | 2.642 |
| 39 | 0.684 | 1.313 | 0.691 | 1.685 | 0.677 | 1.932 | 0.999 | 1.767 | 1.073 | 2.310 | 1.071 | 2.618 | 1.210 | 2.270 | 1.345 | 2.618 | 1.370 | 3.197 |
| 40 | 0.740 | 1.240 | 0.858 | 1.706 | 0.917 | 2.047 | 1.004 | 1.743 | 1.222 | 2.187 | 1.324 | 2.651 | 1.176 | 2.227 | 1.466 | 2.610 | 1.610 | 3.125 |
| 41 | 0.543 | 1.098 | 0.642 | 1.469 | 0.688 | 1.730 | 0.738 | 1.535 | 0.916 | 2.091 | 0.993 | 2.307 | 0.865 | 1.800 | 1.073 | 2.380 | 1.207 | 2.710 |
| 42 | 0.392 | 0.963 | 0.451 | 1.236 | 0.486 | 1.441 | 0.562 | 1.519 | 0.641 | 1.667 | 0.719 | 2.144 | 0.658 | 1.556 | 0.757 | 1.859 | 0.853 | 2.355 |
| 43 | 0.272 | 0.874 | 0.293 | 1.016 | 0.308 | 1.171 | 0.402 | 1.237 | 0.430 | 1.516 | 0.453 | 1.591 | 0.513 | 1.599 | 0.512 | 1.699 | 0.559 | 2.066 |
| 44 | 0.213 | 0.941 | 0.216 | 0.996 | 0.219 | 1.038 | 0.317 | 1.127 | 0.308 | 1.274 | 0.327 | 1.451 | 0.408 | 1.403 | 0.371 | 1.366 | 0.400 | 1.780 |
| 45 | 0.152 | 0.835 | 0.143 | 0.871 | 0.144 | 0.881 | 0.248 | 0.975 | 0.208 | 1.013 | 0.215 | 1.242 | 0.324 | 1.153 | 0.268 | 1.256 | 0.256 | 1.314 |
| 46 | 0.109 | 0.712 | 0.097 | 0.746 | 0.099 | 0.806 | 0.196 | 0.906 | 0.144 | 0.942 | 0.145 | 1.132 | 0.262 | 0.950 | 0.186 | 1.040 | 0.164 | 1.109 |
| 47 | 0.086 | 0.631 | 0.057 | 0.567 | 0.059 | 0.669 | 0.178 | 0.808 | 0.103 | 0.807 | 0.081 | 0.815 | 0.267 | 1.049 | 0.145 | 0.981 | 0.101 | 0.923 |
| 48 | 0.095 | 0.586 | 0.060 | 0.603 | 0.066 | 0.765 | 0.206 | 0.865 | 0.121 | 0.895 | 0.091 | 0.933 | 0.304 | 1.031 | 0.168 | 1.060 | 0.124 | 1.095 |
| 49 | 0.091 | 0.554 | 0.029 | 0.422 | 0.015 | 0.345 | 0.214 | 0.844 | 0.087 | 0.766 | 0.042 | 0.609 | 0.324 | 1.027 | 0.161 | 1.033 | 0.081 | 0.889 |
| 50 | 0.125 | 0.649 | 0.053 | 0.583 | 0.023 | 0.434 | 0.281 | 0.956 | 0.135 | 0.935 | 0.078 | 0.860 | 0.406 | 1.173 | 0.228 | 1.232 | 0.117 | 1.070 |
| 51 | 0.174 | 0.759 | 0.084 | 0.737 | 0.049 | 0.656 | 0.374 | 1.089 | 0.216 | 1.187 | 0.127 | 1.093 | 0.517 | 1.307 | 0.327 | 1.462 | 0.210 | 1.416 |
| 52 | 0.265 | 0.915 | 0.159 | 0.997 | 0.108 | 0.963 | 0.502 | 1.229 | 0.349 | 1.487 | 0.245 | 1.514 | 0.672 | 1.452 | 0.498 | 1.762 | 0.370 | 1.861 |
| 53 | 0.423 | 1.111 | 0.327 | 1.365 | 0.256 | 1.446 | 0.711 | 1.414 | 0.602 | 1.877 | 0.504 | 2.083 | 0.891 | 1.603 | 0.809 | 2.164 | 0.702 | 2.470 |
| 54 | 0.640 | 1.271 | 0.623 | 1.755 | 0.592 | 2.005 | 0.944 | 1.599 | 0.968 | 2.208 | 0.948 | 2.650 | 1.152 | 1.801 | 1.239 | 2.494 | 1.198 | 3.004 |
| 55 | 0.747 | 1.270 | 0.827 | 1.813 | 0.843 | 2.127 | 1.051 | 1.641 | 1.207 | 2.266 | 1.260 | 2.750 | 1.266 | 2.131 | 1.473 | 2.584 | 1.544 | 3.107 |
| 56 | 0.656 | 1.154 | 0.775 | 1.667 | 0.837 | 1.998 | 0.911 | 1.617 | 1.089 | 2.082 | 1.180 | 2.537 | 1.082 | 1.951 | 1.303 | 2.403 | 1.403 | 2.880 |
| 57 | 0.462 | 1.055 | 0.502 | 1.431 | 0.521 | 1.662 | 0.680 | 1.569 | 0.748 | 1.866 | 0.762 | 2.173 | 0.842 | 1.925 | 0.917 | 2.124 | 0.948 | 2.550 |
| 58 | 0.424 | 1.049 | 0.448 | 1.390 | 0.462 | 1.643 | 0.630 | 1.408 | 0.685 | 1.931 | 0.691 | 2.150 | 0.821 | 1.998 | 0.834 | 2.098 | 0.872 | 2.619 |
| 59 | 0.439 | 1.217 | 0.441 | 1.386 | 0.442 | 1.580 | 0.664 | 1.501 | 0.674 | 1.843 | 0.690 | 2.314 | 0.833 | 1.721 | 0.841 | 2.179 | 0.846 | 2.497 |
| 60 | 0.435 | 1.045 | 0.440 | 1.340 | 0.442 | 1.568 | 0.680 | 1.391 | 0.672 | 1.777 | 0.677 | 2.081 | 0.895 | 1.942 | 0.847 | 2.067 | 0.868 | 2.609 |
| 61 | 0.462 | 1.076 | 0.436 | 1.337 | 0.429 | 1.511 | 0.740 | 1.550 | 0.700 | 1.850 | 0.676 | 2.120 | 0.939 | 1.914 | 0.900 | 2.152 | 0.889 | 2.636 |
| 62 | 0.528 | 1.130 | 0.505 | 1.453 | 0.475 | 1.610 | 0.853 | 1.822 | 0.804 | 1.945 | 0.790 | 2.312 | 1.059 | 1.996 | 1.038 | 2.367 | 1.006 | 2.642 |
| 63 | 0.685 | 1.321 | 0.691 | 1.685 | 0.677 | 1.932 | 0.992 | 1.666 | 1.068 | 2.274 | 1.071 | 2.618 | 1.206 | 2.223 | 1.345 | 2.613 | 1.370 | 3.203 |
| 64 | 0.740 | 1.240 | 0.858 | 1.706 | 0.917 | 2.047 | 1.005 | 1.765 | 1.217 | 2.158 | 1.324 | 2.653 | 1.173 | 2.217 | 1.458 | 2.555 | 1.607 | 3.114 |

**TABLE 13.** *(Continued.)* Mean and standard deviation (SD) of $p^{delayed}$ charging profile over the example week with 1-hour resolution by ambient temperature and charging power scenario Low (L), Medium (M), and High (H).

| | | | | | | | | | | | | | | | | | | |
|---|---|---|---|---|---|---|---|---|---|---|---|---|---|---|---|---|---|---|
| 65 | 0.543 | 1.098 | 0.642 | 1.469 | 0.688 | 1.730 | 0.738 | 1.523 | 0.910 | 2.027 | 0.990 | 2.295 | 0.872 | 1.862 | 1.068 | 2.324 | 1.208 | 2.726 |
| 66 | 0.392 | 0.962 | 0.451 | 1.236 | 0.486 | 1.441 | 0.562 | 1.491 | 0.639 | 1.660 | 0.721 | 2.206 | 0.656 | 1.562 | 0.757 | 1.868 | 0.853 | 2.355 |
| 67 | 0.272 | 0.874 | 0.293 | 1.016 | 0.308 | 1.171 | 0.404 | 1.290 | 0.430 | 1.478 | 0.453 | 1.591 | 0.502 | 1.507 | 0.516 | 1.736 | 0.559 | 2.066 |
| 68 | 0.213 | 0.941 | 0.216 | 0.996 | 0.219 | 1.038 | 0.317 | 1.126 | 0.307 | 1.261 | 0.327 | 1.451 | 0.408 | 1.421 | 0.375 | 1.459 | 0.400 | 1.780 |
| 69 | 0.152 | 0.835 | 0.143 | 0.871 | 0.144 | 0.881 | 0.248 | 0.976 | 0.212 | 1.113 | 0.215 | 1.242 | 0.323 | 1.139 | 0.262 | 1.163 | 0.256 | 1.314 |
| 70 | 0.109 | 0.712 | 0.097 | 0.746 | 0.099 | 0.806 | 0.195 | 0.906 | 0.144 | 0.942 | 0.145 | 1.132 | 0.261 | 0.946 | 0.185 | 1.035 | 0.164 | 1.113 |
| 71 | 0.086 | 0.631 | 0.057 | 0.567 | 0.059 | 0.669 | 0.177 | 0.806 | 0.103 | 0.807 | 0.081 | 0.815 | 0.268 | 1.048 | 0.145 | 0.980 | 0.101 | 0.923 |
| 72 | 0.095 | 0.586 | 0.060 | 0.603 | 0.066 | 0.765 | 0.206 | 0.864 | 0.121 | 0.895 | 0.091 | 0.933 | 0.305 | 1.034 | 0.167 | 1.057 | 0.124 | 1.095 |
| 73 | 0.092 | 0.556 | 0.030 | 0.430 | 0.015 | 0.345 | 0.214 | 0.845 | 0.087 | 0.768 | 0.042 | 0.612 | 0.326 | 1.031 | 0.161 | 1.038 | 0.081 | 0.889 |
| 74 | 0.125 | 0.651 | 0.054 | 0.588 | 0.023 | 0.434 | 0.281 | 0.955 | 0.136 | 0.942 | 0.078 | 0.860 | 0.408 | 1.162 | 0.227 | 1.231 | 0.116 | 1.066 |
| 75 | 0.175 | 0.760 | 0.085 | 0.741 | 0.049 | 0.656 | 0.373 | 1.087 | 0.215 | 1.184 | 0.128 | 1.095 | 0.520 | 1.326 | 0.326 | 1.458 | 0.210 | 1.416 |
| 76 | 0.265 | 0.915 | 0.159 | 0.999 | 0.108 | 0.963 | 0.502 | 1.229 | 0.348 | 1.484 | 0.246 | 1.518 | 0.672 | 1.432 | 0.496 | 1.759 | 0.370 | 1.861 |
| 77 | 0.423 | 1.112 | 0.327 | 1.365 | 0.257 | 1.448 | 0.711 | 1.404 | 0.601 | 1.876 | 0.505 | 2.085 | 0.894 | 1.632 | 0.808 | 2.163 | 0.702 | 2.470 |
| 78 | 0.640 | 1.272 | 0.623 | 1.755 | 0.592 | 2.005 | 0.945 | 1.599 | 0.966 | 2.206 | 0.948 | 2.650 | 1.151 | 1.784 | 1.240 | 2.505 | 1.198 | 3.004 |
| 79 | 0.748 | 1.270 | 0.827 | 1.813 | 0.843 | 2.127 | 1.053 | 1.651 | 1.206 | 2.264 | 1.260 | 2.750 | 1.259 | 2.034 | 1.474 | 2.595 | 1.544 | 3.107 |
| 80 | 0.657 | 1.154 | 0.775 | 1.669 | 0.837 | 1.998 | 0.909 | 1.585 | 1.089 | 2.082 | 1.180 | 2.537 | 1.099 | 2.126 | 1.305 | 2.421 | 1.403 | 2.880 |
| 81 | 0.463 | 1.056 | 0.502 | 1.431 | 0.521 | 1.662 | 0.686 | 1.683 | 0.749 | 1.870 | 0.762 | 2.173 | 0.848 | 1.963 | 0.920 | 2.163 | 0.951 | 2.571 |
| 82 | 0.426 | 1.051 | 0.448 | 1.390 | 0.462 | 1.643 | 0.631 | 1.405 | 0.685 | 1.931 | 0.691 | 2.150 | 0.813 | 1.897 | 0.831 | 2.064 | 0.870 | 2.585 |
| 83 | 0.440 | 1.210 | 0.441 | 1.386 | 0.442 | 1.580 | 0.664 | 1.518 | 0.674 | 1.836 | 0.691 | 2.316 | 0.834 | 1.718 | 0.841 | 2.179 | 0.846 | 2.497 |
| 84 | 0.437 | 1.047 | 0.440 | 1.340 | 0.442 | 1.568 | 0.678 | 1.371 | 0.672 | 1.778 | 0.677 | 2.081 | 0.900 | 1.981 | 0.846 | 2.066 | 0.868 | 2.609 |
| 85 | 0.463 | 1.077 | 0.436 | 1.337 | 0.429 | 1.511 | 0.743 | 1.575 | 0.700 | 1.850 | 0.676 | 2.120 | 0.944 | 1.997 | 0.900 | 2.156 | 0.889 | 2.636 |
| 86 | 0.528 | 1.130 | 0.505 | 1.453 | 0.475 | 1.610 | 0.857 | 1.835 | 0.803 | 1.944 | 0.790 | 2.312 | 1.057 | 1.923 | 1.039 | 2.383 | 1.006 | 2.642 |
| 87 | 0.685 | 1.323 | 0.691 | 1.685 | 0.677 | 1.932 | 0.991 | 1.638 | 1.073 | 2.310 | 1.071 | 2.618 | 1.205 | 2.201 | 1.348 | 2.643 | 1.370 | 3.203 |
| 88 | 0.740 | 1.240 | 0.858 | 1.706 | 0.917 | 2.047 | 1.006 | 1.789 | 1.220 | 2.176 | 1.324 | 2.653 | 1.173 | 2.221 | 1.463 | 2.585 | 1.606 | 3.113 |
| 89 | 0.543 | 1.098 | 0.642 | 1.469 | 0.688 | 1.730 | 0.737 | 1.522 | 0.910 | 2.027 | 0.990 | 2.295 | 0.866 | 1.785 | 1.068 | 2.324 | 1.210 | 2.742 |
| 90 | 0.392 | 0.963 | 0.451 | 1.236 | 0.486 | 1.441 | 0.561 | 1.462 | 0.641 | 1.667 | 0.721 | 2.206 | 0.661 | 1.610 | 0.755 | 1.857 | 0.852 | 2.353 |
| 91 | 0.272 | 0.875 | 0.293 | 1.016 | 0.308 | 1.171 | 0.406 | 1.287 | 0.431 | 1.516 | 0.453 | 1.591 | 0.512 | 1.596 | 0.516 | 1.750 | 0.560 | 2.081 |
| 92 | 0.213 | 0.942 | 0.216 | 0.996 | 0.219 | 1.038 | 0.317 | 1.127 | 0.310 | 1.289 | 0.327 | 1.451 | 0.410 | 1.424 | 0.371 | 1.366 | 0.400 | 1.780 |
| 93 | 0.153 | 0.836 | 0.143 | 0.871 | 0.144 | 0.881 | 0.249 | 0.977 | 0.208 | 1.013 | 0.215 | 1.242 | 0.324 | 1.140 | 0.267 | 1.255 | 0.256 | 1.315 |
| 94 | 0.109 | 0.713 | 0.097 | 0.746 | 0.099 | 0.806 | 0.197 | 0.909 | 0.144 | 0.942 | 0.145 | 1.132 | 0.262 | 0.950 | 0.185 | 1.037 | 0.164 | 1.113 |
| 95 | 0.086 | 0.632 | 0.057 | 0.567 | 0.059 | 0.669 | 0.180 | 0.810 | 0.103 | 0.807 | 0.081 | 0.815 | 0.268 | 1.048 | 0.145 | 0.980 | 0.101 | 0.923 |
| 96 | 0.096 | 0.587 | 0.060 | 0.603 | 0.066 | 0.765 | 0.209 | 0.869 | 0.121 | 0.893 | 0.091 | 0.931 | 0.307 | 1.033 | 0.168 | 1.059 | 0.124 | 1.093 |
| 97 | 0.096 | 0.571 | 0.032 | 0.446 | 0.016 | 0.365 | 0.221 | 0.858 | 0.090 | 0.777 | 0.044 | 0.630 | 0.333 | 1.042 | 0.165 | 1.046 | 0.082 | 0.891 |
| 98 | 0.129 | 0.662 | 0.056 | 0.598 | 0.024 | 0.451 | 0.289 | 0.968 | 0.139 | 0.950 | 0.081 | 0.882 | 0.415 | 1.173 | 0.232 | 1.242 | 0.118 | 1.075 |
| 99 | 0.179 | 0.770 | 0.086 | 0.749 | 0.052 | 0.684 | 0.384 | 1.101 | 0.222 | 1.201 | 0.131 | 1.110 | 0.527 | 1.330 | 0.333 | 1.475 | 0.213 | 1.425 |
| 100 | 0.271 | 0.925 | 0.162 | 1.009 | 0.111 | 0.983 | 0.512 | 1.239 | 0.356 | 1.501 | 0.249 | 1.529 | 0.680 | 1.431 | 0.504 | 1.773 | 0.376 | 1.874 |
| 101 | 0.430 | 1.121 | 0.332 | 1.376 | 0.260 | 1.460 | 0.722 | 1.413 | 0.609 | 1.888 | 0.512 | 2.101 | 0.903 | 1.638 | 0.818 | 2.175 | 0.709 | 2.483 |
| 102 | 0.648 | 1.279 | 0.628 | 1.763 | 0.596 | 2.013 | 0.955 | 1.603 | 0.976 | 2.216 | 0.955 | 2.660 | 1.159 | 1.777 | 1.255 | 2.547 | 1.207 | 3.015 |
| 103 | 0.757 | 1.278 | 0.834 | 1.823 | 0.849 | 2.137 | 1.062 | 1.644 | 1.220 | 2.277 | 1.270 | 2.764 | 1.271 | 2.045 | 1.486 | 2.574 | 1.557 | 3.121 |
| 104 | 0.666 | 1.163 | 0.784 | 1.681 | 0.845 | 2.011 | 0.920 | 1.598 | 1.101 | 2.098 | 1.193 | 2.556 | 1.097 | 1.954 | 1.312 | 2.404 | 1.418 | 2.898 |
| 105 | 0.472 | 1.067 | 0.509 | 1.445 | 0.528 | 1.677 | 0.693 | 1.601 | 0.756 | 1.878 | 0.771 | 2.190 | 0.853 | 1.886 | 0.932 | 2.181 | 0.961 | 2.575 |
| 106 | 0.434 | 1.063 | 0.455 | 1.405 | 0.468 | 1.660 | 0.640 | 1.387 | 0.693 | 1.943 | 0.700 | 2.170 | 0.835 | 1.977 | 0.839 | 2.081 | 0.880 | 2.617 |
| 107 | 0.444 | 1.140 | 0.445 | 1.371 | 0.445 | 1.570 | 0.679 | 1.481 | 0.680 | 1.817 | 0.695 | 2.291 | 0.860 | 1.728 | 0.845 | 2.155 | 0.848 | 2.450 |
| 108 | 0.449 | 1.062 | 0.447 | 1.354 | 0.448 | 1.582 | 0.702 | 1.404 | 0.683 | 1.794 | 0.685 | 2.098 | 0.922 | 1.909 | 0.856 | 2.078 | 0.878 | 2.624 |
| 109 | 0.477 | 1.094 | 0.444 | 1.354 | 0.436 | 1.531 | 0.765 | 1.595 | 0.712 | 1.869 | 0.687 | 2.141 | 0.968 | 1.917 | 0.911 | 2.169 | 0.900 | 2.653 |
| 110 | 0.543 | 1.148 | 0.512 | 1.467 | 0.481 | 1.627 | 0.875 | 1.790 | 0.816 | 1.961 | 0.800 | 2.331 | 1.094 | 1.999 | 1.051 | 2.389 | 1.017 | 2.660 |
| 111 | 0.696 | 1.314 | 0.700 | 1.701 | 0.687 | 1.959 | 1.016 | 1.668 | 1.081 | 2.289 | 1.084 | 2.642 | 1.236 | 2.220 | 1.353 | 2.611 | 1.382 | 3.219 |
| 112 | 0.748 | 1.221 | 0.865 | 1.716 | 0.924 | 2.060 | 1.022 | 1.731 | 1.225 | 2.165 | 1.334 | 2.669 | 1.191 | 2.116 | 1.465 | 2.565 | 1.614 | 3.122 |
| 113 | 0.554 | 1.092 | 0.647 | 1.477 | 0.694 | 1.743 | 0.756 | 1.505 | 0.915 | 2.033 | 0.998 | 2.308 | 0.885 | 1.675 | 1.074 | 2.327 | 1.218 | 2.752 |
| 114 | 0.399 | 0.932 | 0.459 | 1.254 | 0.493 | 1.463 | 0.572 | 1.411 | 0.645 | 1.663 | 0.730 | 2.224 | 0.684 | 1.557 | 0.762 | 1.912 | 0.861 | 2.371 |
| 115 | 0.278 | 0.814 | 0.297 | 1.025 | 0.315 | 1.198 | 0.414 | 1.190 | 0.428 | 1.401 | 0.460 | 1.604 | 0.520 | 1.439 | 0.517 | 1.727 | 0.568 | 2.094 |
| 116 | 0.210 | 0.736 | 0.209 | 0.885 | 0.222 | 1.038 | 0.325 | 1.004 | 0.303 | 1.192 | 0.328 | 1.433 | 0.409 | 1.260 | 0.362 | 1.396 | 0.402 | 1.785 |
| 117 | 0.153 | 0.656 | 0.133 | 0.703 | 0.140 | 0.804 | 0.250 | 0.904 | 0.198 | 1.032 | 0.207 | 1.178 | 0.318 | 1.005 | 0.247 | 1.097 | 0.247 | 1.250 |
| 118 | 0.104 | 0.562 | 0.083 | 0.594 | 0.084 | 0.649 | 0.185 | 0.777 | 0.129 | 0.811 | 0.122 | 0.868 | 0.254 | 0.904 | 0.161 | 0.951 | 0.148 | 1.001 |
| 119 | 0.078 | 0.511 | 0.050 | 0.497 | 0.040 | 0.468 | 0.163 | 0.742 | 0.089 | 0.721 | 0.067 | 0.710 | 0.248 | 0.921 | 0.110 | 0.824 | 0.081 | 0.823 |
| 120 | 0.078 | 0.521 | 0.052 | 0.559 | 0.044 | 0.589 | 0.178 | 0.792 | 0.084 | 0.742 | 0.059 | 0.735 | 0.281 | 0.984 | 0.117 | 0.873 | 0.069 | 0.805 |
| 121 | 0.078 | 0.512 | 0.033 | 0.464 | 0.016 | 0.368 | 0.195 | 0.817 | 0.066 | 0.653 | 0.019 | 0.392 | 0.313 | 1.224 | 0.120 | 0.894 | 0.033 | 0.523 |
| 122 | 0.098 | 0.583 | 0.041 | 0.521 | 0.014 | 0.334 | 0.252 | 1.100 | 0.098 | 0.803 | 0.038 | 0.564 | 0.357 | 1.109 | 0.174 | 1.086 | 0.055 | 0.720 |
| 123 | 0.122 | 0.641 | 0.054 | 0.605 | 0.026 | 0.467 | 0.303 | 1.131 | 0.140 | 0.973 | 0.064 | 0.782 | 0.408 | 1.268 | 0.236 | 1.279 | 0.102 | 0.981 |
| 124 | 0.169 | 0.749 | 0.080 | 0.713 | 0.049 | 0.646 | 0.368 | 1.194 | 0.204 | 1.160 | 0.106 | 1.018 | 0.490 | 1.267 | 0.337 | 1.577 | 0.157 | 1.234 |
| 125 | 0.248 | 0.902 | 0.136 | 0.911 | 0.096 | 0.929 | 0.445 | 1.200 | 0.328 | 1.513 | 0.194 | 1.318 | 0.578 | 1.389 | 0.474 | 1.803 | 0.310 | 1.686 |
| 126 | 0.335 | 1.041 | 0.247 | 1.217 | 0.186 | 1.247 | 0.546 | 1.294 | 0.463 | 1.713 | 0.361 | 1.791 | 0.695 | 1.472 | 0.646 | 2.050 | 0.515 | 2.261 |
| 127 | 0.409 | 1.118 | 0.355 | 1.436 | 0.295 | 1.511 | 0.643 | 1.364 | 0.610 | 1.915 | 0.532 | 2.141 | 0.795 | 1.624 | 0.787 | 2.167 | 0.703 | 2.520 |
| 128 | 0.495 | 1.213 | 0.470 | 1.638 | 0.430 | 1.840 | 0.737 | 1.481 | 0.772 | 2.134 | 0.719 | 2.504 | 0.898 | 1.722 | 0.954 | 2.343 | 0.942 | 2.870 |
| 129 | 0.593 | 1.267 | 0.623 | 1.822 | 0.619 | 2.162 | 0.858 | 1.566 | 0.938 | 2.231 | 0.957 | 2.818 | 1.056 | 1.819 | 1.155 | 2.630 | 1.215 | 3.273 |
| 130 | 0.679 | 1.272 | 0.764 | 1.867 | 0.793 | 2.288 | 0.966 | 1.492 | 1.094 | 2.293 | 1.183 | 2.915 | 1.175 | 1.830 | 1.307 | 2.515 | 1.420 | 3.211 |
| 131 | 0.680 | 1.250 | 0.752 | 1.794 | 0.795 | 2.195 | 0.966 | 1.687 | 1.073 | 2.226 | 1.161 | 2.772 | 1.177 | 2.280 | 1.329 | 2.568 | 1.400 | 3.157 |
| 132 | 0.697 | 1.272 | 0.762 | 1.782 | 0.812 | 2.175 | 0.992 | 1.755 | 1.131 | 2.375 | 1.186 | 2.873 | 1.234 | 2.380 | 1.378 | 2.643 | 1.447 | 3.277 |
| 133 | 0.672 | 1.227 | 0.711 | 1.673 | 0.708 | 1.916 | 0.954 | 1.749 | 1.072 | 2.125 | 1.092 | 2.547 | 1.192 | 2.486 | 1.338 | 2.614 | 1.366 | 2.934 |

**TABLE 13.** *(Continued.)* **Mean and standard deviation (SD) of $p^{delayed}$ charging profile over the example week with 1-hour resolution by ambient temperature and charging power scenario Low (L), Medium (M), and High (H).**

| | | | | | | | | | | | | | | | | | | |
|---|---|---|---|---|---|---|---|---|---|---|---|---|---|---|---|---|---|---|
| 134 | 0.647 | 1.287 | 0.746 | 1.785 | 0.786 | 2.118 | 0.962 | 2.290 | 1.063 | 2.212 | 1.142 | 2.715 | 1.126 | 2.529 | 1.378 | 3.310 | 1.500 | 4.113 |
| 135 | 0.555 | 1.122 | 0.626 | 1.584 | 0.669 | 1.927 | 0.852 | 2.031 | 0.976 | 2.505 | 1.035 | 2.968 | 1.039 | 2.670 | 1.139 | 2.618 | 1.288 | 3.658 |
| 136 | 0.511 | 1.150 | 0.564 | 1.493 | 0.560 | 1.656 | 0.719 | 1.666 | 0.851 | 2.140 | 0.905 | 2.567 | 0.885 | 2.218 | 1.029 | 2.412 | 1.091 | 2.785 |
| 137 | 0.457 | 1.185 | 0.500 | 1.452 | 0.532 | 1.761 | 0.636 | 1.649 | 0.722 | 1.860 | 0.777 | 2.264 | 0.763 | 2.053 | 0.891 | 2.441 | 0.977 | 2.892 |
| 138 | 0.413 | 1.363 | 0.454 | 1.453 | 0.488 | 1.699 | 0.525 | 1.607 | 0.639 | 1.884 | 0.719 | 2.313 | 0.637 | 1.893 | 0.802 | 2.576 | 0.932 | 3.329 |
| 139 | 0.244 | 0.769 | 0.286 | 1.067 | 0.316 | 1.297 | 0.364 | 1.225 | 0.413 | 1.547 | 0.474 | 1.858 | 0.427 | 1.334 | 0.449 | 1.465 | 0.515 | 1.855 |
| 140 | 0.184 | 0.851 | 0.180 | 0.833 | 0.193 | 0.963 | 0.269 | 1.092 | 0.264 | 1.240 | 0.282 | 1.358 | 0.340 | 1.255 | 0.318 | 1.341 | 0.339 | 1.551 |
| 141 | 0.150 | 0.711 | 0.130 | 0.736 | 0.141 | 0.886 | 0.240 | 0.986 | 0.196 | 1.018 | 0.196 | 1.101 | 0.321 | 1.253 | 0.248 | 1.237 | 0.258 | 1.429 |
| 142 | 0.120 | 0.616 | 0.101 | 0.661 | 0.105 | 0.752 | 0.196 | 0.921 | 0.154 | 0.906 | 0.158 | 1.096 | 0.268 | 1.199 | 0.186 | 1.040 | 0.190 | 1.171 |
| 143 | 0.094 | 0.575 | 0.071 | 0.615 | 0.063 | 0.663 | 0.175 | 0.771 | 0.115 | 0.835 | 0.101 | 0.906 | 0.280 | 1.273 | 0.131 | 0.889 | 0.118 | 1.001 |
| 144 | 0.117 | 0.663 | 0.105 | 0.779 | 0.107 | 0.892 | 0.211 | 0.897 | 0.148 | 0.980 | 0.135 | 1.054 | 0.306 | 1.070 | 0.181 | 1.103 | 0.156 | 1.170 |
| 145 | 0.081 | 0.524 | 0.034 | 0.470 | 0.017 | 0.375 | 0.194 | 0.814 | 0.066 | 0.655 | 0.019 | 0.392 | 0.304 | 1.100 | 0.119 | 0.892 | 0.033 | 0.523 |
| 146 | 0.101 | 0.594 | 0.042 | 0.531 | 0.015 | 0.353 | 0.244 | 0.919 | 0.100 | 0.810 | 0.038 | 0.564 | 0.360 | 1.174 | 0.174 | 1.084 | 0.055 | 0.720 |
| 147 | 0.125 | 0.650 | 0.055 | 0.615 | 0.027 | 0.481 | 0.298 | 1.011 | 0.141 | 0.975 | 0.065 | 0.782 | 0.403 | 1.154 | 0.234 | 1.257 | 0.104 | 0.993 |
| 148 | 0.174 | 0.762 | 0.082 | 0.724 | 0.050 | 0.656 | 0.370 | 1.140 | 0.205 | 1.163 | 0.108 | 1.026 | 0.496 | 1.352 | 0.332 | 1.489 | 0.158 | 1.239 |
| 149 | 0.253 | 0.912 | 0.139 | 0.922 | 0.099 | 0.946 | 0.457 | 1.358 | 0.322 | 1.439 | 0.198 | 1.332 | 0.589 | 1.417 | 0.475 | 1.781 | 0.312 | 1.690 |
| 150 | 0.340 | 1.050 | 0.250 | 1.227 | 0.191 | 1.264 | 0.551 | 1.317 | 0.466 | 1.717 | 0.366 | 1.802 | 0.713 | 1.630 | 0.653 | 2.076 | 0.510 | 2.170 |
| 151 | 0.416 | 1.127 | 0.360 | 1.446 | 0.301 | 1.528 | 0.658 | 1.528 | 0.613 | 1.917 | 0.537 | 2.150 | 0.807 | 1.590 | 0.795 | 2.227 | 0.718 | 2.587 |
| 152 | 0.501 | 1.222 | 0.477 | 1.651 | 0.434 | 1.851 | 0.748 | 1.494 | 0.778 | 2.146 | 0.724 | 2.510 | 0.940 | 2.002 | 0.956 | 2.366 | 0.947 | 2.877 |
| 153 | 0.601 | 1.275 | 0.630 | 1.835 | 0.626 | 2.176 | 0.869 | 1.604 | 0.944 | 2.238 | 0.963 | 2.827 | 1.113 | 2.198 | 1.157 | 2.618 | 1.220 | 3.280 |
| 154 | 0.687 | 1.281 | 0.773 | 1.881 | 0.800 | 2.300 | 0.993 | 1.652 | 1.105 | 2.359 | 1.194 | 2.935 | 1.221 | 2.123 | 1.309 | 2.483 | 1.429 | 3.227 |
| 155 | 0.691 | 1.309 | 0.761 | 1.809 | 0.803 | 2.215 | 0.995 | 1.767 | 1.076 | 2.202 | 1.171 | 2.792 | 1.237 | 2.553 | 1.357 | 2.712 | 1.407 | 3.171 |
| 156 | 0.706 | 1.307 | 0.770 | 1.794 | 0.822 | 2.200 | 1.050 | 2.142 | 1.131 | 2.325 | 1.193 | 2.890 | 1.236 | 2.272 | 1.414 | 2.797 | 1.453 | 3.289 |
| 157 | 0.684 | 1.340 | 0.718 | 1.686 | 0.714 | 1.938 | 1.008 | 2.191 | 1.078 | 2.140 | 1.098 | 2.562 | 1.213 | 2.432 | 1.334 | 2.560 | 1.372 | 2.945 |
| 158 | 0.647 | 1.237 | 0.755 | 1.797 | 0.793 | 2.130 | 0.933 | 1.893 | 1.081 | 2.344 | 1.152 | 2.729 | 1.192 | 2.900 | 1.348 | 3.110 | 1.508 | 4.121 |
| 159 | 0.569 | 1.261 | 0.631 | 1.594 | 0.675 | 1.944 | 0.865 | 2.193 | 0.992 | 2.575 | 1.042 | 2.978 | 1.089 | 2.791 | 1.166 | 2.836 | 1.288 | 3.648 |
| 160 | 0.511 | 1.115 | 0.569 | 1.501 | 0.564 | 1.666 | 0.714 | 1.448 | 0.846 | 2.062 | 0.914 | 2.580 | 0.925 | 2.505 | 1.037 | 2.401 | 1.096 | 2.783 |
| 161 | 0.449 | 1.068 | 0.503 | 1.458 | 0.539 | 1.779 | 0.669 | 1.813 | 0.719 | 1.830 | 0.781 | 2.271 | 0.768 | 1.895 | 0.904 | 2.501 | 0.977 | 2.893 |
| 162 | 0.388 | 1.090 | 0.456 | 1.446 | 0.498 | 1.711 | 0.553 | 1.708 | 0.642 | 1.893 | 0.723 | 2.304 | 0.644 | 1.934 | 0.804 | 2.556 | 0.937 | 3.310 |
| 163 | 0.235 | 0.744 | 0.287 | 1.071 | 0.318 | 1.301 | 0.358 | 1.292 | 0.410 | 1.532 | 0.473 | 1.858 | 0.433 | 1.224 | 0.452 | 1.613 | 0.514 | 1.829 |
| 164 | 0.168 | 0.636 | 0.179 | 0.831 | 0.191 | 0.959 | 0.267 | 1.099 | 0.266 | 1.335 | 0.272 | 1.247 | 0.358 | 1.378 | 0.324 | 1.346 | 0.325 | 1.412 |
| 165 | 0.131 | 0.586 | 0.124 | 0.699 | 0.131 | 0.829 | 0.218 | 0.790 | 0.191 | 1.098 | 0.187 | 1.053 | 0.307 | 1.090 | 0.253 | 1.362 | 0.242 | 1.391 |
| 166 | 0.097 | 0.519 | 0.086 | 0.590 | 0.091 | 0.647 | 0.184 | 0.783 | 0.137 | 0.823 | 0.130 | 0.875 | 0.254 | 0.944 | 0.174 | 0.966 | 0.159 | 1.037 |
| 167 | 0.067 | 0.449 | 0.039 | 0.412 | 0.036 | 0.407 | 0.161 | 0.723 | 0.082 | 0.675 | 0.058 | 0.619 | 0.248 | 0.900 | 0.118 | 0.830 | 0.077 | 0.758 |
| 168 | 0.075 | 0.494 | 0.033 | 0.399 | 0.029 | 0.411 | 0.180 | 0.779 | 0.090 | 0.747 | 0.048 | 0.574 | 0.274 | 0.954 | 0.133 | 0.922 | 0.080 | 0.796 |

Although keeping in mind, that here the factors were presented per location type, which had a large effect on the factors. However, as near all BEVs in this study visited the location 'Home', especially the coincidence factors for it, presented a reasonably close comparison, and results, to the previous studies. The driving profiles formed in this study were based on travel survey data of 12 773 responses, with 40 321 trips, and thus the profiles can be considered to represent well the average passenger vehicle driving behavior.

However, no analysis was conducted weather the driving patterns of BEVs would differ from the driving patterns of vehicles with internal combustion engines (ICEs), which can be assumed that the majority of the respondents in the travel survey, conducted in 2016, used. Instead, the underlying assumption was that the BEVs would be preferred to be used similarly to ICE vehicles, to satisfy the travelling patterns of the respondents. In addition, charging was assumed widely available in this study, to represent a situation where the transport sector is widely electrified, and thus the availability of charging can be assumed high. Moreover, the temperature and driving speed dependence of the BEV consumption, was based on several studies, instead of particular BEV models, which was considered better to describe the average consumption of a large-scale BEV fleet. However, the energy consumption rate of BEVs, based on ambient temperature (Table 3), had high variation for the very low temperature of −20°C, and hence included some uncertainty. In addition, some of the studies considered were already a couple years old, and thus due to technological advancements, the rates presented can be rather considered pessimistic than optimistic.

The share of electrifiable vehicles after fast charging was 93.9%. The method for adding the fast-charging events can be considered rather simple, and by allowing either the addition of further stops or to alter the consecutive trips of the vehicle profiles together, the share of electrifiable vehicles could be increased. However, these would either increase the computational burden or, in the case of altering the profiles further, assume a change in the driving behavior of the driver, which was beyond the scope of this study. In addition, regardless of fast charging or not, the driving profiles were fixed, which is inherent when using DUOATS type modeling, and thus effects of e.g., EV policy changes are not possible to be conducted. Moreover, utilizing the results for a small number of BEVs includes uncertainties, due to high variation of charging for individual BEVs, whereas for analyses including a large number of BEVs, the results should represent the charging behavior well. These analyses could include generation planning, power system security of supply, and grid expansion planning, to include e.g., a new district which includes certain types of charging locations.

For future studies, the timing of charging could be modeled based on external parameters, such as the price of electricity, which could also affect the coincidence of charging. Furthermore, the flexibility of charging, including vehicle-to-grid, could be modeled. In addition, the effects of the charging load to a complete energy system could be analyzed.

## APPENDIX A
## GROUPING OF LOCATION TYPES

In Table 10 the grouping of all locations available for the respondents in the national household travel survey is presented.

In Table 11 the original values are presented for the studies which required conversion from them to the relative values presented in Table 3 in Section II-C. Moreover, the conversion is presented in the column with 'calculated as' heading. Study [37] studied maximum range of two vehicles which are both presented in table 11, together with the mean value of them, which was utilized in this study.

## APPENDIX B
## ADDITIONAL FIGURES

See Figs. 14–16.

## APPENDIX C
## TIME SERIES FOR CHARGING PROFILES

The Tables 12 and 13 present the hourly mean and standard deviation of weekly charging loads for the $p^{immediate}$ and $p^{delayed}$ charging profiles considering the ambient temperatures of 15°C, −5°C, and −20°C, and the three charging power scenarios.

## REFERENCES

[1] International Energy Agency. (2021). *Global EV Outlook 2021*. Accessed: Feb. 20, 2023. [Online]. Available: https://www.iea.org/reports/global-ev-outlook-2021
[2] European Environmental Agency. *New Registrations of Electric Vehicles in Europe*. Accessed: Feb. 20, 2023. [Online]. Available: https://www.eea.europa.eu/ims/new-registrations-of-electric-vehicles
[3] European Commission. *Zero Emission Vehicles: First 'Fit for 55' Deal Will End the Sale of New $CO_2$ Emitting Cars in Europe by 2035*. Accessed: Feb. 20, 2023. [Online]. Available: https://ec.europa.eu/commission/presscorner/detail/en/ip_22_6462
[4] The Finnish Transport and Communications Agency. *Henkilöautojen Ensirekisteröinnit Ennätysmatalalla—Vaihtoehtoisten Käyttövoimien Osuus Lähenee jo 40 Prosenttia*. (in Finnish). Accessed: Feb. 20, 2023. [Online]. Available: https://www.traficom.fi/fi/ajankohtaista/henkiloautojen-ensirekisteroinnit-ennatysmatalalla-vaihtoehtoisten-kayttovoimien
[5] L. Calearo, M. Marinelli, and C. Ziras, "A review of data sources for electric vehicle integration studies," *Renew. Sustain. Energy Rev.*, vol. 151, Nov. 2021, Art. no. 111518, doi: 10.1016/j.rser.2021.111518.
[6] J. Zhang, J. Yan, Y. Liu, H. Zhang, and G. Lv, "Daily electric vehicle charging load profiles considering demographics of vehicle users," *Appl. Energy*, vol. 274, Sep. 2020, Art. no. 115063, doi: 10.1016/j.apenergy.2020.115063.
[7] C. Gaete-Morales, H. Kramer, W.-P. Schill, and A. Zerrahn, "An open tool for creating battery-electric vehicle time series from empirical data, emobpy," *Sci. Data*, vol. 8, no. 1, p. 152, Jun. 2021, doi: 10.1038/s41597-021-00932-9.
[8] T. Yi, C. Zhang, T. Lin, and J. Liu, "Research on the spatial-temporal distribution of electric vehicle charging load demand: A case study in China," *J. Cleaner Prod.*, vol. 242, Jan. 2020, Art. no. 118457, doi: 10.1016/j.jclepro.2019.118457.
[9] G. Pareschi, L. Küng, G. Georges, and K. Boulouchos, "Are travel surveys a good basis for EV models? Validation of simulated charging profiles against empirical data," *Appl. Energy*, vol. 275, Oct. 2020, Art. no. 115318, doi: 10.1016/j.apenergy.2020.115318.
[10] Z. Darabi and M. Ferdowsi, "Aggregated impact of plug-in hybrid electric vehicles on electricity demand profile," *IEEE Trans. Sustain. Energy*, vol. 2, no. 4, pp. 501–508, Oct. 2011, doi: 10.1109/tste.2011.2158123.
[11] Z. Liu, Q. Wu, A. Nielsen, and Y. Wang, "Day-ahead energy planning with 100% electric vehicle penetration in the Nordic region by 2050," *Energies*, vol. 7, no. 3, pp. 1733–1749, Mar. 2014, doi: 10.3390/en7031733.
[12] N. Daina, A. Sivakumar, and J. W. Polak, "Modelling electric vehicles use: A survey on the methods," *Renew. Sustain. Energy Rev.*, vol. 68, pp. 447–460, Feb. 2017, doi: 10.1016/j.rser.2016.10.005.
[13] D. Fischer, A. Harbrecht, A. Surmann, and R. McKenna, "Electric vehicles' impacts on residential electric local profiles—A stochastic modelling approach considering socio-economic, behavioural and spatial factors," *Appl. Energy*, vols. 233–234, pp. 644–658, Jan. 2019, doi: 10.1016/j.apenergy.2018.10.010.
[14] H. Jahangir, H. Tayarani, A. Ahmadian, M. A. Golkar, J. Miret, M. Tayarani, and H. O. Gao, "Charging demand of plug-in electric vehicles: Forecasting travel behavior based on a novel rough artificial neural network approach," *J. Cleaner Prod.*, vol. 229, pp. 1029–1044, Aug. 2019, doi: 10.1016/j.jclepro.2019.04.345.
[15] G. Storti Gajani, L. Bascetta, and G. Gruosso, "Data-driven approach to model electrical vehicle charging profile for simulation of grid integration scenarios," *IET Electr. Syst. Transp.*, vol. 9, no. 4, pp. 168–175, Dec. 2019, doi: 10.1049/iet-est.2019.0002.
[16] Y. Zhao, Z. Wang, Z.-J.-M. Shen, and F. Sun, "Data-driven framework for large-scale prediction of charging energy in electric vehicles," *Appl. Energy*, vol. 282, Jan. 2021, Art. no. 116175, doi: 10.1016/j.apenergy.2020.116175.
[17] X. Zhang, Y. Zou, J. Fan, and H. Guo, "Usage pattern analysis of Beijing private electric vehicles based on real-world data," *Energy*, vol. 167, pp. 1074–1085, Jan. 2019, doi: 10.1016/j.energy.2018.11.005.
[18] H. Saele and I. Petersen, "Electric vehicles in Norway and the potential for demand response," in *Proc. 53rd Int. Univ. Power Eng. Conf. (UPEC)*, Glasgow, U.K., Sep. 2018, pp. 1–6, doi: 10.1109/UPEC.2018.8541926.
[19] H. M. Louie, "Time-series modeling of aggregated electric vehicle charging station load," *Electric Power Compon. Syst.*, vol. 45, no. 14, pp. 1498–1511, Dec. 2017, doi: 10.1080/15325008.2017.1336583.
[20] L. Buzna, P. De Falco, S. Khormali, D. Proto, and M. Straka, "Electric vehicle load forecasting: A comparison between time series and machine learning approaches," in *Proc. 1st Int. Conf. Energy Transition Medit. Area (SyNERGY MED)*, Cagliari, Italy, May 2019, pp. 1–5, doi: 10.1109/SyNERGY-MED.2019.8764110.
[21] S. Xydas, A. S. Hassan, C. E. Marmaras, N. Jenkins, and L. M. Cipcigan, "Electric vehicle load forecasting using data mining methods," in *Proc. IET Hybrid Electr. Vehicles Conf. (HEVC)*, London, U.K., Nov. 2013, pp. 10.1–10.1, doi: 10.1049/cp.2013.1914.
[22] T. Simolin, K. Rauma, R. Viri, J. Mäkinen, A. Rautiainen, and P. Järventausta, "Charging powers of the electric vehicle fleet: Evolution and implications at commercial charging sites," *Appl. Energy*, vol. 303, Dec. 2021, Art. no. 117651, doi: 10.1016/j.apenergy.2021.117651.
[23] Finnish Transport and Communications Agency. (2018). *Henkilöliikennetutkimus 2016: Suomalaisten liikkuminen*, (in Finnish). Accessed: Mar. 8, 2018. [Online]. Available: https://urn.fi/URN:ISBN:978-952-317-513-6
[24] I. Graabak, Q. Wu, L. Warland, and Z. Liu, "Optimal planning of the Nordic transmission system with 100% electric vehicle penetration of passenger cars by 2050," *Energy*, vol. 107, pp. 648–660, Jul. 2016, doi: 10.1016/j.energy.2016.04.060.
[25] A. Rautiainen, S. Repo, P. Jarventausta, A. Mutanen, K. Vuorilehto, and K. Jalkanen, "Statistical charging load modeling of PHEVs in electricity distribution networks using national travel survey data," *IEEE Trans. Smart Grid*, vol. 3, no. 4, pp. 1650–1659, Dec. 2012, doi: 10.1109/tsg.2012.2206411.
[26] O. Lehtinen, S. Pitkaniemi, A. Weckman, M. Aikio, M. Mabano, and M. Lehtonen, "Electric vehicle charging loads in residential areas of apartment houses," in *Proc. 21st Int. Sci. Conf. Electr. Power Eng. (EPE)*, Prague, Czech Republic, Oct. 2020, pp. 1–6, doi: 10.1109/epe51172.2020.9269191.

[27] M. Aunedi, M. Woolf, G. Strbac, O. Babalola, and M. Clark, "Characteristic demand profiles of residential and commercial EV users and opportunities for smart charging," presented at the 23rd Int. Conf. Electr. Distrib., Lyon, France, Jun. 2015. [Online]. Available: http://cired.net/publications/cired2015/papers/CIRED2015_1088_final.pdf

[28] L. Calearo, A. Thingvad, K. Suzuki, and M. Marinelli, "Grid loading due to EV charging profiles based on pseudo-real driving pattern and user behavior," *IEEE Trans. Transport. Electrific.*, vol. 5, no. 3, pp. 683–694, Sep. 2019, doi: 10.1109/tte.2019.2921854.

[29] J. Quiros-Tortos, L. F. Ochoa, and B. Lees, "A statistical analysis of EV charging behavior in the U.K.," in *Proc. IEEE PES Innov. Smart Grid Technol. Latin America (ISGT LATAM)*, Montevideo, Uruguay, Oct. 2015, pp. 445–449, doi: 10.1109/isgt-la.2015.7381196.

[30] B. Thormann and T. Kienberger, "Evaluation of grid capacities for integrating future E-mobility and heat pumps into low-voltage grids," *Energies*, vol. 13, no. 19, p. 5083, Sep. 2020, doi: 10.3390/en13195083.

[31] X. Tong, C. Guo, X. Yang, and C. Chen, "Research on characteristics of electric vehicle charging load and distribution network supportability," in *Proc. IEEE PES Asia–Pacific Power Energy Eng. Conf. (APPEEC)*, Xi'an, China, Oct. 2016, pp. 1539–1542, doi: 10.1109/appeec.2016.7779748.

[32] J. Bollerslev, P. B. Andersen, T. V. Jensen, M. Marinelli, A. Thingvad, L. Calearo, and T. Weckesser, "Coincidence factors for domestic EV charging from driving and plug-in behavior," *IEEE Trans. Transport. Electrific.*, vol. 8, no. 1, pp. 808–819, Mar. 2022, doi: 10.1109/tte.2021.3088275.

[33] A. Rautiainen, A. Mutanen, S. Repo, P. Jarventausta, A. Tammi, R. Ryymin, J. Helin, A. Unkuri, and M. Pekkinen, "Case studies on impacts of plug-in vehicle charging load on the planning of urban electricity distribution networks," in *Proc. 8th Int. Conf. Exhib. Ecol. Vehicles Renew. Energies (EVER)*, Monte Carlo, Monaco, Mar. 2013, pp. 1–7, doi: 10.1109/ever.2013.6521542.

[34] Statistics Finland. *Population According to Age (5-Year) and Sex, 1865–2021*. Accessed: Jan. 5, 2023. [Online]. Available: https://pxdata.stat.fi/PxWeb/pxweb/en/StatFin/StatFin__vaerak/statfin_vaerak_pxt_11rc.px/

[35] Statistics Finland. *Vehicle Stock by Area, 2011–2022*. Accessed: Jan. 5, 2023. [Online]. Available: https://pxdata.stat.fi/PxWeb/pxweb/en/StatFin/StatFin__mkan/statfin_mkan_pxt_11ic.px/

[36] H. Zhang, Z. Hu, Z. Xu, and Y. Song, "Evaluation of achievable vehicle-to-grid capacity using aggregate PEV model," *IEEE Trans. Power Syst.*, vol. 32, no. 1, pp. 784–794, Jan. 2017, doi: 10.1109/tpwrs.2016.2561296.

[37] J. R. M. Delos Reyes, R. V. Parsons, and R. Hoemsen, "Winter happens: The effect of ambient temperature on the travel range of electric vehicles," *IEEE Trans. Veh. Technol.*, vol. 65, no. 6, pp. 4016–4022, Jun. 2016, doi: 10.1109/TVT.2016.2544178.

[38] Y. Al-Wreikat, C. Serrano, and J. R. Sodré, "Effects of ambient temperature and trip characteristics on the energy consumption of an electric vehicle," *Energy*, vol. 238, Jan. 2022, Art. no. 122028, doi: 10.1016/j.energy.2021.122028.

[39] A. Lajunen, "Evaluation of energy consumption and carbon dioxide emissions for electric vehicles in Nordic climate conditions," in *Proc. 13th Int. Conf. Ecol. Vehicles Renew. Energies (EVER)*, Monte Carlo, Monaco, Apr. 2018, pp. 1–7, doi: 10.1109/EVER.2018.8362390.

[40] K. Liu, J. Wang, T. Yamamoto, and T. Morikawa, "Exploring the interactive effects of ambient temperature and vehicle auxiliary loads on electric vehicle energy consumption," *Appl. Energy*, vol. 227, pp. 324–331, Oct. 2018, doi: 10.1016/j.apenergy.2017.08.074.

[41] Finnish Meteorological Institute. *Energialaskennan Testivuodet 2020*. (in Finnish). Accessed: Dec. 20, 2022. [Online]. Available: https://www.ilmatieteenlaitos.fi/energialaskenta-try2020

[42] Finnish Meteorological Institute. *Kuukausitilastot*. (in Finnish). Accessed: Dec. 16, 2022. [Online]. Available: https://www.ilmatieteenlaitos.fi/kuukausitilastot

[43] Official Statistics of Finland. *Motor Vehicle Stock*. Accessed: Dec. 16, 2022. [Online]. Available: https://www.stat.fi/til/mkan/2020/mkan_2020_2021-02-26_tie_001_en.html

[44] G. M. Fetene, S. Kaplan, S. L. Mabit, A. F. Jensen, and C. G. Prato, "Harnessing big data for estimating the energy consumption and driving range of electric vehicles," *Transp. Res. D, Transp. Environ.*, vol. 54, pp. 1–11, Jul. 2017, doi: 10.1016/j.trd.2017.04.013.

[45] Y. Xiao, Y. Zhang, I. Kaku, R. Kang, and X. Pan, "Electric vehicle routing problem: A systematic review and a new comprehensive model with nonlinear energy recharging and consumption," *Renew. Sustain. Energy Rev.*, vol. 151, Nov. 2021, Art. no. 111567, doi: 10.1016/j.rser.2021.111567.

[46] G. Wager, J. Whale, and T. Braunl, "Driving electric vehicles at highway speeds: The effect of higher driving speeds on energy consumption and driving range for electric vehicles in Australia," *Renew. Sustain. Energy Rev.*, vol. 63, pp. 158–165, Sep. 2016, doi: 10.1016/j.rser.2016.05.060.

[47] X. Yuan, C. Zhang, G. Hong, X. Huang, and L. Li, "Method for evaluating the real-world driving energy consumptions of electric vehicles," *Energy*, vol. 141, pp. 1955–1968, Dec. 2017, doi: 10.1016/j.energy.2017.11.134.

[48] Finnish Meteorological Institute. *Havaintojen Lataus*, (in Finnish). Accessed: Dec. 21, 2023. [Online]. Available: https://www.ilmatieteenlaitos.fi/havaintojen-lataus

[49] B. Wang, D. Zhao, P. Dehghanian, Y. Tian, and T. Hong, "Aggregated electric vehicle load modeling in large-scale electric power systems," *IEEE Trans. Ind. Appl.*, vol. 56, no. 5, pp. 5796–5810, Sep. 2020, doi: 10.1109/tia.2020.2988019.

[50] J. S. Milton and J. Arnold, *Introduction to Probability and Statistics: Principles and Applications for Engineering and the Computing Sciences*. New York, NY, USA: McGraw-Hill, 1995, p. 809.

**ILKKA JOKINEN** received the M.Sc. degree in advanced energy solution from the School of Electrical Engineering, Aalto University, Finland, in 2020, where he is currently pursuing the Ph.D. degree. His research interests include sector coupling, renewable energy integration, decarbonization, and power and energy system planning together with economics.

**MATTI LEHTONEN** received the master's and Licentiate degrees in electrical engineering from the Helsinki University of Technology (nowadays Aalto University), in 1984 and 1989, respectively, and the Ph.D. degree in technology from the Tampere University of Technology, in 1992. He was with VTT Energy, Espoo, Finland, from 1987 to 2003. Since 1999, he has been a Professor with Aalto University, where he is currently the Head of Power Systems and High Voltage Engineering. His research interests include power system planning and asset management, power system protection, including earth fault problems, harmonic related issues, and the applications of information technology in distribution systems.